EVALUATING THE TIME-DEPENDENT DEFORMATIONS AND BOND CHARACTERISTICS OF A SELF-CONSOLIDATING CONCRETE MIX AND THE IMPLICATION FOR PRETENSIONED BRIDGE APPLICATIONS

by

KYLE HATCH LARSON

B.S., Bradley University, 2002
M.S., Kansas State University, 2003

AN ABSTRACT OF A DISSERTATION

submitted in partial fulfillment of the requirements for the degree

DOCTOR OF PHILOSOPHY

Department of Civil Engineering
College of Engineering

KANSAS STATE UNIVERSITY
Manhattan, Kansas

2006

Abstract

Results of an extensive experimental program conducted to determine the material, bond characteristics, and time-dependent deformations of a proposed self-consolidating concrete (SCC) mixture for bridge girders are presented. This research program was completed in three phases. The first phase consisted of 15 full-scale, pretensioned SCC flexural specimens tested to evaluate their transfer and development lengths. These specimens included both single-strand and multiple-strand beams, as well as specimens designed to evaluate the so-called “top-strand" effect. The top-strand specimens, with more than 20 inches of concrete below the strand, were tested to evaluate the current American Association of State Highway Officials requirement of a 30% increase in the development length when the concrete below the strand is more than 12 inches. Strand end-slip measurements, used to estimate transfer lengths, indicated the proposed SCC mixture meets ACI and AASHTO requirements. In addition, flexural tests confirmed the proposed SCC mixture also meets current code requirements for development length.

The second phase was to evaluate the elastic shortening, creep, and shrinkage properties of the proposed SCC mixture for bridge girders. Four bridge girders with an inverted-T profile were used to measure these time-dependent deformations. In two of the specimens, the strands were tensioned to 75% of the ultimate tensile strength, simulating a girder at service. Strands of the other two specimens were left untensioned to evaluate shrinkage effect of the concrete alone. The shrinkage was then subtracted from the fully tensioned specimens and elastic shortening and creep were isolated after

relaxation losses were calculated from code expressions. In addition, the fully tensioned specimens were used to determine transfer lengths of the prestressing strand.

The final phase of the program was to record strain measurements of the actual bridge girders used in the field. Elastic shortening, creep, and shrinkage prestress losses of the proposed SCC mixture were compared with current design equations. Instrumentation of seven pretensioned girders in a five-span bridge located in Cowley County, Kansas, was used to measure time-dependent deformations. Three of these girders utilized SCC, while the other four were cast with conventional concrete.

EVALUATING THE TIME-DEPENDENT DEFORMATIONS AND BOND CHARACTERISTICS OF A SELF-CONSOLIDATING CONCRETE MIX AND THE IMPLICATION FOR PRETENSIONED BRIDGE APPLICATIONS

by

KYLE HATCH LARSON

B.S., Bradley University, 2002
M.S., Kansas State University, 2003

A DISSERTATION

submitted in partial fulfillment of the requirements for the degree

DOCTOR OF PHILOSOPHY

Department of Civil Engineering
College of Engineering

KANSAS STATE UNIVERSITY
Manhattan, Kansas

2006

Approved by:

Major Professor
Robert J Peterman

Copyright

Abstract

Results of an extensive experimental program conducted to determine the material, bond characteristics, and time-dependent deformations of a proposed self-consolidating concrete (SCC) mixture for bridge girders are presented. This research program was completed in three phases. The first phase consisted of 15 full-scale, pretensioned SCC flexural specimens tested to evaluate their transfer and development lengths. These specimens included both single-strand and multiple-strand beams, as well as specimens designed to evaluate the so-called “top-strand" effect. The top-strand specimens, with more than 20 inches of concrete below the strand, were tested to evaluate the current American Association of State Highway Officials requirement of a 30% increase in the development length when the concrete below the strand is more than 12 inches. Strand end-slip measurements, used to estimate transfer lengths, indicated the proposed SCC mixture meets ACI and AASHTO requirements. In addition, flexural tests confirmed the proposed SCC mixture also meets current code requirements for development length.

The second phase was to evaluate the elastic shortening, creep, and shrinkage properties of the proposed SCC mixture for bridge girders. Four bridge girders with an inverted-T profile were used to measure these time-dependent deformations. In two of the specimens, the strands were tensioned to 75% of the ultimate tensile strength, simulating a girder at service. Strands of the other two specimens were left untensioned to evaluate shrinkage effect of the concrete alone. The shrinkage was then subtracted from the fully tensioned specimens and elastic shortening and creep were isolated after

relaxation losses were calculated from code expressions. In addition, the fully tensioned specimens were used to determine transfer lengths of the prestressing strand.

The final phase of the program was to record strain measurements of the actual bridge girders used in the field. Elastic shortening, creep, and shrinkage prestress losses of the proposed SCC mixture were compared with current design equations. Instrumentation of seven pretensioned girders in a five-span bridge located in Cowley County, Kansas, was used to measure time-dependent deformations. Three of these girders utilized SCC, while the other four were cast with conventional concrete.

Table of Contents

List of Figures

List of Tables

ACKNOWLEDGMENT

I would like to express my deepest and sincere gratitude to Dr. Robert J. Peterman for his advising and guidance. His knowledge and insight for helping with the difficulties that arose along the way and introducing me to the industry of prestressed concrete was much appreciated. Thanks are extended to the Federal Highway Administration and the Kansas Department of Transportation for funding this research. Extended thanks are given to Mr. David Meggers of KDOT for all his help and ideas throughout the project. I would like to thank Dr. Asad Esmaeily for his many contributions to the project and also serving on my committee. I also thank Dr. Stefan Romanoschi and Dr. Kevin Lease for also serving on my committee and Dr. Bruce Law for being the outside committee chair.

Special thinks is given to Prestressed Concrete Inc, of Newton Kansas for all their help on the project. They were always willing to help me out and make "it" happen. I would also like to thank Mr. Tom Bergquist of Prestressed Concrete Inc for helping with all the planning of the test specimens. Thanks are also given to Bridges, Inc of Newton Kansas for working with me while I hooked up all the strain gages onsite.

I would like to acknowledge my fellow graduate students that helped me out along the way: Chris Harker, Bob Harrison, and Mike Stein and all the other faculty (especially Dr. Hayder Rasheed), staff (especially Danita Deters, Angie Fairbanks, Peggy Selvidge, and David Suhling), and undergraduates (especially Logan Benteman and Patrick Sheedy) who helped me complete this research.

Finally I would like to thank Sarah Grotheer for all her help and support throughout the writing of this dissertation.

CHAPTER ONE - INTRODUCTION

Self-consolidating concrete (SCC) has rapidly become a widely used material in the construction industry. SCC is defined as a highly workable concrete that can flow through densely reinforced or geometrically complex structural elements under its own weight, and adequately fill voids without segregation or excessive bleeding without the need for vibration.[1] The workability can be characterized by the following properties.[1]

- Filling ability: the ability of SCC to flow under its own weight into all spaces in the formwork.
- Passing ability: the ability of SCC to flow through openings close to the size of the coarse aggregate without segregation or aggregate blocking.
- Stability: the ability of SCC to remain homogeneous during transport and placing, and after placement.

The "Interim Guidelines for the Use of Self-Consolidating Concrete in PCI Member Plants"[1] recommends that "strand bond tests shall be run with new SCC mixes to verify that the bond with SCC is equivalent or better than a conventional concrete of similar design when using similar strand." These guidelines state that "this can be done using a flexural development length test or by direct load testing." Because SCC does not require any external vibration during placement, some design engineers have expressed concern about its ability to achieve adequate bond with the strand.

At the onset of this research program very few studies had been conducted to evaluate the bond strength between the prestressing strand and SCC. Most of the current research on SCC had been focused on development of SCC mixtures, comparisons of hardened concrete properties of SCC mixtures to conventional (needing vibration)

concrete, and testing methods for evaluation of fresh SCC mixture. As summarized in the literature review (Chapter Two), most studies on bond have been done with conventional concrete (CC) and those done with SCC have highly inconclusive results. In addition to the lack of data about SCC and bond, but also on long-term performance of pretensioned, prestressed bridge girders cast with SCC. This manuscript will address the issues of bond and time-dependent deformations associated with long-term prestress losses for prestressed bridge girders containing SCC.

1.1 Background

The Kansas Department of Transportation (KDOT) would like to use SCC in pretensioned bridge members to enhance the aesthetics and improve consolidation in congested areas. Kansas precasters want to use this type of concrete for a variety of reasons. A drawback with conventional concrete is that, in hard to vibrate areas such as the flange of inverted T-shape members, air is trapped at the surface of the form producing "bug" holes. SCC will help ensure proper consolidation and improve the finish on these surfaces.

However, before allowing the use of SCC in state bridge girders, KDOT wanted to investigate the bond and flexural characteristics of an SCC mixture proposed by the local precaster, Prestressed Concrete Inc, in Newton, Kansas. Prestressed Concrete Inc developed their proposed SCC mixture proportions with the help of their admixture supplier. Because SCC is placed without external vibration, KDOT was concerned that the bond between the SCC and strand may not be as strong as that achieved with a conventional concrete mix. At the onset of this study, information about the transfer and development lengths of prestressing steel in SCC, and the applicability of the American

Concrete Institute (ACI) and American Association of State Highway Transportation Officials (AASHTO) equations to these members were essentially absent from the literature.

Transfer length is the distance required to transfer the fully effective prestressing force from the strand to the concrete. Development length is the bond length required to anchor the strand as it resists external loads on a member.[2] As external loads are applied to a flexural member, the member resists the increased moment demand through increased internal tensile and compressive forces. Increased tension in the strand is achieved through anchorage to the surrounding concrete.[3] Transfer and development length are defined in detail in Chapter Two of this dissertation.

Current American Concrete Institute Building Code Requirements (ACI 318-05)[4] and American Association of State Highway Transportation Officials (AASHTO)[5] design requirements do not specifically address the use of SCC in prestressing applications. The ACI 318 and AASHTO expressions for transfer and development lengths are based on tests performed with conventional concrete (CC) and are as follows:

Transfer length (L_{tr}):

$$L_{tr} = \frac{f_{se}}{3} d_b \qquad (0.1)$$

Development length (L_{dev}):

$$L_{dev} = \left(f_{ps} - \tfrac{2}{3} f_{se} \right) d_b \qquad (0.2)$$

where

d_b = diameter of strand in inches;
f_{se} = effective stress is prestressing strand after allowance of prestress losses (ksi); and
f_{ps} = stress in prestressing strand at calculated ultimate capacity of section (ksi).

The AASHTO[5] specifications require an additional 1.6 multiplier to equation 1.2 for precast, prestressed beams.

The Kansas Department of Transportation (KDOT) funded an initial investigation in which large-block pullout tests[6] (LBPTs) were performed at Kansas State University (KSU), using both the standard concrete recommended by Logan[6] and the proposed SCC mix, Table 1.1. The concrete compressive strength of the Logan mixture was 5,600 psi and 6,800 psi for the SCC mixture. The results with SCC had both lower first-slip and ultimate-load values compared to those values when the Logan concrete was used (Tables A.2 and A.3). A comparison of the values for both the conventional concrete and SCC mixtures are shown in Figure 1.1. Note, Logan[6] recommends that all 0.5-inch strand should have an average minimum pullout capacity of 36 kip, with a maximum coefficient of variation of 10% for a six-sample group. Logan has since added an additional recommendation that the minimum average value of first-observed slip of 0.5-inch strand should be 16 kip. Furthermore, the values with SCC were below the values of 16 kip and 36 kip for first-observed slip and maximum pullout force, respectively. Both of these LBPTs used strand from the same unweathered reel, which had exhibited satisfactory bond performance in flexural beam tests. This strand is referred to as the control strand.

Based on these initial pullout results, it was determined that full-scale, development length girder tests were necessary to further investigate the bond between SCC and the prestressing strand. Thus, KDOT funded an experimental program to evaluate the flexural performance of pretensioned concrete members with the proposed SCC mixture.

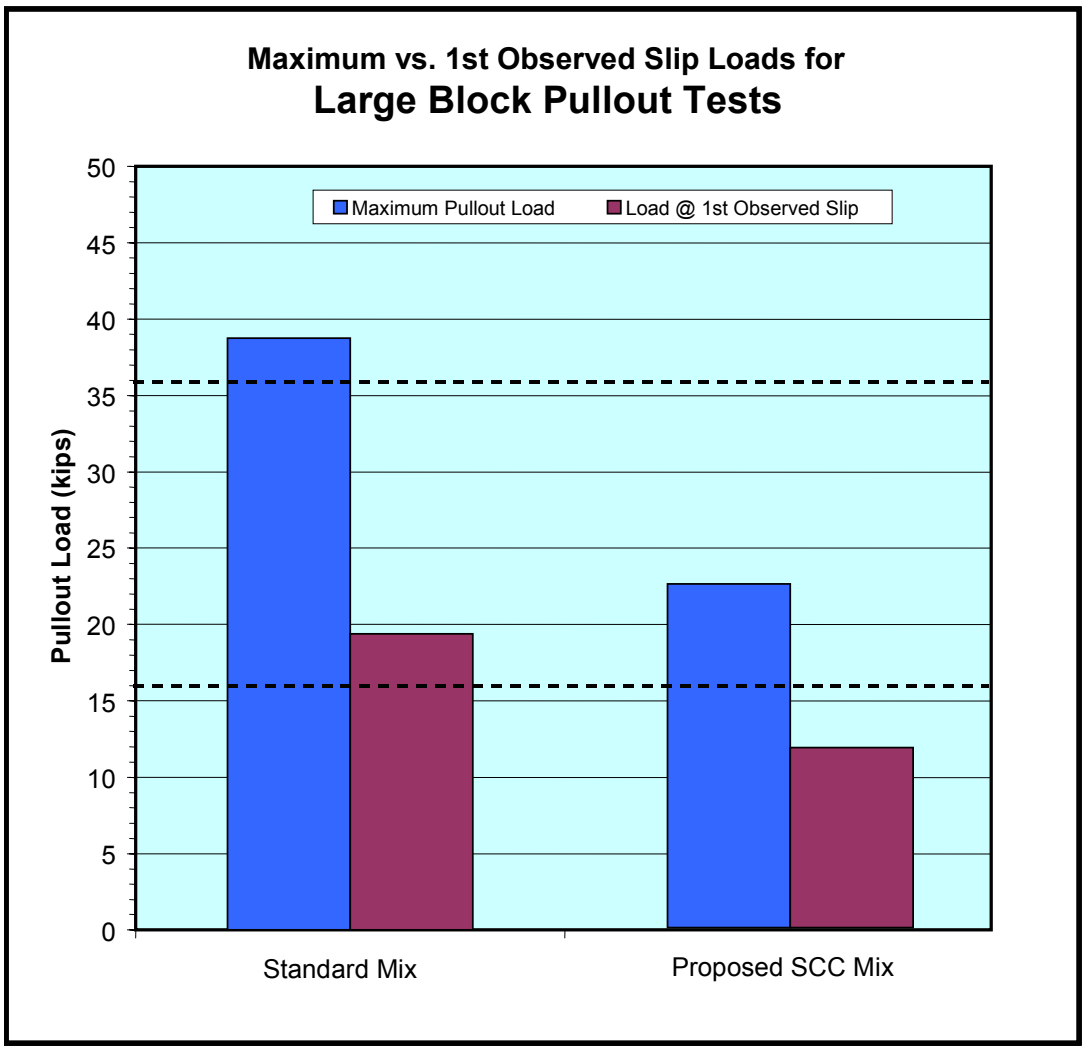

Figure 1.1 Pullout values for conventional concrete versus SCC

Table 1.1 Comparison of Logan and proposed SCC mixture

Materials	Logan	SCC
Cement (Type III)	660 lbs	750 lbs
3/4" Max Limestone	0 lbs	1360 lbs
3/4" Max Crushed Gravel	1900 lbs	0 lbs
Concrete Sand	1100 lbs	1360 lbs
HRWR (ASTM C 494 Type F)	0 oz	70 oz
Normal Range WR (ASTM C 494 Type A)	26 oz	0 oz
Air-entraining agent (ASTM Designation C260)	0 oz	5 oz
Water	35 gal	27 gal

1.2 Test Program

1.2.1 Overview of Experimental Program

Girders were cast with different cross sections and embedment lengths to test the flexural capacities of these different configurations. Single-strand, top-strand, and multiple-strand girders were all cast and tested.

1.2.1.1 Transfer Length

Transfer lengths were estimated for 16 specimens by measuring strand end-slip at each specimen end. The SCC mix design and prestressing strand reel were constant for all specimens, with the primary variables being the number of strands and the location of the strand from the bottom of the specimen.

1.2.1.1 Development Length

A series of development length tests were performed on the flexural specimens that were cast. Specimens were tested with embedment lengths equal to that of development lengths (L_{dev}) predicted by code equations. Specimens with embedment lengths of 80% of L_{dev} were also tested.

1.2.2 Inverted-T-Shape Specimens

Specimens with an Inverted-T (IT) shaped cross-section were cast in order to determine time-dependent deformations. The IT section was chosen because KDOT is beginning to use this section more in their bridges. Elastic shortening, creep, and shrinkage losses were determined from experimental results. In addition, companion

creep-and-shrinkage prisms were cast in order to compare with current ACI code recommendations.

1.2.3 Cowley County Bridge

Thirty-five bridge girders were cast and placed in the field to analyze combined creep and shrinkage effects of SCC. Of these 35 girders, 14 were cast with SCC and the remaining 21 with conventional concrete. Vibrating wire strain gages were embedded in seven of the girders to record these time-dependent deformations. The bridge is located in Cowley County, approximately five miles west of Winfield, Kansas, on US Highway 160.

1.3 Scope

Chapter Two presents a literature review of past research completed and defines key terms.

Chapter Three addresses different types of girders used in the flexural specimen test program.

Chapter Four discusses material properties of prestressing strand and concrete, along with different test methods used to evaluate fresh concrete properties.

Chapter Five presents methods for measuring transfer length in the development length girders and inverted-T-shape specimens.

Chapter Six shows fabrication, loading conditions, and test setup configurations for the flexural specimens.

Chapter Seven presents transfer and development length results of the flexural specimens.

Chapter Eight gives the properties of the inverted-T-shape section used for determining creep and shrinkage properties.

Chapter Nine shows results yielded from the inverted-T-shape section. These results include both transfer length and prestress losses.

Chapter Ten presents the setup for the creep-and-shrinkage prisms, along with code equations.

Chapter Eleven gives results for the creep-and-shrinkage prisms, along with comparisons with ACI 209 design recommendations.

Chapter Twelve shows fabrication of the girders used for the bridge that was instrumented with strain gages, along with the erection process of the bridge.

Chapter Thirteen presents prestress loss results of the girders from the bridge that was instrumented.

Chapter Fourteen presents conclusions and recommendations resulting from this project.

CHAPTER TWO - BACKGROUND & LITERATURE REVIEW

2.1 Prestressed Concrete

2.1.1 Concepts

Prestressing can be defined as the preloading of a structure, before the application of service loads, so as to improve its performance in specific ways.[7] Concrete is widely regarded as a compression material. The idea of prestressing is to take full advantage of this material property. The original concept of prestressing concrete was to introduce sufficient axial precompression in beams so that all tension in the concrete was eliminated at service load[7]. The following equation is used to analyze stresses in the prestressed member:

$$f_c = \frac{P}{A} \mp \frac{P \cdot e \cdot y}{I} \pm \frac{M \cdot y}{I} \tag{1.1}$$

where

f_c = stress at a given point;
P = prestressing force;
e = eccentricity (distance from the geometric centroid of the beam to geometric centroid of the steel);
I = moment of inertia;
y = distance from centroid of the cross section to the point in question; and
M = moment due to applied external loads.

There are two common methods to prestress concrete: pretensioning and post-tensioning. For the purpose of this research, only pretensioned concrete members will be examined. The general process of pretensioning has the following characteristics:

- Uses a bed.

- Strand is tensioned first.
- Concrete is cast around the strand.
- Strand is cut after a time period allowing the concrete to harden, transferring prestressing force by bond.
- Some prestressing force is lost because the concrete shortens elastically under released prestressing load and the strand shortens along with it.

Prestressed concrete is heavily dependent on the bond between prestressing strands and concrete. This bond is thoroughly investigated in this study.

2.1.2 Definitions

In this section, transfer length, development length, and embedment length are defined. A list of other terms used throughout this manuscript are shown in the Notations section.

Transfer length (L_{tr}) is the distance required to transfer the fully effective prestressing force from the strand to the concrete. In other words, transfer length is the length of bond between the free end of the strand, where there is zero stress, to the point where the prestressing force is fully effective. Strand tension increases due to bond stresses that restrain or hold back the strand. The idealized stress in the prestressing strand along the length of the specimen is shown in Figure 2.1, where both transfer length and development length regions are labeled. This diagram is the ACI assumed variation of steel stress.

Development length (L_{dev}) is defined as the bond length required to anchor the strand as it resists external loads on the member. In the case where the bonded length

exceeds the development length, while the member is under external loads, then strand tension has adequately developed and bond length is sufficient. However, if the bonded length of the strand is less than the development length, then strand slip occurs throughout the concrete while under the influence of external loads.

Embedment length (L_e) is defined as the length of bond from the critical section to the beginning of bond. The critical section is located where the steel stress is at its maximum point, usually the point of maximum moment. The beginning of bond usually occurs at the end of a fully bonded member. In order to prevent bond failure, embedment length must be equal to or greater than development length.

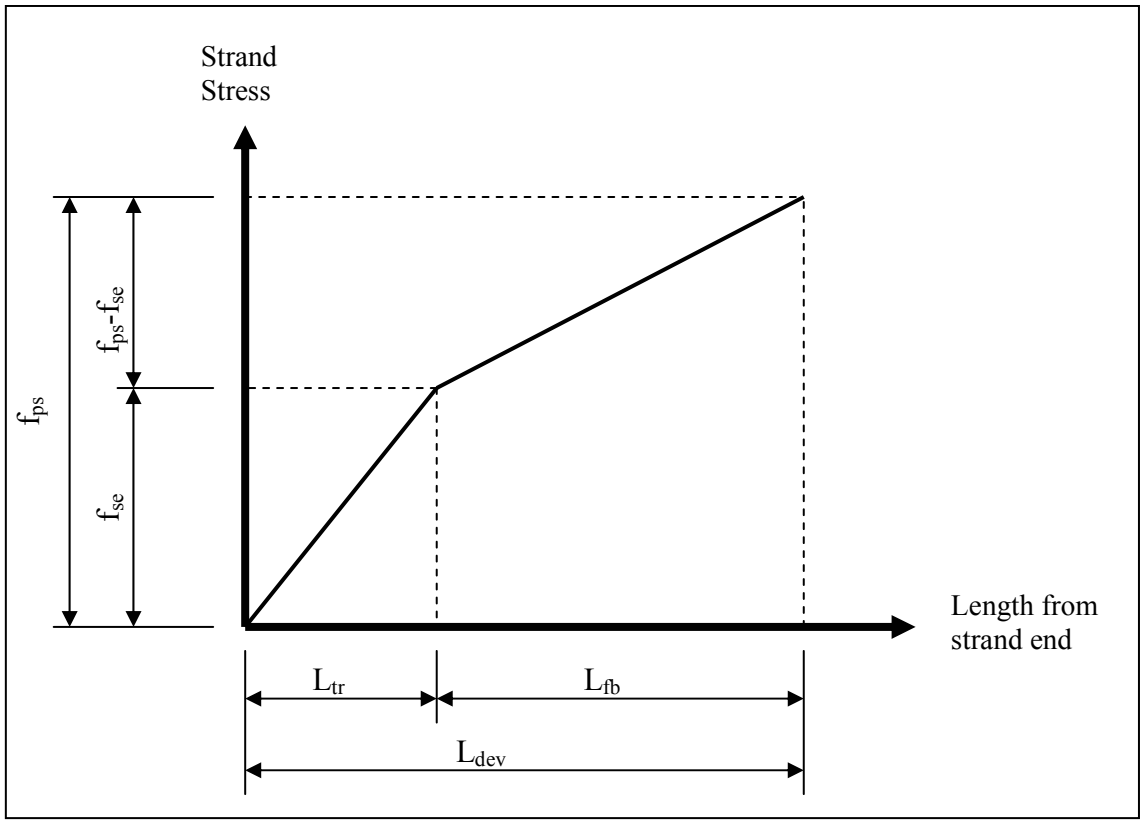

Figure 2.1 ACI variation of steel stress with distance from free end[4]

2.1.3 Prestress Loss Equations

ACI 318,[4] AASHTO LRFD Bridge Design Specifications,[5] KDOT,[8] and The PCI Design Handbook[9] all have slight differences in determining losses of prestressed members. Each method is detailed in section A.2. The ACI 209 Committee[10] procedure for determining prestress losses is also shown. This method uses creep coefficient and shrinkage strains resulting from laboratory tests.

2.2 Self-Consolidating Concrete

Self-consolidating concrete was first developed in Japan in the mid-1980s. Ouchi (2001)[11] reports that durability of concrete structures was a major topic of interest in Japan. One of the key components of making durable concrete is to have proper compaction. However, getting this proper compaction was becoming a major concern because the number of skilled workers in Japan was declining, thus leading to the deficient structures. A solution to this lack of proper compaction by skilled workers was to develop a concrete that could be compacted into every corner of formwork purely by means of its own self-weight and without the need for vibrating compaction.

SCC gets its flowable properties from admixtures that are added to the concrete. Bury and Christensen (2003)[12] describe how the admixtures give the concrete its fluid characteristics. The high-range water-reducing (HRWR) admixtures, as defined by ASTM C494, allow the concrete to remain stable during and after placement, along with a high degree of workability. HRWR admixtures allow improved cement dispersion over older, water-reducing admixtures. According to Bury and Christensen HRWR admixtures impart a negative charge on the cement particles, causing them to repel from

one another. In addition, admixtures have side chains of varying lengths, which are engineered to be part of the backbone of the molecule and help keep the cement particles apart. This allows more water to surround more surface area of the cement particles. The dual action of the admixtures allows for improved cement dispersion, more complete hydration of the cement, and improved workability.[12]

Ouchi et al. (2003)[13] completed a study in which applications of SCC in Japan, Europe and the United States were examined. Japan has been using SCC in large quantities since the early 1990's and within the last 6-8 years Europe has constructed a number of bridges with SCC while the main use of SCC in the U.S. is still mainly for architectural concrete. One of the major differences between the SCC being produced in Japan and Europe as compared to the SCC produced in the U.S. is the improved bond quantity of the SCC in Japan and Europe. Ouchi et al. report that in general the SCC bond strength when expressed in terms of compressive strengths are higher with SCC than with conventional concrete.

2.3 Elements of Bond

This section details the past research that has been completed on the subject of bond (transfer and development length) between prestressing strand and concrete. Most of the research has been completed with conventional concrete, as only recently has SCC been used in prestressed concrete members.

Janney (1954)[14] completed one of the first studies of bond in pretensioned, prestressed concrete girders. Prismatic specimens were used to study the bond near the end of the prestressed member. Beam specimens were also used to study flexural bond

and the interrelation between flexural bond and the resulting bond from the transfer of prestress. Several variables were considered, which included strand diameter and surface condition. The study was set out to answer the following questions:

- To what extent does wire diameter influence transfer of pretension from steel to concrete?
- How are prestress transfer bond properties of wire and strand influenced by surface conditions?
- What is the effect of concrete strength on the transfer of stress from pretensioned steel to concrete?

Janney concluded that strand diameter size used in the study will result in sufficient strength through bond. Also, the transfer bond is a large function of the friction between the concrete and steel. The author noted that results were only taken after release and did not take into account the effect of time, fatigue, and impact.

Hanson and Kaar (1959)[15] carried out an investigation of flexural bond on 47 prestressed beams. The principal factor investigated was variation of strand embedment length with different strand diameters. Strand surface condition, reinforcement percentage, and reduction in concrete strength were also investigated in a limited manner. It was found that strand with a rusted surface condition did exhibit better bond. The following design guidelines were proposed:

- Calculate steel stress at ultimate flexural strength, assuming that no general bond slip occurs.
- Check embedment length of strand, that is, the distance from the free end of the strand to the section of maximum steel stress.

- From given charts, determine maximum steel stress that can be developed in the embedment length provided for the chosen size of strand.

Kaar et al. (1963)[16] investigated the influence of concrete strength on transfer length at the time of release over a one-year period. Rectangular, concentrically prestressed members fabricated with different concrete strengths and strand diameters were used in this investigation. Surface strains measured by a Whittemore gage, were used to determine transfer lengths of each specimen. Immediately before transfer, and then at 1, 3, 7, 14, 28, 56, 90, 180, and 365 days, readings were taken. The authors concluded that

- concrete strengths at transfer of prestress had little influence on the transfer lengths;
- for specimens using strand up to 0.5-inch in diameter, transfer lengths measured adjacent to the flame-cutting end were approximately 20 percent greater than transfer length at the opposite end;
- for 0.6-inch-diameter strands, transfer length increase was 30 percent;
- average increase in transfer length over a period of one year following prestress transfer was 6 percent; and
- increase in transfer length with time was independent of concrete strength at the time of transfer.

Janney (1963)[17] evaluated stress-transfer characteristics of a new type of prestressing strand that had a higher minimum breaking strength than previously used strand. Six specimens were cast and tested. Two were prestressed with conventional 0.5-inch-diameter clean and bright strand. Two other specimens were prestressed with 0.5-

inch-diameter clean and bright high strength strand. Finally, the remaining two specimens were prestressed with 0.5-inch-diameter, high-strength strand with a medium coat of rust over the surface. The test specimens were 3.5 inches (*H*) by 4.25 inches (*B*) and eight feet in length. Each member was prestressed with a single prestressing strand located at the centroid. Mechanical gage points were mounted on the concrete surface, and resulting compressive strains were used in determining transfer lengths. Results yielded a slightly greater transfer length for the specimens with high-strength strand. However, the author argues that this slight increase should not be significant from a design standpoint.

Kaar and Hanson (1975)[18] completed a study in which 108 pretensioned concrete beams were tested under cyclic loading, simulating the loads sustained by a railroad crosstie. Repeated loads were applied to one of the four selected locations near the end of the beam. The load used was one that would open the crack 0.001 inches or 15% greater than the crack-opening load. Different surface conditions of strand and release of prestress were also evaluated. The authors concluded that the load cannot be applied nearer than 2.2 times the strand transfer length for smooth 3/8-inch diameter strand to obtain a bond-fatigue life of more than 3 million cycles. The authors also concluded that these railroad ties should be constructed with short transfer lengths and to decrease transfer lengths, the strand should be roughened without reducing its diameter.

Martin and Scott (1976)[19] presented equations for designing precast, pretensioned members for spans too short to provide an embedment length enough to develop the full strength of the strand. Test results obtained from Hanson and Kaar (1959)[14] were used in developing their equations. For embedment lengths less than $80d_b$

$$f_{ps} \le \frac{l_e}{80 d_b}\left(\frac{135}{d_b^{1/6}} + 31\right) \tag{1.2}$$

and for embedment lengths greater that $80d_b$

$$f_{ps} \le \frac{135}{d_b^{1/6}} + \frac{0.39 l_e}{d_b} \tag{1.3}$$

where

f_{ps} = stress in prestressing strand at calculated ultimate capacity of section (ksi);
d_b = diameter of strand in inches;
l_e = embedment length in inches.

Also, f_{ps} shall not be greater than the results given by strain compatibility.

The investigation conducted by Zia and Mostafa (1977)[20] centered on developing new equations for both transfer and development lengths. Previous research found that transfer length can be affected by a large number of parameters including

- type of steel (wire or strand)
- steel size (diameter)
- steel stress level
- surface condition of steel (clean, oiled, rusted)
- concrete strength
- type of loading (static, repeated, impact)
- type of release (gradual, sudden (flame cutting, saw-cutting))
- confining reinforcement around steel (helix or stirrups)
- time-dependent effect
- consolidation and consistency of concrete around steel
- amount of concrete coverage around steel

After analyzing all transfer length results that were tabulated, the authors came up with new equations for both transfer and development length.

$$L_t = 1.5\frac{f_{si}}{f_{ci}^{'}}d_b - 4.6 \tag{1.4}$$

$$L_{dev} = 1.5\frac{f_{si}}{f_{ci}^{'}}d_b - 4.6 + 1.25\left(f_{su} - f_{se}\right)d_b \tag{1.5}$$

The equation for transfer length is applicable for concrete strength ranging between 2,000 and 8,000 psi. This expression formulated by the authors takes into account the effect of strand size, initial prestress, and concrete strength at release. In addition, the equations are conservative from the actual lengths that were observed and would make a suitable transfer length for the ACI expression.

Cousins et al. (1990)[21] present development of analytical equations for transfer length and flexural bond lengths for prestressed members. Experimental results gathered from previous work were used in deriving these equations. The suggested equation for transfer length is

$$L_t = 0.5\left(\frac{U_t^{'}\sqrt{f_{ci}^{'}}}{B}\right) + \frac{f_{se}A_s}{\pi d U_t^{'}\sqrt{f_{ci}^{'}}} \tag{1.6}$$

where recommended values of $U_t^{'}$ are 6.7 for uncoated strand, 10.6 for coated strand with low grit, and 16.5 for strand coated with medium to high grit. The value of *B*, the bond modulus, had an average value of 300 psi/in and used for equation 2.6. The equation for flexural bond lengths was suggested as

$$L_{fb} = \left(f_{ps} - f_{se}\right)\left(\frac{A_s/\pi d}{U_d^{'}\sqrt{f_c^{'}}}\right) \tag{1.7}$$

where the recommended values of $U_d^{'}$ are 1.32 for uncoated strand, 6.40 for coated strand with medium to high density of grit, and 4.55 for coated strand with low-density grit. Finally, the development length is just the sum of the proposed equations for transfer and flexural bond length ($L_t + L_{fb}$).

Cousins et al. (1992)[22] present a method for evaluating the bond of prestressing strand to concrete. The purpose of this research was to develop a standard test for determining bonding characteristics of prestressing strand to concrete and to correlate the test to transfer length. An experimental program was conducted to compare transfer lengths of the proposed test to a direct tension pullout test. The authors concluded that the proposed standard test was simple and easy to perform. Plus, test results were very similar to those obtained from direct tension pullout tests.

Shahawy et al. (1992)[23] conducted an investigation in which full-scale pretensioned AASHTO girders were examined for transfer length. Different prestressing strand diameter sizes were used. Concrete surface strains were used in determining the transfer length of each girder. Results showed that ACI/AASHTO predictions for transfer length were inadequate. The authors showed that if f_{si} was used instead of f_{se}, a much better comparison between experimental transfer length and results from using code expressions exist. They recommend this change be made for the ACI/AASHTO expression for transfer length.

Mitchell et al. (1993)[24] cast 22 pretensioned concrete beam specimens to determine the influence of concrete strength on transfer and development lengths. The two main variables in this study were concrete strength and strand diameter. Concrete compressive strengths varied from 3,050 to 7,250 psi at transfer to 4,500 to 12,900 psi at

time of testing. Strand diameters used in the specimens were 0.375 inches, 0.5 inches, and 0.62 inches. Concrete surface strains were used to assess transfer lengths. Strain measurements were taken before release, just after release, and just prior to testing. Test results showed that an increase in concrete strength gives smaller transfer lengths. The following equation for transfer length was derived from the experimental data:

$$L_t = 0.33 f_{pi} d_b \sqrt{\frac{3}{f'_{ci}}} \tag{1.8}$$

The following equation for development length was derived:

$$L_{dev} = 0.33 f_{pi} d_b \sqrt{\frac{3}{f'_{ci}}} + \left(f_{ps} - f_{se} \right) d_b \sqrt{\frac{4.5}{f'_c}} \tag{1.9}$$

Alternatively a simpler, more conservative expression for transfer length was also recommended:

$$L_t = 50 d_b \sqrt{\frac{3}{f'_{ci}}} \tag{1.10}$$

This expression can be conservatively used in checking stresses but should not be used to calculate the transfer length component of the development length.

Buckner (1995)[25] summarizes FHWA's independent review of design recommendations for transfer and development length. The objectives of the study were to

- conduct a review of literature related to strand transfer and development length research;
- analyze data from recent studies and rationalize discrepancies among conclusions drawn from those studies; and

- recommend equations for strand transfer and development length consistent with current practices.

The author recommends the following equation be used for transfer length:

$$L_t = \frac{f_{si} d_b}{3} \tag{1.11}$$

Also, for strands either straight or draped that have more than 12 inches of concrete cast beneath the strand, transfer length should be multiplied by 1.3. These recommendations apply only to Grade 270, seven-wire, low-relaxation uncoated strand used in pretensioned members with normal-weight concrete having compressive strengths at release of 3,500 psi or higher. The study also recommends a conservative expression for development length:

$$L_{dev} = \frac{f_{si} d_b}{3} + \lambda\left(f_{ps} - f_{se}\right) d_b \tag{1.12}$$

where for general application, the multiplier λ is taken as ($0.6+40\varepsilon_{ps}$). For λ, it shall be taken greater than or equal to 1.0 and less than or equal to 2.0. As was the case in the transfer length expression, if more than 12 inches of concrete is below the strand, the development length expression should be multiplied by 1.3.

Martin and Korkosz (1995)[26] present a strain compatibility method for calculating nominal flexural capacity for sections in which the strand is not completely developed. This is critical at the ends of members where strands may be debonded to reduce release stresses. The authors contend that in short-span members, the prestressing strand may not be fully developed at sections of high moment and this could cause a premature failure. Equations are presented in which concrete strains are used in determining the nominal flexural capacity. They also recommend that the strength-reduction factor of $\phi =$

0.85 be applied to the calculated nominal-moment strength, when the failure end point is strand slip.

Russell and Burns (1996)[27] conducted a study in which transfer lengths were measured and compared to the current AASHTO and ACI code provisions. A wide variety of research variables were used in conducting this research, including

- number of strands (1, 3, 4, 5, and 8),
- size of strand (0.5 and 0.6 inch diameter),
- debonding (fully bonded or debonded strands),
- confining reinforcement (with or without), and
- size and shape of the cross section.

A total of 44 specimens were tested and transfer lengths were measured on both ends of the specimens. Transfer lengths were measured using concrete surface strains along the length of each specimen. End slips and use of electrical-resistance strain gages were also used in determining transfer lengths. Resulting data confirms the current code expressions that transfer length varies proportionately with strand diameter. It was also found that transfer length is not a linear, but rather that transfer length is an exponential function of strand diameter. Another relationship found in this study was that test specimens with a larger cross sections and multiple strands possess significantly shorter transfer lengths. Strand end slips were also used to find a correlation between end slip and transfer length. The equation

$$L_t = 294.4 L_{es} \tag{1.13}$$

where

L_{es} = measured end slip (inch)

was derived from the data by performing a regressional analysis. The reported correlation of $r = 0.717$ indicates that a good correlation exists between transfer length and strand-end slip. It was also found that confining reinforcement had little or no effect in lessening transfer lengths. A safe expression for transfer length was derived:

$$L_t = \frac{f_{se} d_b}{2} \tag{1.14}$$

This expression is proposed to be used in all design considerations.

Rose and Russell (1997)[28] sought to evaluate three different bond-performance tests and their potential to predict bond characteristics. Simple pullout tests, tensioned pullout tests, and measured strand-end slips were compared to companion transfer lengths with varying surface conditions. It was concluded that strand-end slips provide a reliable indication of transfer length. It was found that the theoretically derived expression

$$L_t = 2L_{es}\left(\frac{E_{ps}}{f_{st}}\right) \tag{1.15}$$

can reliably predict transfer length. The research demonstrates that strand end slip is the most reliable assessment of bond performance when compared to simple and tensioned pullout tests. Use of strand end slip was found to be independent of strand surface conditions. They found that a roughened surface enhances bond, whereas a lubricated surface hinders bond performance. Also it was noted that transfer lengths can increase as much as 60 percent when adjacent to flame cutting.

Logan (1997)[6] wrote an extensive paper on the acceptance criteria for bond quality for prestressed concrete applications. This paper also addressed the procedure for performing large-block pullout tests and requirements for these tests. For this study, prestressing strand was collected from a wide variety of places throughout the country to

evaluate strand-bond performance. More than 200 tests were conducted on specimens that included large-block pullout tests, end slip at release and 21 days, and development length tests. The author concluded that the large-block pullout tests are an accurate predictor of general transfer and development length characteristics of the strand in prestressed concrete applications. The author also concluded, that based on the results of the large-block pullout tests, one can determine if the transfer and development length equations predicted by ACI will pass. It was also concluded that there are high-bond quality and poor-bond quality strands in the marketplace. Initial end-slip measurements do not detect poor-bonding strand; however, end-slip values at 21 days do provide a warning of potential bond problems. Residue that comes off during a wipe test provides no indication of subsequent bond performance.

Lane (1998)[29] introduce new development and transfer length equations after a long study performed by the Federal Highway Administration (FHWA). The research was brought on by a 1988 Memorandum issued by the FHWA which disallowed the use of 0.6 inch diameter strands in pretensioned applications, restricted the minimum center-to-center strand spacing to four times the nominal diameter of the strand, and increased the required development length for fully-bonded and debonded strands by 1.6 and 2.0 times AASHTO Equations 9.32 (Equations 1.1 and 1.2 in this dissertation). The memorandum was only a interim measure until further research could be conducted and AASHTO adopted the new regulations. In 1996 the memorandum was changed due to the results of new research and the use of 0.6 inch diameter strand was allowed and the spacing of strands was returned to their original values. During this time the FHWA also conducted a study to evaluate and introduce a new equation for both development and

transfer length. The study consisted of measuring the development and transfer length of different prestressed members. After analyzing their experimental results and reviewing the work of many others, the FHWA produced the following equations for transfer and development length and that a 1.3 multiplier be applied for any strand (straight or draped) in any member that has 12 inches or more of concrete cast below the strand.

$$L_t = \frac{4 f_{pt} D}{f_c'} - 5$$

$$L_d = \left[\frac{4 f_{pt} D}{f_c'} - 5 \right] + \left[\frac{6.4 \left(f_{su}^* - f_{se} \right) D}{f_c'} + 15 \right]$$

where

f_{pt} = stress in prestressing strand prior to transfer of prestress (ksi);
D = nominal diameter of prestressing strand (inch);
f'_c = concrete compressive strength at 28 days (ksi);
f^*_{su} = average stress in prestressed reinforcement at ultimate load (ksi); and
f_{se} = effective stress in prestressed reinforcement after all losses (ksi).

Peterman et al. (2000)[3] conducted a study in which 18 development length tests were carried out on single-strand, rectangular and multiple-strand, T-shaped specimens. Concrete used in this study was semi-lightweight. Transfer lengths of the specimens tested were also conducted by measuring concrete surface strains. Results from transfer lengths yielded values that were less than AASHTO and ACI code provisions for shear, except in one case where splitting of concrete was noted. In rectangular beam tests, all specimens exceeded their design-moment capacities. However, in the T-beams, bond failures at loads below the design capacity occurred in some of the specimens. Failure occurred due to a flexure-shear crack near the loading point. The authors then conducted further tests and recommended that current AASHTO and ACI requirements for strand-development length be enforced at a critical section located a distance d_p from the point

of maximum moment towards the free end of the strand. An alternative solution was noted that the designer may elect to provide enough transverse reinforcement to minimize the shift in tensile demand that will occur in the event of diagonal cracking.

Steinberg et al. (2001)[30] conducted an experimental study in which concrete strains of three pretensioned concrete beams were monitored. The strains were evaluated through use of electrical-resistance strain gages embedded in the beam and surface mounted to the beams. Transfer lengths were determined by concrete strains and by strand end slip. The researchers concluded that the manual method (concrete surface strains) provided comparable values to the end-slip method. Results also showed that longitudinal tensile strains existed near the end of the beams prior to cutting all the strands. These strains were large enough to cause cracking, which was not visible after release of all the strands.

Oh et al. (2001)[31] completed a comprehensive experimental program in which they compared current ACI design code for transfer length against experimental results. Major variables focused on were strand diameter, concrete strength, concrete cover size and strand spacing. Their results showed that as transfer length decreases with an increase in concrete strength, it also decreases with an increase in concrete cover. Transfer lengths were determined using both concrete surface strains and strand end slip. It was found that a good correlation exists between measuring transfer lengths by strand end slip and concrete surface strains. The author concluded the following:

- The current ACI code equation for transfer length overestimates actual measured transfer lengths.

- Transfer length increases with an increase in strand diameter; however, the ACI code expression assumes this relationship to be linear and experimental results do not support this.
- Transfer lengths tend to increase slightly with time due to creep effects and the increase of transfer length is about 5% at 90 days after prestress transfer.
- The ACI code expression for transfer length should include concrete strength and concrete cover size.

Barnes et al. (2003)[32] conducted a study on 36 full-scale, development length girders. Girders cast each had a unique strand surface condition and concrete strength. Since some of the specimens had debonding of the strands, a total of 184 zones were used in determining transfer lengths. Unlike some previous studies, this one consisted of 0.6-inch-diameter prestrssing stand. Strand surface condition was a major component of this study, so for half of the specimens, the strand used had a bright surface condition and the other half were prestressed with rusted strand. Strand surface condition did not play a major role in increased transfer lengths over time. A mechanical strain gage was used to determine surface strains along both sides of the specimens and from this data, transfer lengths were obtained. It was found that transfer lengths increase approximately 10 to 20% over time. Almost all the increase occurred within the first 28 days after release. Average transfer length of the rusted strands was shorter than those of bright strands. However, it was found that the transfer lengths of rusted strands did see a much greater scatter in data than that of the bright strands. The method of prestress release did not affect transfer lengths of the bright strands; however, a sudden release with the rusted

strand did see a 30 to 50% increase in transfer length. The authors concluded that the expression

$$L_t = 0.17\,ksi^{-0.5}\left(f_{pt}\Big/\sqrt{f'_{ci}}\right)d_b \tag{1.16}$$

provides a lower bound for long-term transfer lengths measured in this study.

Khayat et al. (2003)[33] studied bond strength of prestressing strands in wall elements. The strands were placed in the horizontal position and at different heights, and the pullout tests were performed on the strand. Four SCC and two conventional concrete mixtures were used for this study. Different types of curing methods were used on the concrete wall. The following conclusions were made:

- A top-bar effect did exist; however, it was different depending on the method of curing. The top-bar effect was greater for those mixtures cured by steam.
- Overall, the strand bond was not comprised in a stable SCC mixture.
- The top-bar effect is shown to be sensitive to the type of VMA used.
- For all mixtures, the top-bar effect in air-cured concrete was lower than stream-cured concrete.

Girgis and Tuan (2005)[34] performed Moustafa pullout tests with SCC to determine bond strength. In addition, the transfer length of three pretensioned concrete bridge girders was measured. Three concrete mixtures were used in this study, two SCC and one conventional. The authors found that maximum pullout value was larger for the SCC mixture than the conventional concrete mixture. However, transfer lengths were greater for the girders utilizing SCC. It was concluded that

- Use of a viscosity-modifying admixture may adversely affect early compressive strengths and bond strength of the SCC, which will lead to greater transfer lengths;
- SCC mixtures experience higher transfer lengths than mixtures with conventional concrete;
- Moustafa pullout tests failed to reveal any early-age bond-strength reduction when using SCC;
- SCC had higher bond strength at 28 days, which may warrant shorter development lengths for girders with SCC; and
- Both SCC and conventional concrete in the pullout tests, the smaller the deformed bar, the higher the bond strength.

Burgueno and Haq (2005)[35] evaluated transfer and development lengths of prestressed girders using both SCC and conventional concrete mixtures. Transfer lengths were determined by strand draw-in and concrete surface strains, while development lengths were obtained through flexural tests. The authors found that the ACI expression for transfer length was conservative for both SCC and conventional concrete mixtures. However, development lengths for the SCC mixtures were slightly larger than that predicted by code equations.

The 2005 "European Guidelines for Self-Compacting Concrete"[36] state that no special provisions should be used for transfer and development length when using SCC. Studies have shown that the transfer length for strands embedded in SCC were on the safe side when compared with calculated values according to their current code

equations. Plus, a "top-strand" effect was not seen in members with SCC due to the fact that SCCs fluidity and cohesion minimize the negative effect of bleed water.

2.4 Current Development and Transfer Length Equations

Tabatabai and Dickson (1993)[37] conducted a research study to determine the history behind strand development and transfer length equations. It was found that the current transfer length (equation 1.1) dates back to 1963 and was derived using data from the Portland Cement Association. It states that three factors affect bond; adhesion between concrete and steel, friction between concrete and steel and mechanical resistance between concrete and steel. An average transfer bond stress of 400 psi was used in determining the equation, but it is not clear as to where that number originated. The current equation for development length (equation 1.2) was first introduced in the 1963 ACI Building Code. The equation was based on published reports by Hanson and Kaar (1959) along with the work of Kaar et al(1963). However, those two reports do not propose equations for development length. It was also determined that Alan H. Mattock, who worked for the Portland Cement Association, was involved with proposing the current equations for both transfer and development length.

2.5 Bridge Monitoring

Detailed below are a few other projects that used vibrating-wire strain gages to monitor long-term strains in prestressed bridge girders. It must be noted that all of the projects used high-performance concrete, not SCC. At the time of this study, no literature on the monitoring of bridge girders with SCC could be found.

Ahlborn et al. (2000)[38] investigated long-term prestress losses of two long-span, high-strength composite prestressed bridge girders in the state of Minnesota. They also determined the adequacy of AASHTO provisions for design. Vibrating-wire strain gages were embedded into the concrete to account for losses after the time of strand release. The authors believed the gages could not account for losses in the prestressing strand before the concrete hardened. They calculated total prestress losses from flexural cracking and crack-reopening loads. Losses that occurred before release were then back-calculated by taking total prestress losses and subtracting losses after release. The authors concluded the AASHTO design method overestimated the concrete modulus, leading to lower initial losses. Plus, the AASHTO design equations overpredicted creep and shrinkage losses, thus leading to higher long-term losses. They recommended great caution be used when using AASHTO design guidelines with high-strength concrete.

Barr et al. (2000)[39] presented results of using high-performance concrete in prestressed, precast concrete bridge girders in the state of Washington. Vibrating wire-strain gages were embedded into the girders to measure temperature and long-term strains. From this data, a comparison with current design equations could be made. The authors concluded that by using high-performance concrete, engineers could reduce the number of girder lines used in a bridge. They also found that prestress losses were higher with girders using high-performance concrete than those girders using conventional concrete.

Ramakrishnan and Sigl (2001)[40] instrumented two, three-span high-performance concrete bridges in the state of South Dakota. For the project, trial concrete mixes were first tested and the mixture that resulted in the best performance was used in the bridge

girders. The girders that were instrumented had vibrating wire transducers embedded into them. It was found that prestress losses were slightly larger than those predicted by code equations. The authors also recommend the concrete mixture be used for all state girders utilizing high-performance concrete. Also, a change for the calculation for modulus of elasticity of the concrete was also recommended.

Onyemelukwe et al. (2003)[41] embedded vibrating wire-strain gages into an actual prestressed bridge in the state of Florida to examine time-dependent losses. They discuss the monitoring process and techniques used throughout their study. The authors compared experimental data with code estimates of PCI and AASHTO. It was determined that code estimates gave very close predications to actual experimental data. They also concluded that the methods used to instrument the bridge were very satisfactory.

Yang and Myers (2005)[42] reported prestress losses observed for the first two years of the first high-performance superstructure concrete bridge in the state of Missouri. The authors compared the recorded losses to eight commonly used models for predicting prestress losses. Standard AASHTO Type-II girders were instrumented with vibrating wire-strain gages to obtain long-term losses. In all, 20 girders were used for the bridge, with four of those being instrumented. It was found that the girders behaved as expected and code equations used to predict prestress losses were fairly accurate.

CHAPTER THREE - DESIGN OF FLEXURAL SPECIMENS

Three separate cross sections were tested to evaluate current development length equations. The single strand specimens had identical cross sectional properties at the critical section tested in flexure (mid-span); however, at the specimen ends the cross sections were different in order to test the "top-strand" effect. Table 3.1 summarizes the three different specimens tested. More detail for each specimen type is given below.

Table 3.1 Properties of different cross sections

Specimen	Overall Height* (inch)	Depth to Strand* (inch)	Number of Strands
SSB	12	10	1
TSB	24	2	1
TB	21	19	5

* dimension at specimen end, not critical section at mid-span

3.1 Single-Strand Development Length Specimens

Twelve, single-strand, development length specimens with two different embedment lengths were fabricated and tested. However, due to a handling error with one of the specimens, only 11 were tested to failure. In addition, these specimens utilized two different cross sections in order to evaluate the so-called "top-strand" effect, where 12 inches or more of concrete is cast below the strand. ACI requires a 1.3 multiplier on development length on deformed bars for "horizontal reinforcement so placed that more than 12 in. of fresh concrete is cast in the member below the development length or splice."[4] AASHTO uses a similar 1.3 multiplier for strand development length when using an alternate development length equation in section 5.11.4.2.[5]

The first cross section cast was an 8-inch x 12-inch rectangular section. The nomenclature used for these specimens was **s**ingle-**s**trand **b**eams (SSB). The section contained a single prestressing strand at a depth d_p of 10 inches (Figure 3.1). This section was chosen slightly larger than the 6.5-inch wide specimen tested by Logan[6] in order to provide increased shear capacity. This was desirable because these specimens did not have any shear reinforcement (see A.3 for shear-capacity calculations). The strain in the strand at nominal flexural capacity (see A.4 for sample calculations) was estimated to be 2.94%, using strain compatibility analysis. This value is lower than the 3.5% recommended by Buckner[24] for minimum strand strains in development length specimens. However, it is larger than the 2.0% value calculated by Logan[6] for single-strand beams tested in his investigation and failed in flexure by strand rupture.

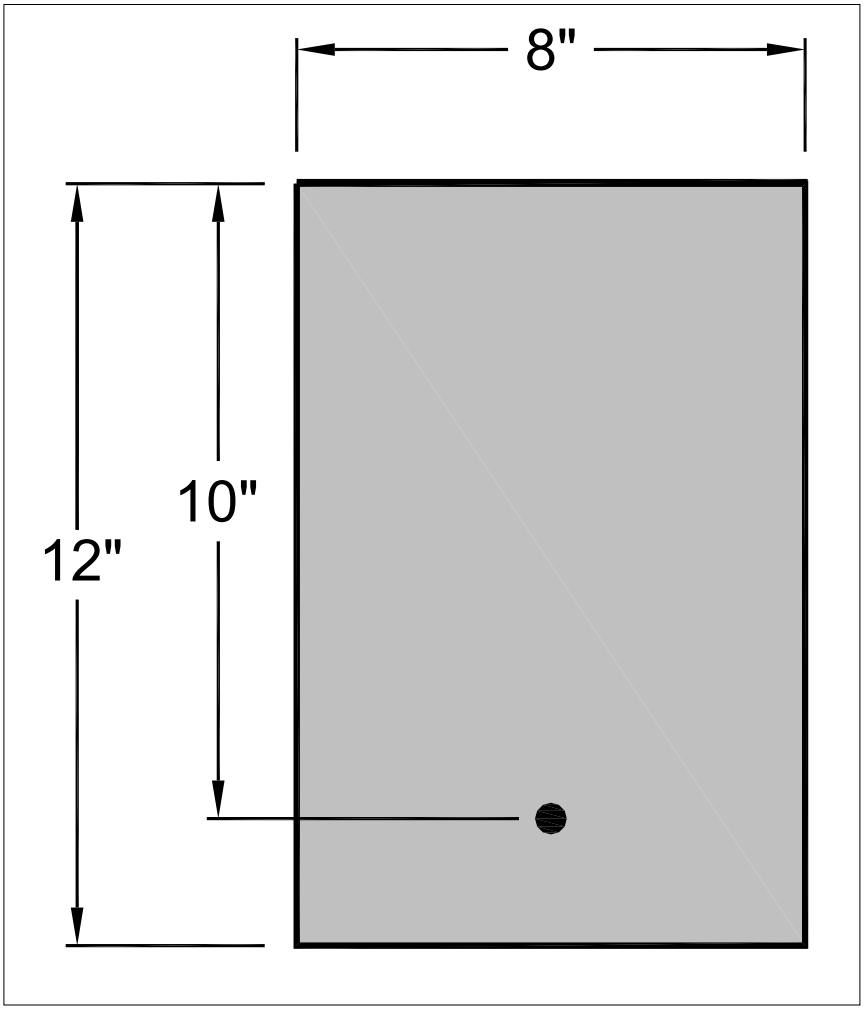

Figure 3.1 Cross section of bottom-strand specimens

Specimens used to evaluate the "top-strand" effect, are denoted **t**op-**s**trand **b**eams (TSB). These specimens had a width of 8 inches and an overall height of 24 inches (Figure 3.2). The strand in these specimens was located 22 inches from the bottom, and thus greatly exceeded the 12-inch height requiring a 1.3 multiplier for development length by AASHTO.[5] However, at mid span, a Styrofoam® block-out was used to reduce the height from 24 inches to 12 inches, as shown in Figure 3.3. These specimens were inverted prior to testing. Note that at mid span, which is the critical section, these

specimens had identical cross sections to the SSB specimens. Therefore, direct comparison between results is justified.

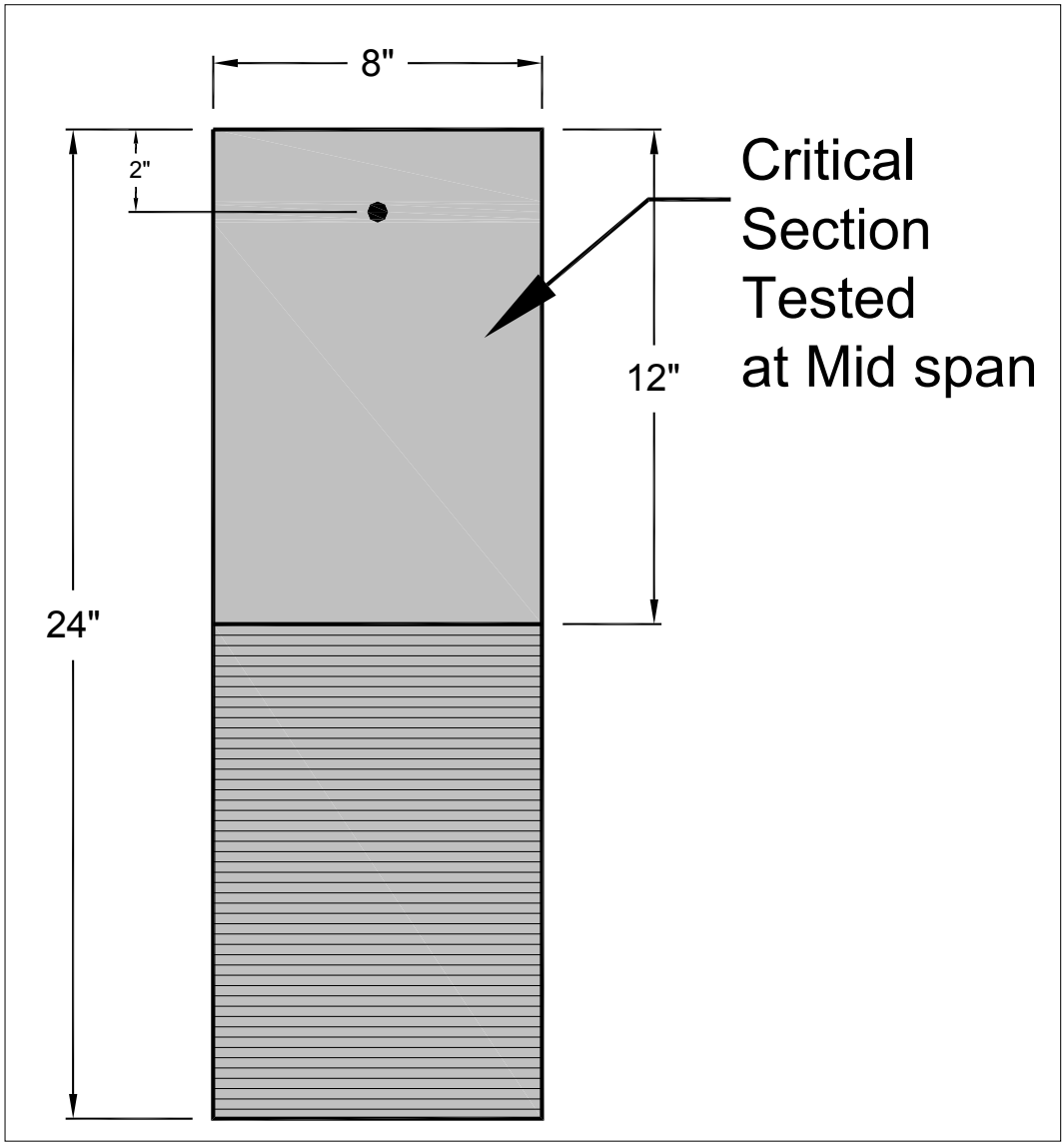

Figure 3.2 Cross section of top-strand specimens

Figure 3.3 Block-out used for top-strand beams

3.2 Multiple-Strand Development Length Specimens

In addition to the single-strand specimens, four multiple-strand specimens were cast in order to investigate the development length of multiple strands at close spacing. These specimens had a T-shape in order to provide the necessary compression area to produce high-tensile strains in the strand at nominal-moment capacity. The calculated strain in the strand was larger than 3.5%, based on strain compatibility (see A.5 for nominal-moment calculation). The nomenclature used for these **T**-**b**eams was simply TB. The cross section of these specimens was identical to the ones used by Peterman et al.[3] in their test program. The cross section had five bottom 0.5-inch-diameter strands at a depth of 19 inches and an overall height of 21 inches, and a compression flange width of 36 inches (Figure 3.4). Half-inch-diameter rebar stirrups at 6 inches on center were

used in both the web and flange, which satisfied ACI code provisions for shear (Figure 3.5).[4]

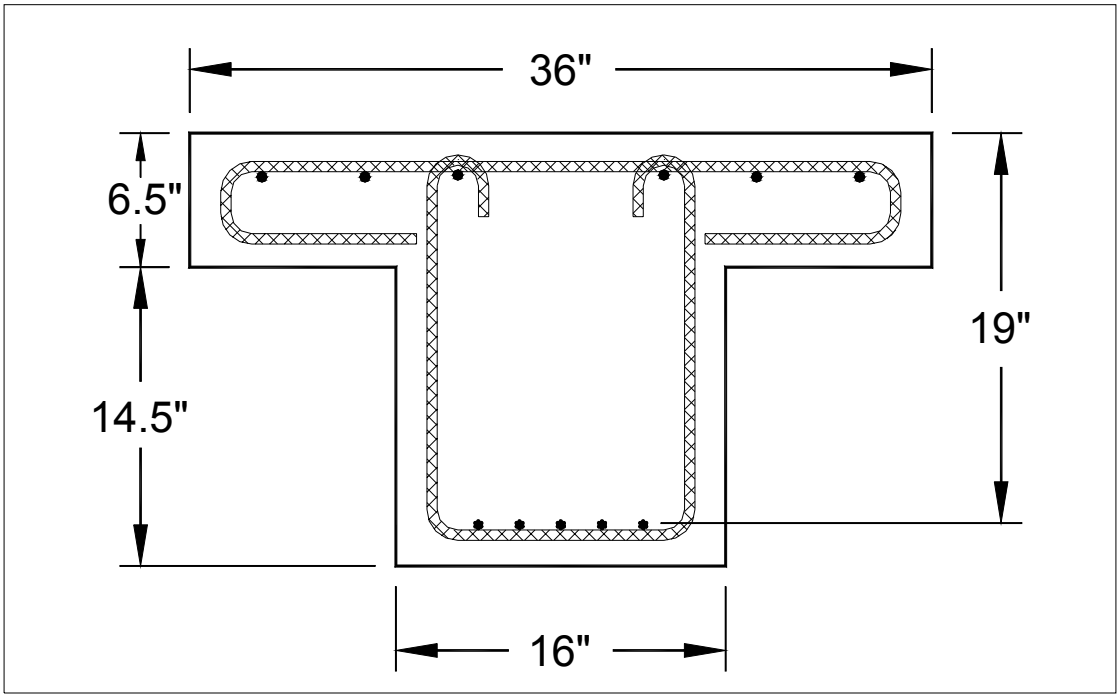

Figure 3.4 Cross section of T- beam specimen

Figure 3.5 Shear reinforcement for T-beams

3.3 Embedment Lengths

At the outset of this experimental program, it was determined that two different embedment lengths, l_e, were to be tested. Crack formers, as in Figure 3.6 for the SSB specimens, Figure 3.7 for the TSB specimens, and Figure 3.8 for the TB specimens, were cast at the embedment length to ensure that during loading the first cracks would open at these locations.

Figure 3.6 Crack former in SSB specimens

Figure 3.7 Crack former for TSB specimen

Figure 3.8 Crack former used for TB specimens

The first set of specimens were tested at an embedment length equal to 100% (6'-1") of the calculated development length, l_{dev}, as shown in Figure 3.9 for SSB setup (and very

similar for the TB setup) and Figure 3.10 for TSB setup. The second set of specimens were tested at either 80% l_{dev} or 120% l_{dev}, depending on results obtained from the 100% l_{dev} specimen tests. The second set of specimens were specifically designed to allow for testing at either embedment length as explained in the following.

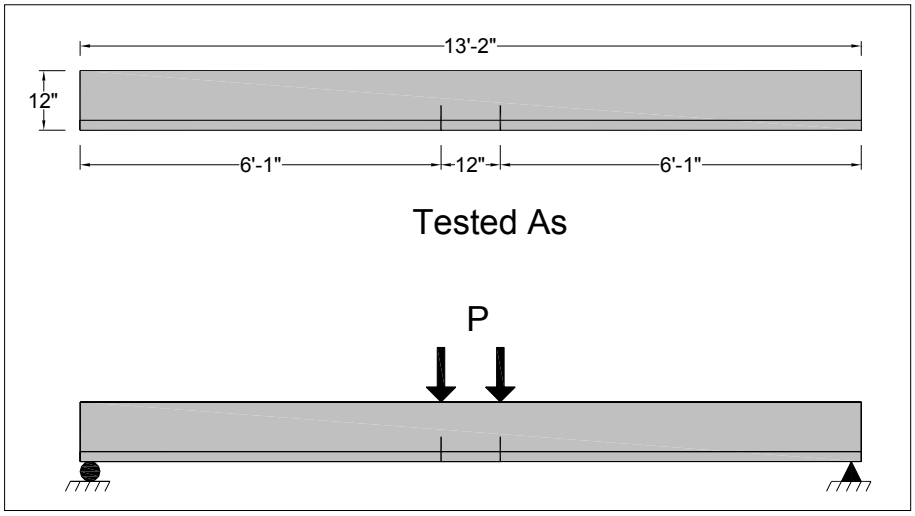

Figure 3.9 Test setup for 6'-1" embedment length (SSB and TB)

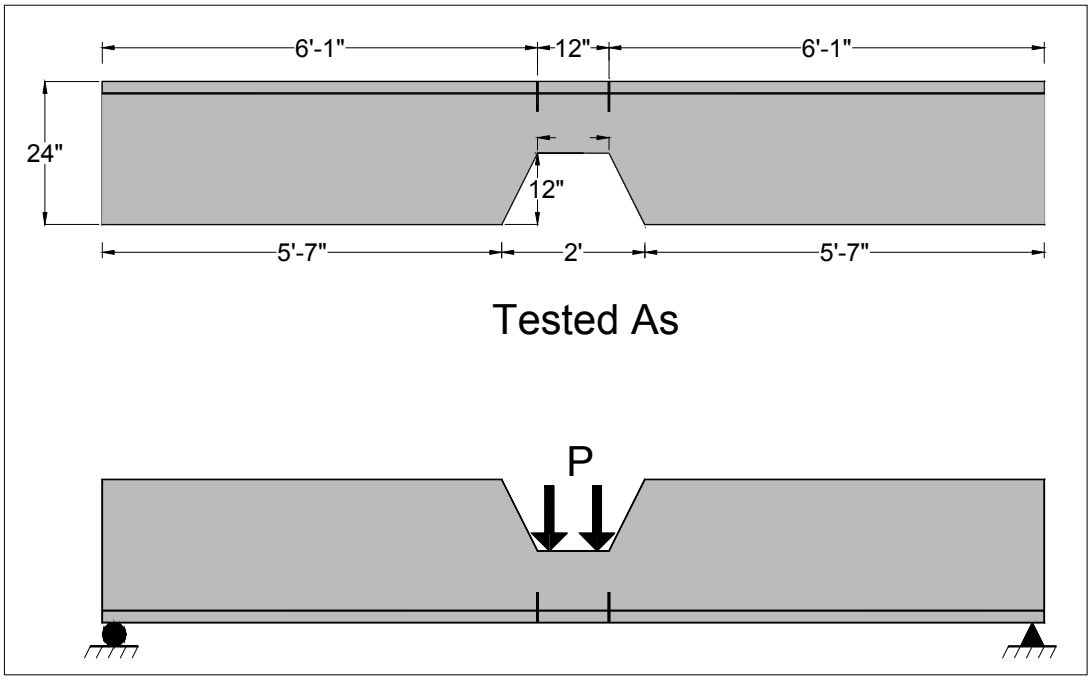

Figure 3.10 Test setup for 6'-1" embedment length for TSB specimens

If the 100% l_{dev} specimens failed (by flexure) at a moment greater than or equal to the calculated nominal-moment capacity M_n, then the second set of specimens would be tested at an embedment length equal to 80% l_{dev} (4'-10"). However, if the 100% l_{dev} specimens failed (by bond) at a moment less than the calculated nominal-moment capacity M_n, then the second set of specimens would be tested at an embedment length equal to 120% l_{dev} (7'-3"). Because all of the 100% l_{dev} specimens failed by flexure (as will be discussed in the Chapter Seven of this dissertation), the second set of specimens were all tested at an embedment length equal to 80% l_{dev}. TSB setup is shown in Figure 3.11.

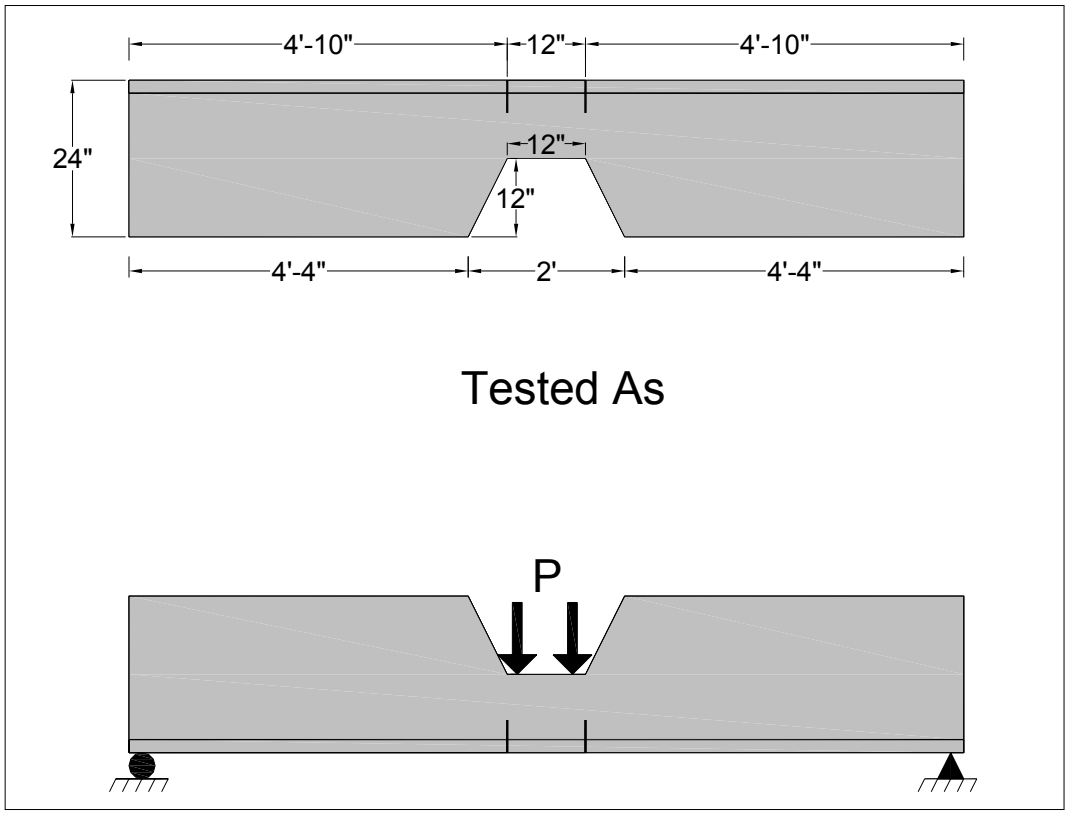

Figure 3.11 Test setup for 4'-10" embedment length TSB specimens

The different embedment length testing of the second set of specimens was made possible by utilizing four crack formers per beam (Figure 3.12). As shown in this figure, the 80% l_{dev} tests required use of the spreader beam with loading points directly above the outer-most crack former, as shown in Figures 6.34 and 6.35.

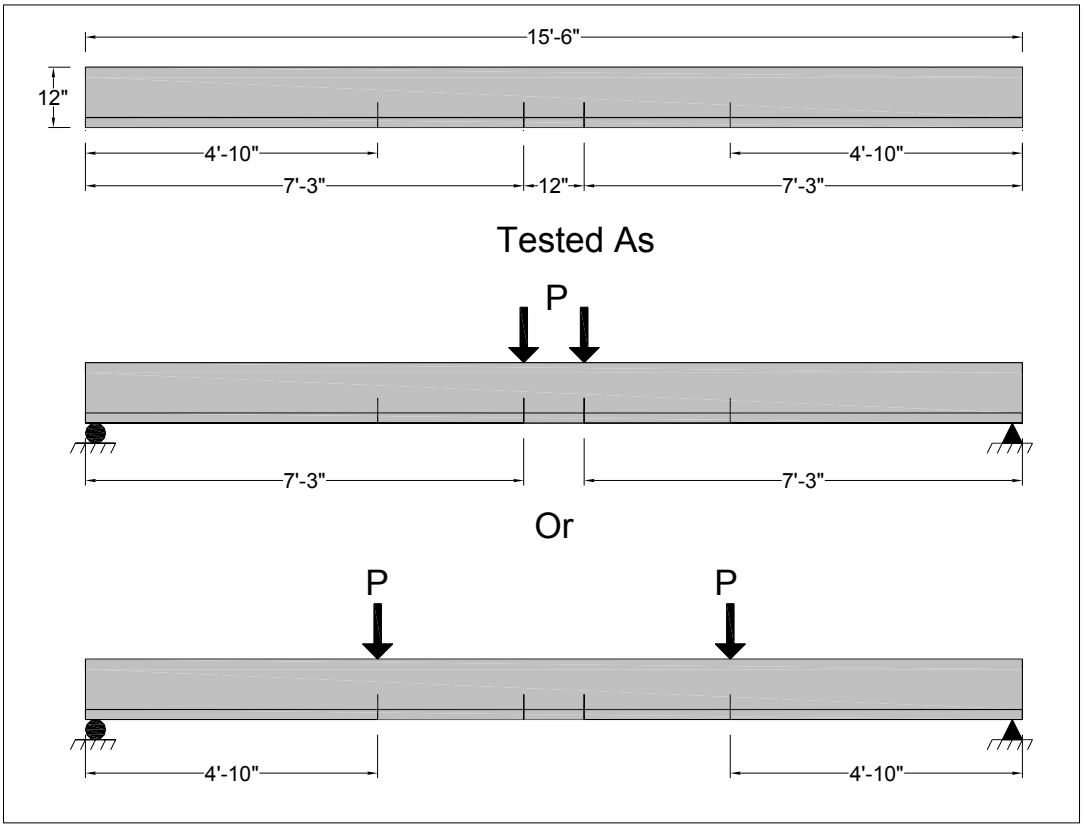

Figure 3.12 Test setup for 4'-10" embedment length SSB and TB specimens

CHAPTER FOUR - MATERIAL PROPERTIES

4.1 Large-Block Pullout Tests

Prior to casting any flexural test specimens, the prestressing strand that would be used for all test girder specimens was pre-qualified using the LBPT procedure, Figure 4.1. Standard LBPT procedures, as stipulated by Logan,[6] were followed in these tests. These strand qualification tests were performed with the standard mix proposed by Logan[6] (Table A.1) and not with SCC. Results of these tests are shown in Table 4.1. the compressive strength of the Logan mixture was 5,600 psi. The average first-observed slip was at 21.6 kip, and the average ultimate pullout was 39.6 kip. The values are both above the minimum recommended values of 16 kip and 36 kip, respectively, and meet the maximum coefficient of variation of 10% for a six–sample group. Thus, the strand reel was deemed acceptable for use in this study. This reel was then covered to prevent weathering and used for all flexural beam tests and IT specimens reported herein.

Figure 4.1 LBPT setup

Table 4.1 LBPT with Logan concrete and project strand

Logan Concrete with Project Strand		
Specimen	**Max Load (kip)**	**Load at 1st Slip (kip)**
1	41.3	21.9
2	41.4	20.8
3	41.5	23.4
4	40.5	19.4
5	35.8	20.2
6	37.1	23.8
Average	**39.6**	**21.6**
Coeff. of Var.	**6.3%**	**8.1%**

4.2 Mix Design

Casting of test specimens was performed at Prestressed Concrete Inc., Newton, Kansas, which is a PCI-certified plant that produces bridge members. They developed their proposed SCC mixture design with the help of their admixture supplier. The SCC mixture used in this study, along with the conventional concrete mixture that this plant uses, is presented in Table 4.2. This conventional concrete mixture is used in some of the girders for the Cowley County Bridge, as described in Chapters 12 and 13. It should be noted that both mixes use a ¾-inch maximum aggregate size and have a 0.30 and 0.41 water-to-cementicious materials ratio for the SCC and the conventional concrete mixtures, respectively. Also note that a different high-range water reducer is used for the SCC and conventional concrete mixtures.

Table 4.2 SCC and conventional concrete mixture proportions

	SCC	Conventional
Materials	**Quantity per yd^3**	**Quantity per yd^3**
Cement (Type III)	750 lbs	650 lbs
Fine Aggregate	1500 lbs	1480 lbs
Coarse Aggregate	1360 lbs	1457 lbs
Air Entrainment	5 oz	6 oz
HRWR	70 oz	26 oz
VMA	0 oz	0 oz
Water	27 gal	31.6 gal
w/c ratio	0.30	0.41

4.3 Fresh Concrete Evaluation

During casting of the specimens, the SCC mixture was tested to determine its workability. At the time of casting, there were no existing ASTM standards for testing SCC, but the PCI Interim Guidelines[1] documents have many test methods to evaluate the plastic properties of SCC for production qualifications. However, since the time of testing ASTM has adopted two standards for the evaluations of SCC. The two standards were ASTM C1611 "Standard Test Method for Slump Flow of Self-Consolidating"[43] and ASTM C1621 "Standard Test Method for Passing Ability of Self-Consolidating Concrete by J-Ring."[44] In this study, inverted-slump flow and visual stability index (VSI) (Figure 4.2), J-Ring (Figure 4.3), and L-Box (Figure 4.4) tests were all performed on the concrete during casting. Khayat et al.[45] outlined the procedures for performing these tests. The inverted-slump flow (spread) measures SCC consistency. It also evaluates the capability of concrete to deform under its own weight.[45] The J-Ring and L-Box are used to evaluate passing ability and blocking resistance of the SCC mix. Khayat et al.[45] reported the

difference between the inverted-slump flow (spread) and J-Ring should not exceed two inches. A schematic of the L-Box is located in the "Interim Guidelines for the Use of Self-Consolidating Concrete in PCI Member Plants".[1] Khayat et al.[45] reported that an 0.80 to 1.0 ratio for h_2/h_1 for L-Box tests has been proposed, but has not been passed into ASTM standard test methods.

Figure 4.2 Inverted slump for SCC

Figure 4.3 J-Ring test for SCC

Figure 4.4 L-Box test for SCC

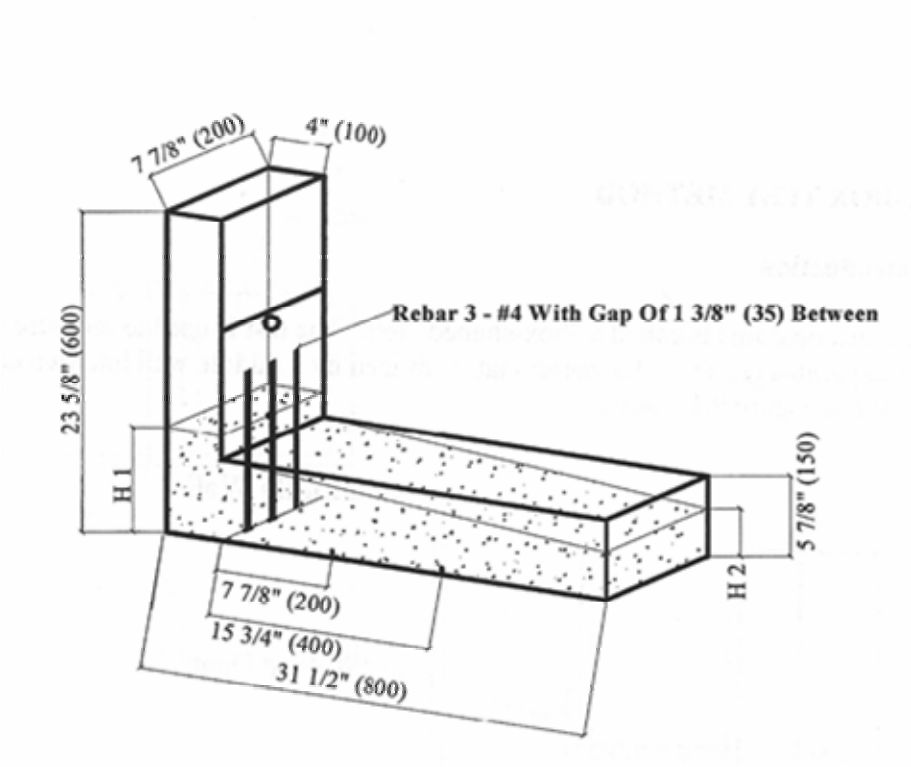

Figure 4.5 Schematic of L-Box[1]

4.4 Hardened Concrete Properties

The compressive strength and modulus of elasticity of the concrete were measured for future use in analytical computations. Standard ASTM procedures were followed for compressive strength and modulus of elasticity testing. In addition to measuring one-day (release) compressive strengths, compressive strengths were determined just prior to loading the flexural specimens to failure. A set of three, 4-inch x 8-inch cylinders were tested for each flexural specimen, and average values were determined. A typical compressive strength versus time curve for the proposed SCC mixture is shown in Figure 4.6.

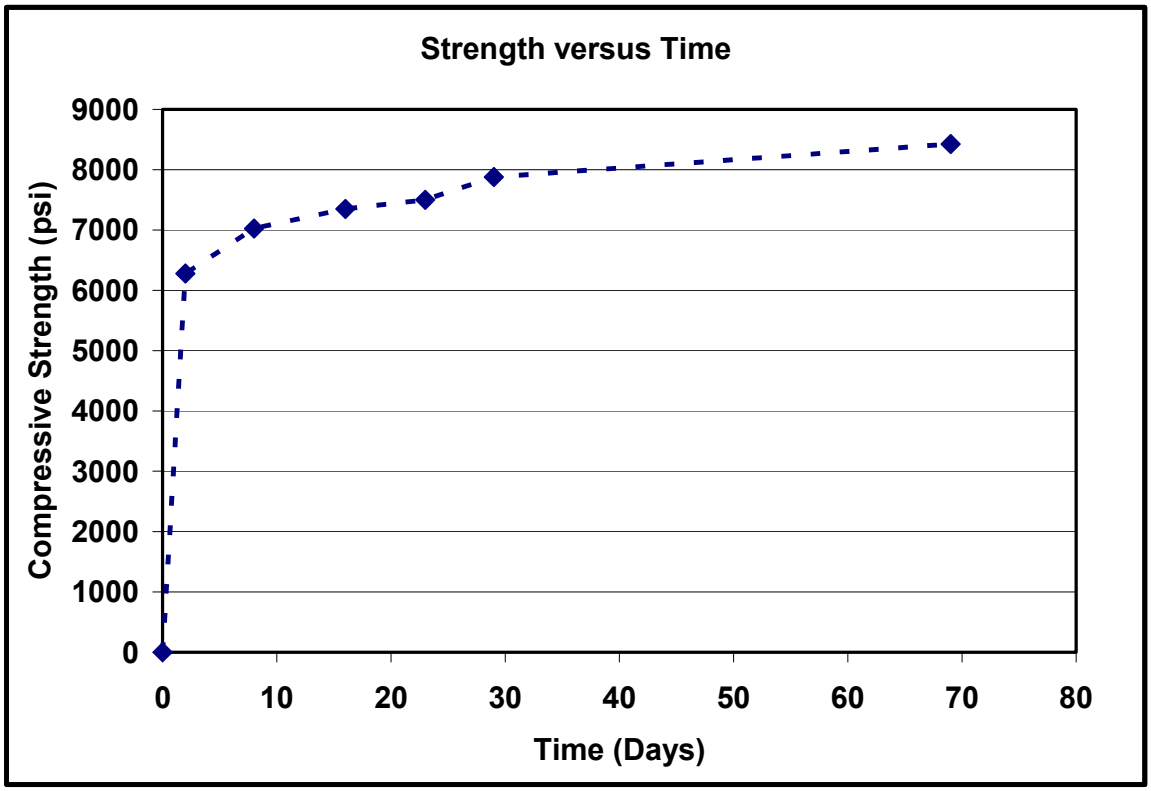

Figure 4.6 Compressive strength development for SCC

CHAPTER FIVE - DETERMINATION OF TRANSFER LENGTH

5.1 End Slip Measurements

End-slip measurements were used in determining transfer lengths of each end for the flexural specimens. End slip can also be described as the amount that the strand "draws" into the specimen end. Transfer length is a key parameter for shear design of prestressed concrete members. If the actual transfer length of the member is larger than the assumed value of 50 strand diameters (governed by ACI), then a possible shear deficiency may occur in the member. For this reason, it is important that transfer length of a member be accurately determined.

Measuring the amount of end slip that the strand undergoes has proven to be an effective way of determining transfer lengths. Russell and Burns (1996)[27] state that "a statistical correlation does exist between transfer length and strand end slips," and suggest that end slips may reliably predict transfer lengths. Logan (1997)[6] also measured strand end slip and found it to be a very accurate measure of transfer length.

Mast's strand-slip theory as presented by Logan (1997)[6] was used to determine transfer length of the girders experimentally. Many publications have shown that a theoretical relationship exists that relates transfer length as a function of strand slip. The equation was derived by assuming a straight-line variation in strand stress from zero at the end of the beam to full prestress at the transfer length (Logan 1997).[6] The end slip can then be expressed in terms of the reduction of the stress in the strand due to release of

the prestressing strand. The following equation can be used to determine the implied transfer length of a member.

$$L_{tr} = \frac{2E_{ps}\Delta}{f_{si}} \tag{4.1}$$

where

E_{ps} = modulus of elasticity of the prestressing strand (ksi);
Δ = amount of strand slip (inches); and
f_{si} = stress in prestressing strand immediately after transfer of prestress force to concrete (ksi).

Different methods have been used to measure the amount of strand slip the strand undergoes. The following method outlines the procedure that was used in this study:

- Prior to detensioning, a mark was made on the strand with a saw blade at a distance approximately 1 inch from the specimen end, Figure 5.1.
- After detensioning, the elastic shortening that occurred in this one inch distance was subtracted from the total amount of end slip, as seen in the following sample calculation,
- A steel block having an exact width of 0.500 inches was held against the concrete at the strand location.
- The distance between this machined block and the mark on the strand was then measured using a digital caliper having a precision of 0.001 inch, Figure 5.2.
- This value was used as the baseline for measurements taken after detensioning to determine the amount of end slip.
- Subsequent end-slip measurements were taken up to the time of testing for each specimen.

Figure 5.1 Making notch on prestressing strand

Figure 5.2 Measuring distance between notch and steel block

The following sample calculation, for the single-strand specimens, detail the equations used in determining the implied transfer length values from the end-slip measurement data.

Measured distance before detensioning = 0.524 inches
Measured distance after detensioning = 0.463 inches
Raw end slip = 0.524 inch -0.463 inch = 0.061 inches

$$\text{Elastic shortening of strand} = \frac{PL}{A_{ps}E_{ps}} = \frac{31(1)}{0.153(28,500)} = 0.0071$$

where

P = force in strand, kips;
L = length of strand between notch and specimen end, inch;
A_{ps} = area of pestressing strand, inch^2; and
E_{ps} = modulus of elasticity of prestressing strand, ksi.

End slip = Δ = raw end slip – elastic shortening of strand
Δ = 0.061 inch – 0.0071 inch = 0.054 inches

$$L_{tr} = \frac{2E_{ps}\Delta}{f_{si}} = \frac{2(28,500)0.054}{196} = 16 \text{ inches}$$

with the calculation of f_{si} shown in A.6.

5.2 Surface Strain Measurements

Concrete surface strains were used in determination of the transfer length for the IT specimens. A mechanical strain gage (Whittemore gage, Figure 5.3) was used to measure the surface strains. Whittemore points, stainless steel discs with a machined hole in the center, were adhered along the bottom flange of the specimen prior to detensioning, Figure 5.4. Readings were taken just prior to detensioning and after detensioning. Then the concrete strain at transfer was determined by taking the numerical difference between the initial reading and the final reading. The measured concrete strains were then plotted against the length of the specimen. To reduce any

anomalies, measured strains were smoothed by averaging the data over three gage lengths. The equation used to smooth the data is shown as follows:

$$(strain)_i = \frac{(strain)_{i-1} + (strain)_i + (strain)_{i+1}}{3} \quad (4.2)$$

where

i = the current strain reading.

Hence, at any given strain point, strain and the values just ahead and behind were averaged to obtain the "smoothed" curve.

Transfer lengths for each specimen end were then determined by plotting the concrete strains versus the specimen length and evaluating the strain profile. Russell and Burns (1993)[2] developed a simple procedure for determining transfer lengths from the strain profiles. The procedure is known as the "95% average maximum strain" and is outlined below.

- Plot the "smoothed"-strain profile by taking the average of three consecutive strain points.
- Determine the "average maximum strain" by computing the average of all strains contained within the strain plateau of the fully effective prestress force.
- Take 95% of the above calculated "average maximum strain" and construct a line corresponding to this value.
- Transfer length is determined by taking the intersection of the 95% maximum strain line and the "smoothed"-strain profile line.

Figure 5.3 Whittemore gage

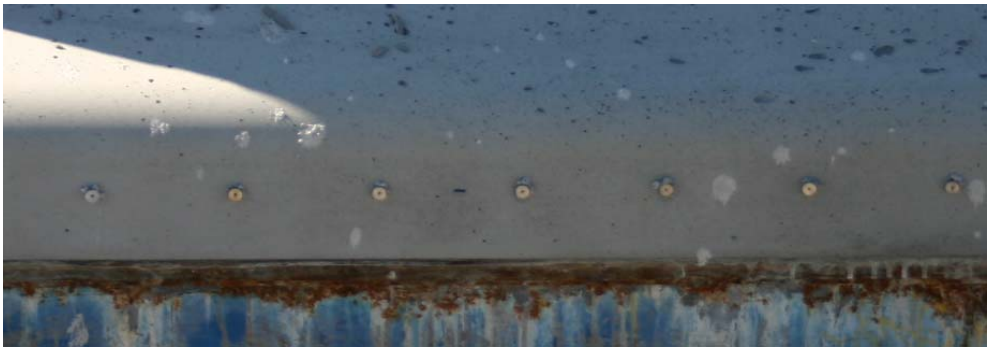

Figure 5.4 Whittmore locating points

CHAPTER SIX - FABRICATION AND TEST SETUP OF FLEXURAL SPECIMENS

6.1 Flexural Specimen Fabrication

Fabrication of all flexural specimens was performed at Prestressed Concrete Inc., Newton, Kansas. All six bottom strand beams along with TB A and TB C were cast in the afternoon of March 29, 2004, and detensioned the next morning, March 30, 2004. The remaining two T-beams, TB B and TB D, were cast in the afternoon of March 30, 2004, and detensioned the next morning, March 31, 2004. On the afternoon of April 8, 2004, nine top-strand beams were cast and detensioned the next morning, April 9, 2004. Table 6.1 presents a review of the cast date and detensioning date for each specimen.

Table 6.1 Review of cast and detensioning dates

	Beam	Date Cast	Date of Detensioning
Bottom Strand	SSB A	3/29/2004	3/30/2004
	SSB C	3/29/2004	3/30/2004
	SSB D	3/29/2004	3/30/2004
	SSB E	3/29/2004	3/30/2004
	SSB F	3/29/2004	3/30/2004
Top Strand	TSB A	4/8/2004	4/9/2004
	TSB B	4/8/2004	4/9/2004
	TSB C	4/8/2004	4/9/2004
	TSB D	4/8/2004	4/9/2004
	TSB E	4/8/2004	4/9/2004
	TSB F	4/8/2004	4/9/2004
T-Beams	TB A	3/29/2004	3/30/2004
	TB B	3/30/2004	3/31/2004
	TB C	3/29/2004	3/30/2004
	TB D	3/30/2004	3/31/2004

Two vibrating wire strain gages (VWSG) were embedded in three of the specimens (SSB A, TSB D, and TB A) to monitor long-term strains before testing. For SSB A, one gage was placed at strand height, two inches from the bottom and the other at 8.5 inches from the bottom, Figure 6.1. TSB D had one gage at strand height two inches from the bottom once the specimen was flipped, and the other at 8.5 inches from the bottom after the specimen was flipped, Figure 6.2. For TB A, one gage was located at strand height two inches from the bottom and the other at 19 inches from the bottom, Figure 6.3. To record the temperatures while the SCC was curing, digital temperature data loggers, Figure 6.4, were also placed in those three specimens to develop a temperature versus time curve.

Figure 6.1 VWSGs for SSB A

Figure 6.2 VWSG for TSB D

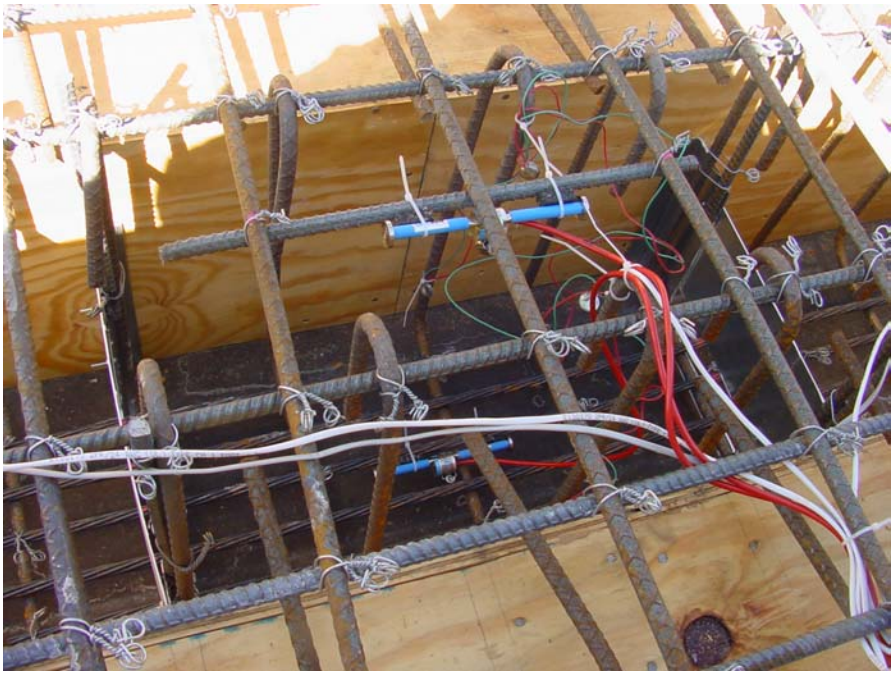

Figure 6.3 VWSGs for TB A

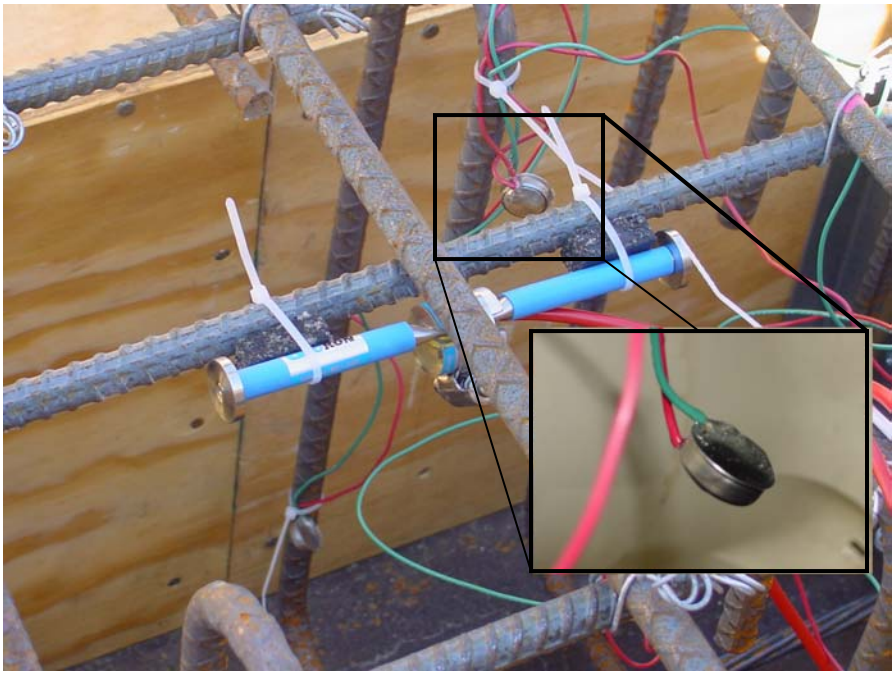

Figure 6.4 Digital temperature data logger to record temperature

Casting of the SSB specimens was a relatively short process. Forms with the dimensions of one foot wide by one foot deep were used to cast these specimens and Styrofoam sheets were used to get the correct width of the beams, Figure 6.5. The crack formers were held in place with use of wood across the top because no internal shear stirrups were used in these test specimens, as shown in Figure 6.6.

Figure 6.5 SSB bed

Figure 6.6 Crack former held in with wood 2 x 4

Once the forms were set to the correct dimensions and all test equipment was put in place, the SCC was poured into them, Figure 6.7, and then finished with a float, Figure 6.8. After release strength was met, Figure 6.9, the strand was torched and the specimens

removed from the beds and moved to the field. They were then shipped up to Manhattan, Kansas, for testing.

Figure 6.7 Pouring of SCC into forms

Figure 6.8 Finishing of SSB specimens

Figure 6.9 Cured SSB

The TSB specimens utilized the rollaway bed for their casting, Figure 6.10. The walls were spaced at eight inches to accomplish this task. As noted earlier, a Styrofoam block was used to reduce the height at mid-span from 24 inches to 12 inches, Figure 6.11. Two, 0.75-inch-diameter rebar, which can be seen in Figures 6.10 and 6.11, was placed at the bottom of the beams to reduce the risk of cracking while the specimens were flipped over. The Styrofoam blocks were removed and rebar cut prior to testing.

Figure 6.10 TSB bed with headers in place

Figure 6.11 Block used to reduce height at mid span

Coil inserts, Figure 6.12, were cast in the ends of each TSB specimen because no lift loops could be cast into the top of the specimens. These would later be used to remove the specimens from the bed and flip them over.

Figure 6.12 Inserts cast into ends so specimens could be flipped over

After the forms were set to the proper dimensions, the SCC was poured into the forms, Figure 6.13, and then finished, Figure 6.14.

Figure 6.13 Pouring of SCC into forms

Figure 6.14 Finishing of specimens

After the specimens had cured and release strength had been met, they were detensioned and the walls were removed, Figure 6.15. Once they had cured to the specified shipping strength, they were shipped to Manhattan, Kansas, for testing.

Figure 6.15 Removal of TSB from beds

The TB specimens were also cast on the rollaway bed, two at a time. The beds were first prepped and the headers were spaced at the proper distance, Figure 6.17. The web stirrups were placed and the strand was then pulled into place. The web and flange stirrups were tied into place, Figures 6.17 and 6.18.

Figure 6.16 Headers spaced for TB specimens

Figure 6.17 Placement of internal shear stirrups

Figure 6.18 Finished shear stirrups in TBs

Once the stirrups were all tied into place, the outside form walls were put in place, Figure, 6.19. The SCC was then poured into the forms, Figure 6.20, and finished using a float, Figure 6.21.

Figure 6.19 Placement of outside walls

Figure 6.20 Pouring of SCC into forms

Figure 6.21 Finishing of top surface

The next morning, after release strength was achieved, the strand was detensioned by flame cutting, Figure 6.22. Once the specimens had reached the proper strength, they

were shipped to Manhattan, Kansas. As-built dimensions of each specimen can be seen in Table A.7.

Figure 6.22 Torching of strand of TBs

6.2 Flexural Specimen Setup

6.2.1 Test Setup

The flexural specimens were tested using MTS servo-controlled actuators in the KSU Civil Engineering Structural Mechanics Laboratory. The SSB and TSB specimens were moved into the testing laboratory by carts as shown in Figure 6.23. Larger carts had to be constructed to handle the larger TB specimens, Figure 6.24.

Figure 6.23 Carts used for SSB and TSB specimens

Figure 6.24 Carts for TB specimen

Data was collected for load, mid-span deflection, and strand end slip. End-slip readings were monitored using a linear variable differential transformer (LVDT), as shown in Figure 6.25 for the single-strand specimens and Figure 6.26 for the TB specimens.

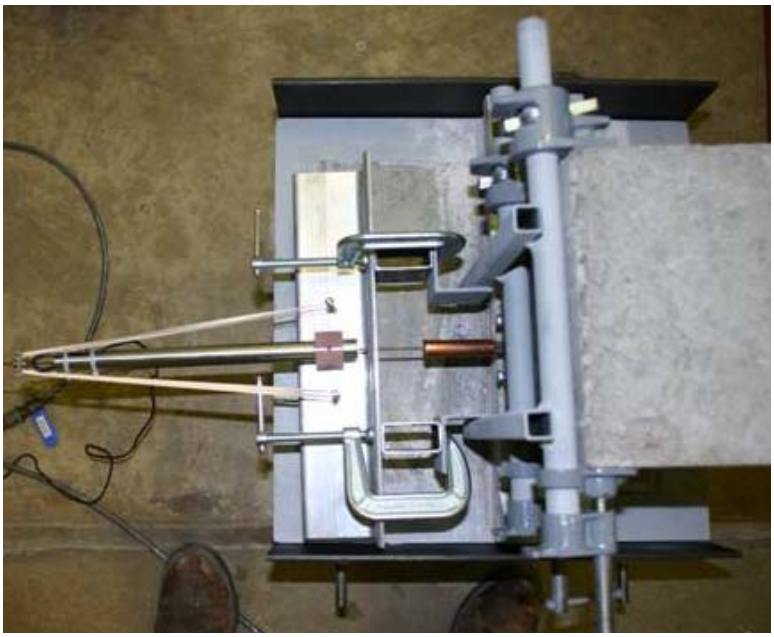

Figure 6.25 End-slip device used for SSB and TSB

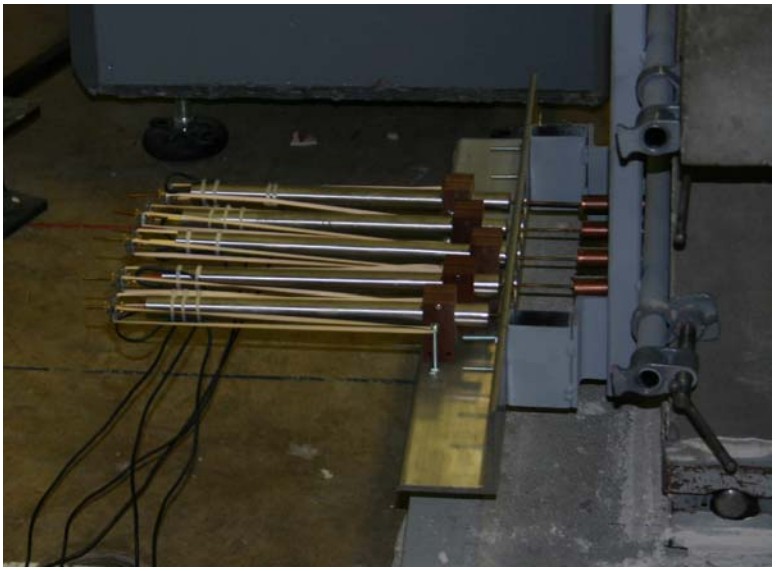

Figure 6.26 End-slip device used for TB specimens

LVDTs were also used to measure mid-span deflection. One on either side of the specimen was used, and the average value was used for data analysis, Figure 6.27.

Figure 6.27 LVDTs used for mid-span deflection

Figure 6.28 shows the test frame setup that was used to load all single-strand specimens. A spreader beam with rollers was used to apply point loads directly above the crack formers. Roller connections applied the point load at these locations. Figure 6.29 shows the TSB specimens in the loading frame. The TB specimens were loaded in the frame as shown in Figure 6.30.

Figure 6.28 Setup used for SSB specimens

Figure 6.29 Setup used for TSB specimens

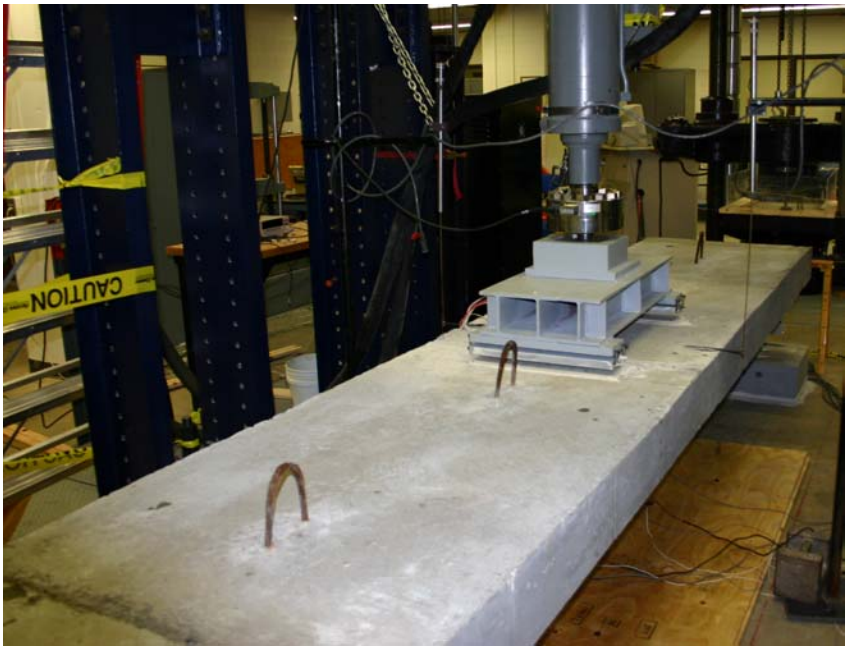

Figure 6.30 Setup for TB specimens

The SSB and TB specimens, with 80% embedment lengths, had to utilize a spreader beam to apply the load. This was discussed in the embedment length section (section

3.3). The spreader beam used for the SSB specimens is shown in Figure 6.31 and Figure 6.32 for the TB specimens.

Figure 6.31 Spreader beam for SSB specimens

Figure 6.32 Spreader beam used for TB specimens

All specimens were taken to failure and are shown in Figures 6.33 to 6.35 for all three specimen types.

Figure 6.33 Failure for SSB specimen

Figure 6.34 Failure for TSB specimen

Figure 6.35 Failure for TB specimen

6.2.2 Loading Conditions

Three types of loading-rate conditions were used for evaluating the different embedment lengths. The first loading condition was designated as the SLOW test and was targeted to take about 10 hours. During a SLOW test, the specimen was loaded at 100 lb/min until cracking. Then the loading rate was reduced to 10 lb/min until failure. This slow loading rate was used to accurately measure the amount of strand slip, if any, occurring prior to failure. For the second loading condition, designated as 76.5 % M_n, the specimen was loaded at 100 lb/min up to 76.5% of nominal capacity of the specimen and this load maintained for 24 hours. This load condition was modeled after ACI 318 section 20.3.2 for the testing and evaluation of existing structures. If the specimen successfully withstood the load for 24 hours, it was then loaded at 10 lb/min to failure. The final loading condition, designated as 100% M_n, was similar to the 76.5% M_n procedure, except that load was maintained at 100% M_n for 24 hours. Because only two types of the TB specimens were cast, the 76.5 % M_n and 100% M_n were combined for the

second specimen to produce a more severe loading condition. Table 6.2 shows the loading condition of each specimen tested, along with the corresponding development length.

Table 6.2 Loading conditions for all specimens

	Beam	Embedment Length	Loading Condition
Bottom Strand	SSB A	6'-1"	76.5% M_n
	SSB C	6'-1"	SLOW
	SSB D	4-10"	100% M_n
	SSB E	4-10"	SLOW
	SSB F	4-10"	76.5% M_n
Top Strand	TSB A	4'-10"	76.5% M_n
	TSB B	4'-10"	100% M_n
	TSB C	4'-10"	SLOW
	TSB D	6'-1"	100% M_n
	TSB E	6'-1"	76.5% M_n
	TSB F	6'-1"	SLOW
T-Beams	TB A	6'-1"	SLOW
	TB B	6'-1"	SLOW
	TB C	4'-10"	Combined
	TB D	4'-10"	Combined

CHAPTER SEVEN - FLEXURAL SPECIMEN RESULTS

7.1 Material Properties

Spread, VSI, J-Ring, and L-Box tests were performed before the casting of all flexural specimens. In addition, the compressive strength of concrete cylinders, that were matched-cured up to detensioning, were completed at the time of prestress release and just before the specimens were brought to failure. The ASTM C 39 standard for performing compressive strength tests was followed. Table 7.1 summarizes all of the measured concrete properties. The inverted-slump flow (spread), J-Ring, and L-Box tests were all performed before pouring of SCC into the forms. The VSI was determined by the author and the other tests were performed by the author and plant personal. .

Table 7.1 Concrete properties of specimens tested

	Specimen	Slump Flow (inch)	VSI	J-Ring (in.)	L-Box (h_2/h_1)	Strength @ Release (psi)	Strength @ Testing (psi)
Bottom Strand	SSB A	21	0.5	19	0.80	5,000	8,250
	SSB C	21	0.5	19	0.80	5,000	6,960
	SSB D	22	0.5	21	0.83	5,000	7,430
	SSB E	22	0.5	21	0.83	5,000	7,710
	SSB F	22	0.5	21	0.83	5,000	7,190
Top Strand	TSB A	28	0.5	26 1/2	0.88	3,600	6,570
	TSB B	28	0.5	26 1/2	0.88	3,600	7,150
	TSB C	28	0.5	26 1/2	0.88	3,600	6,940
	TSB D	28	0.5	26 1/2	0.88	3,600	7,790
	TSB E	28	0.5	26 1/2	0.88	3,600	7,330
	TSB F	28	0.5	26 1/2	0.88	3,600	6,100
T-Beams	TB A	17	0.5	14	0.78	5,200	7,550
	TB B	22	0.5	21	0.83	4,800	7,920
	TB C	21	1.0	18 1/2	0.83	5,200	8,300
	TB D	22	0.5	21	0.83	4,800	8,070

The temperature of the SCC was recorded during curing for three of the flexural specimens and a typical heat development curve for 24 hours is shown, Figure 7.1, Figure 7.2, and Figure 7.3 for the SSB, TSB, and TB specimens, respectively. It must be noted that the TSB and TB specimens had greater mass and thus were able to generate more heat during curing.

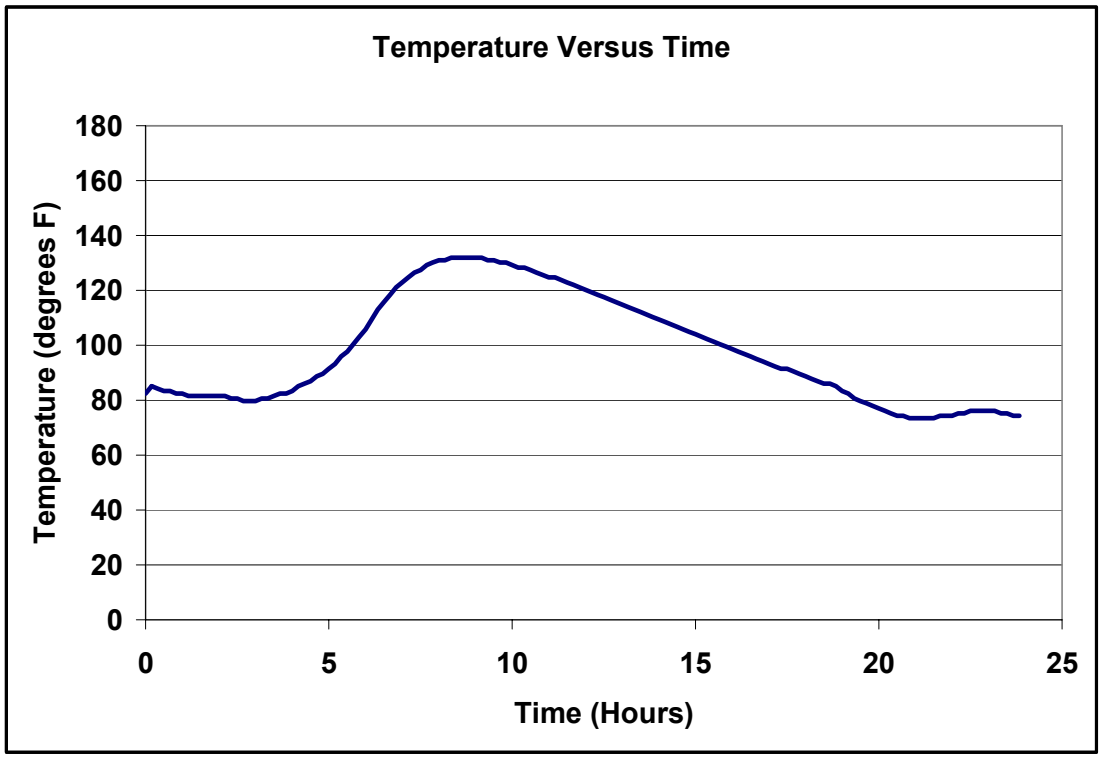

Figure 7.1 Temperature curve during curing for SSB specimen

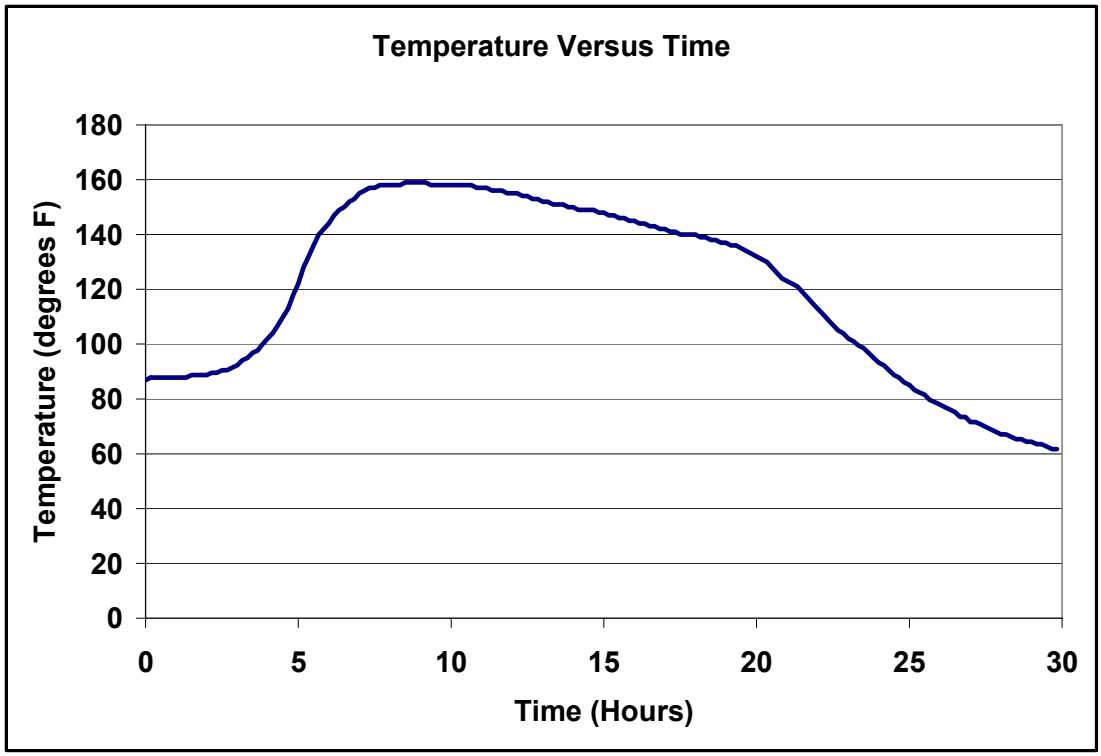

Figure 7.2 Temperature curve during curing for TSB specimen

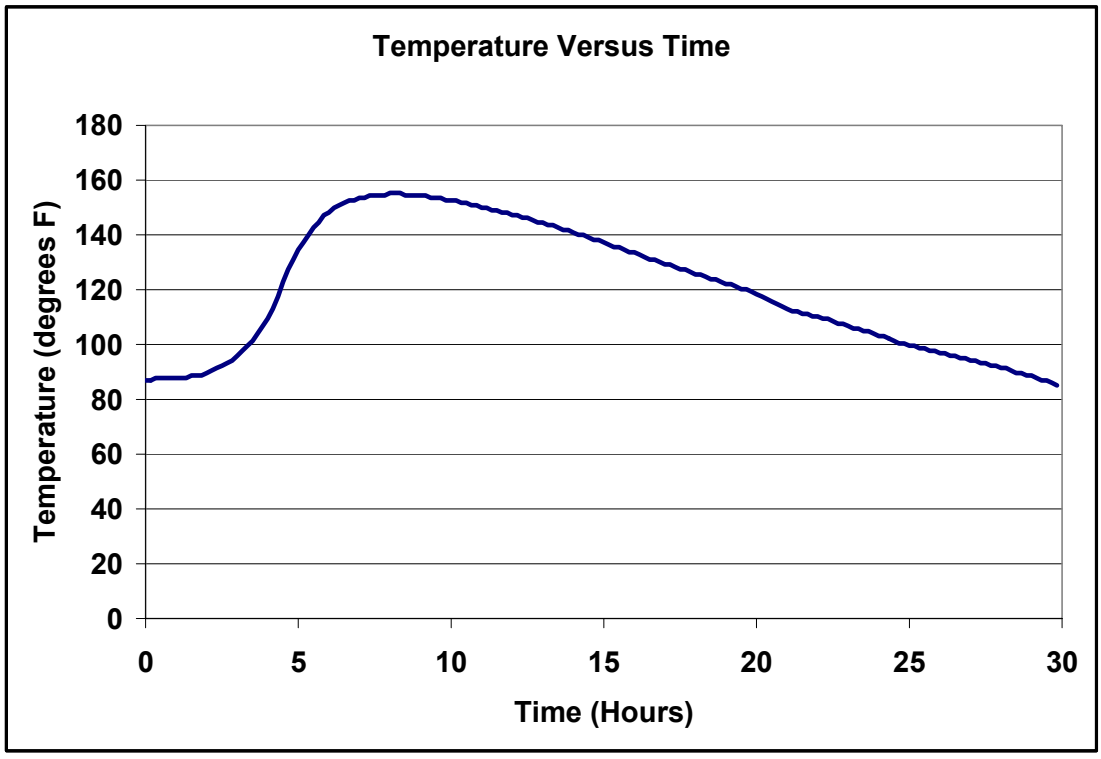

Figure 7.3 Temperature curve during curing for TB specimen

7.2 Transfer Length

As described previously, end-slip measurements were used to evaluate the transfer length of each girder. In these calculations, f_{si} was assumed to be 196 ksi for all single-strand specimens and 192 ksi for the T-beams (loss calculations in A.6).

For all SSB specimens, no end had a longer implied (18-day) transfer length than the value assumed by the AASHTO and ACI codes (33 inches as calculated from equation 1.1). The average 18-day transfer length for the SSB specimens was 21 inches and values for each specimen end can be seen in Table 7.2. However, ACI 11.4.3 for shear design of prestressed members assumes the transfer length to be 50-strand diameters. Although five specimen ends did exceed this limit, the average value was well below the value of 50-strand diameters (25 inches). AASHTO 5.11.4.1 assumes a value of 60-strand diameters (30 inches) for shear design of prestressed members. Only one specimen end exceeded this value. A 15% increase was seen in the transfer length from release to 18 days. From 18 days to testing day, a noticeable increase in transfer length was not seen.

Table 7.2 Implied transfer lengths (in inches) for SSB specimens

Transer Lengths for Single-Strand Beams								
Beam	Embedment Length	Spread (in)	Release		18 Days		Test Day	
			A	B	A	B	A	B
SSB A	6'-1"	21	16	17	26	30	27	30
SSB B	6'-1"	21	18	24	16	30	16	30
SSB C	6'-1"	21	17	7	24	11	23	11
SSB D	4-10"	22	30	25	29	31	29	31
SSB E	4-10"	22	19	19	13	17	14	17
SSB F	4-10"	22	12	15	10	16	10	16
Average			18		21		21	

The average 18-day implied transfer length for the TSB specimens was 28 inches, once again below the implied transfer length value predicted by the AASHTO and ACI code provisions. Values for each specimen end can be seen in Table 7.3. There were several specimen ends that did exceed the 25-inch (ACI) and 30-inch (AASHTO) assumed values that ACI and AASHTO require for shear design. Unlike the SSB specimens, a noticeable increase in transfer length was seen from release to 18 days. This value was close to 100%. Just like the SSB specimens, a noticeable increase from 18 days to testing day was not seen.

Table 7.3 Implied transfer lengths (in inches) for TSB specimens

Transfer Lengths for Top-Strand Beams								
Beam	Embedment Length	Spread (in)	Release		18 Days		Test Day	
			A	B	A	B	A	B
TSB A	4'-10"	28	17	19	30	34	30	34
TSB B	4'-10"	28	21	13	30	24	30	25
TSB C	4'-10"	28	15	13	34	31	34	31
TSB D	6'-1"	28	15	17	22	19	23	19
TSB E	6'-1"	28	8	21	20	31	22	31
TSB F	6'-1"	28	8	15	32	23	36	25
Average			15		28		28	

The average 18-day implied transfer length for the TB specimens was 26 inches, once again below the implied transfer length (32 inches) value predicted by the AASHTO and ACI code provisions. Values for each specimen end can be seen in Table 7.4. There were several specimen ends that did exceed the 25-inch (ACI) and 30-inch (AASHTO) assumed values that ACI and AASHTO require for shear design. Similar to the SSB specimens, a noticeable increase in transfer length was not seen from release to 18 days and from 18 days to testing.

Table 7.4 Implied transfer lengths (in inches) for TB specimens

Transfer Lengths for T-Beams															
Beam-Side	Release					18 Days					Test Day				
	A	B	C	D	E	A	B	C	D	E	A	B	C	D	E
A1			19	25	6			28	34	13			28	34	14
A2	18	28	16	41	20	24	36	30	44	25	25	36	30	44	25
B1		11	40	19	7		22	41	11	16		22	41	15	17
B2	11				6	14				8	18				11
C1	20	18	25	28	19	23	20	28	31	17	23	20	28	31	19
C2	26	28	42	31	25	28	38	42	40	31	28	38	42	41	31
D1	28	32		11	10	30	35		15	21	30	35		16	22
D2	22	28	17	30	20	25	22	19	31	21	25	24	20	31	22
Ave	22					26					27				

Increases in transfer length over time for the specimens with strands less than 12 inches above the bottom were in general accordance with results by Barnes et al.[32] Barnes et al. found that the transfer lengths were found to increase approximately 10 to 20% over time, on average. All specimens that had the strand cast only two inches above the bottom (SSB and T-beam specimens) were found to increase approximately 10 to 20%. The TSB specimens had an increased implied transfer length of nearly 100% and this could be attributed to the "top-strand" effect. Russell and Burns[2] also completed a study on transfer lengths and found similar results.

Zia and Mostafa, Cousins et al., Mitchell et al., Buckner, Russell and Burns and Barnes et al. all proposed equations for estimating transfer lengths. These equations are given in Chapter Two of this dissertation. The equation given by Buckner is the current transfer length implied by the ACI code. The experimental results are compared against other equations and are graphed in Figure 7.4. The vertical line represents the range of the experimental results.

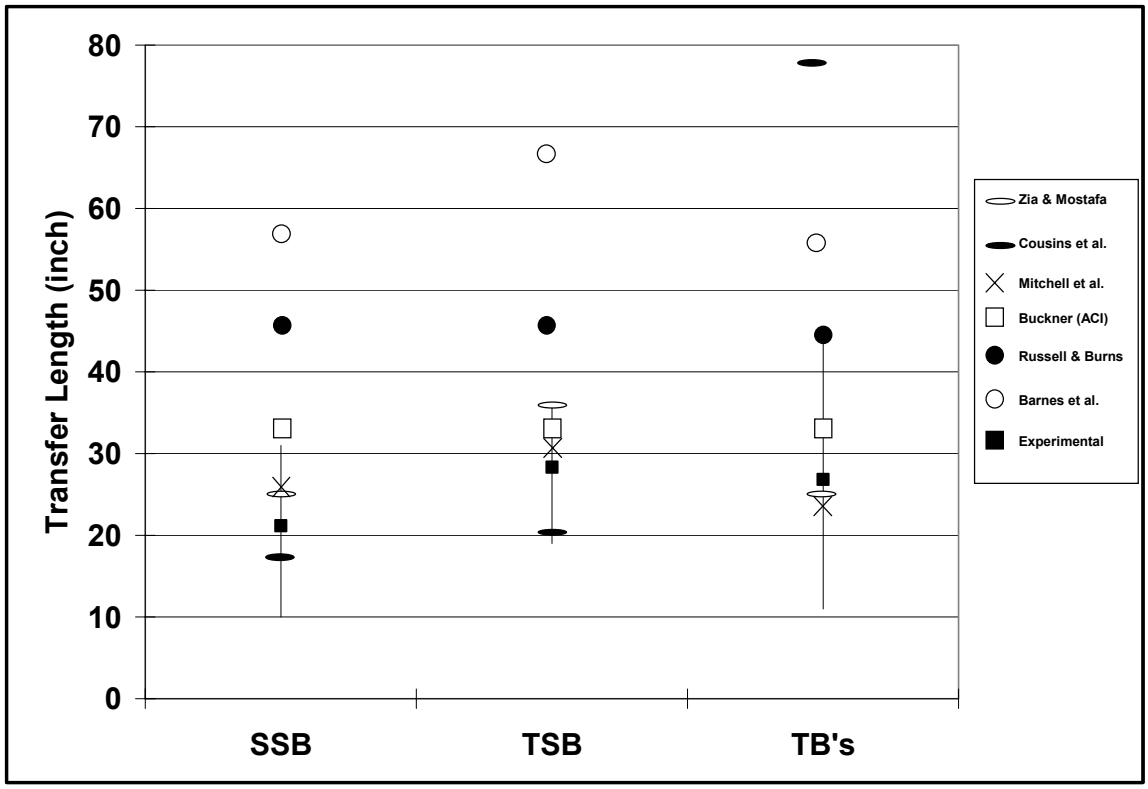

Figure 7.4 Experimental results for transfer length versus other prediction models

7.3 Development Length

Flexural failure by strand rupture was the failure mode of all specimens tested. In each case, the failure moment exceeded the calculated nominal-moment capacities by 10 to 20% for specimens with an embedment length of 6'-1". All specimens with an embedment length of 4'-10" had an increase of 25 to 35% over the calculated partially-developed nominal capacity. It must be noted that a decreased nominal-moment capacity was calculated for specimens with an embedment length shorter than the calculated development length. Calculations for both the fully-developed and partially-devoloped nominal moment capacities can be found in sections A.4 and A.5. Table 7.5 presents all

results of the specimens tested. Furthermore, the maximum end slip recorded for all specimens during testing was less than 0.01 inches.

Table 7.5 Summary of tested specimens

	Beam	% I_e	Nominal Moment (M_n)	Experimental Moment (M_{exp})	M_{exp}/M_n	Strand Rupture	Strand Slip >0.01 in.
Bottom Strand	SSB A	100	33.0	36.6	1.11	Yes	No
	SSB C	100	33.0	38.2	1.16	Yes	No
	SSB D	80	29.4	39.6	1.35	Yes	No
	SSB E	80	29.4	37.5	1.28	Yes	No
	SSB F	80	29.4	38.8	1.32	Yes	No
Top Strand	TSB A	80	29.4	38.9	1.32	Yes	No
	TSB B	80	29.4	39.1	1.33	Yes	No
	TSB C	80	29.4	38.6	1.31	Yes	No
	TSB D	100	33.0	36.6	1.11	Yes	No
	TSB E	100	33.0	37.3	1.13	Yes	No
	TSB F	100	33.0	35.7	1.08	Yes	No
T-Beams	TB A	100	319	370	1.16	Yes	No
	TB B	100	319	383	1.20	Yes	No
	TB C	80	280	359	1.28	Yes	No
	TB D	80	280	376	1.34	Yes	No

7.3.1 SSB Specimen Flexural Results

A moment versus deflection graph for each SSB specimen shows that each one surpassed its nominal-moment capacity and that each failure by strand rupture, Figures 7.5 – 7.14. Also, end slip during loading is plotted for each specimen.

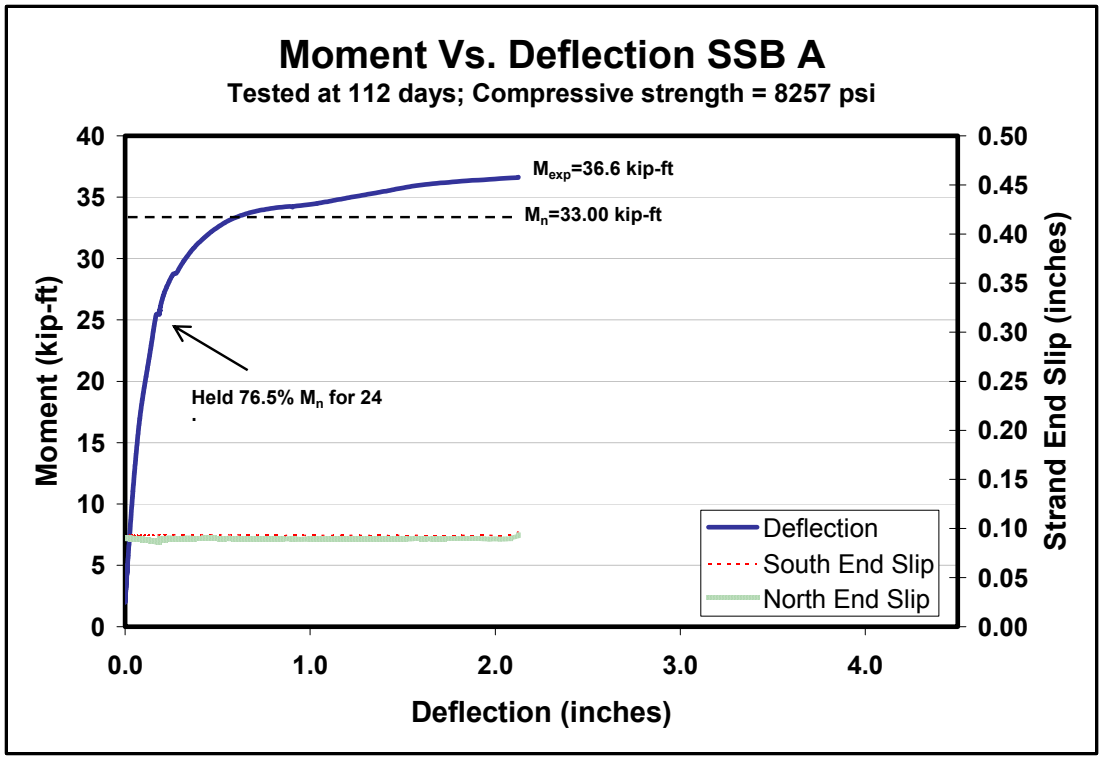

Figure 7.5 Moment versus deflection for SSB A

Figure 7.6 Failure of SSB A

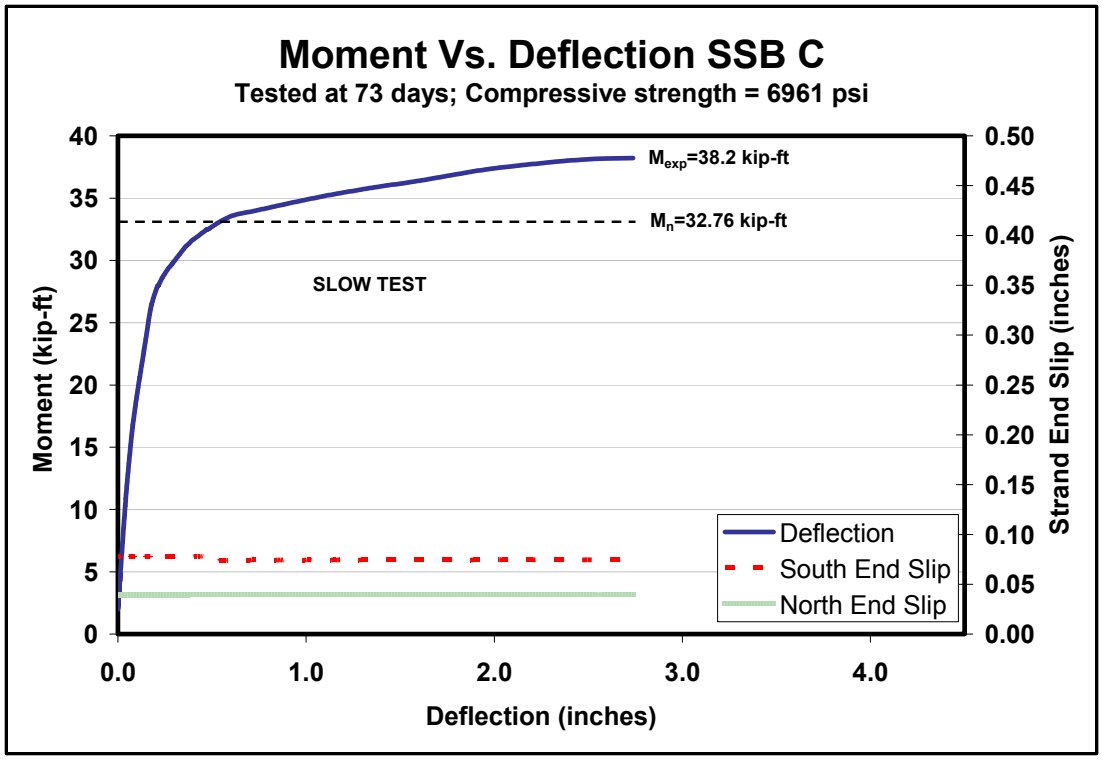

Figure 7.7 Moment versus deflection for SSB C

Figure 7.8 Failure of SSB C

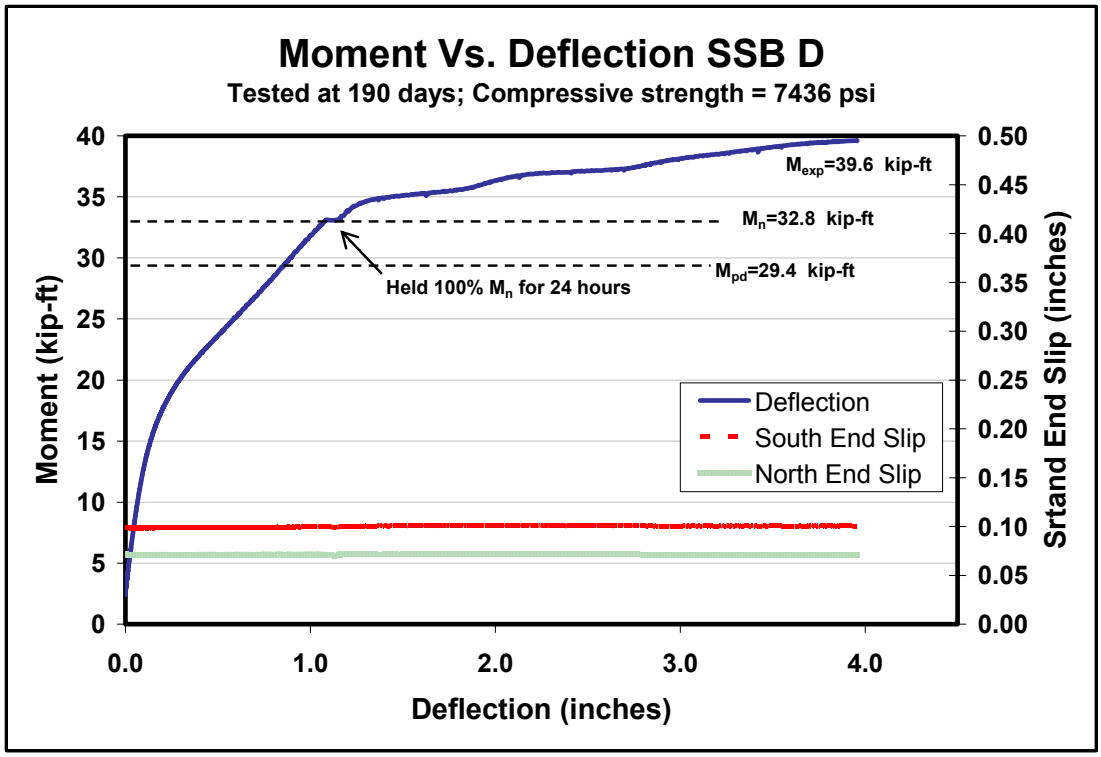

Figure 7.9 Moment versus deflection for SSB D

Figure 7.10 Failure of SSB D

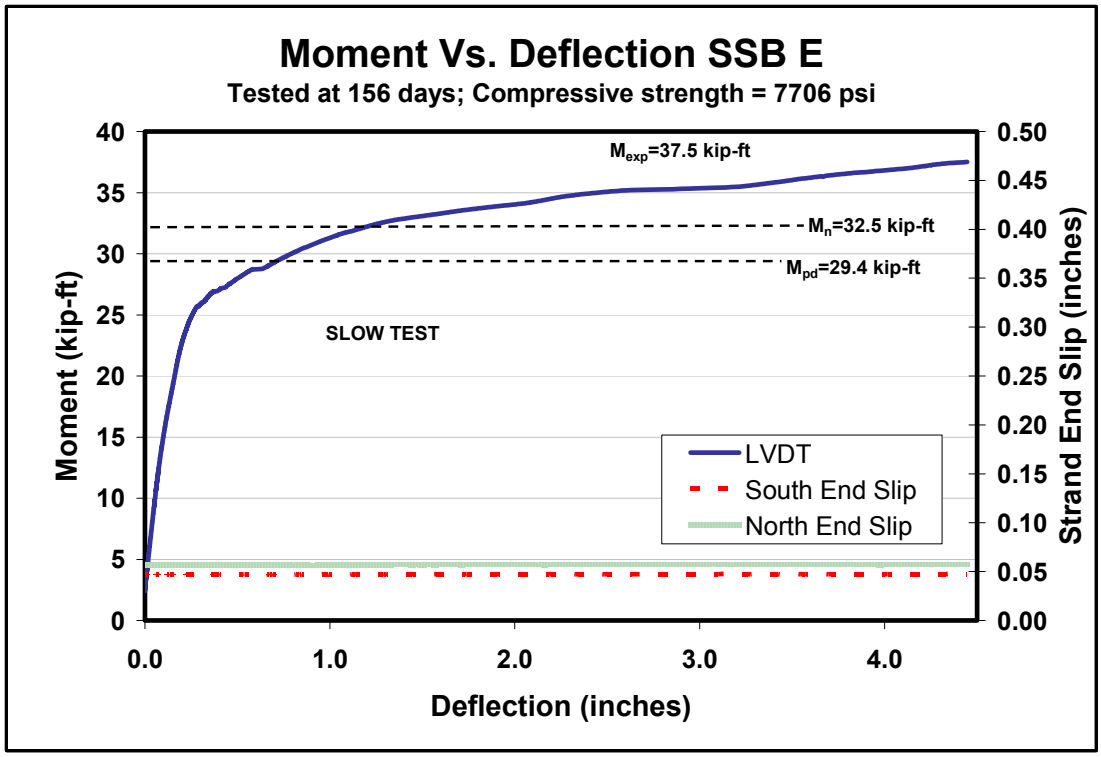

Figure 7.11 Moment versus deflection for SSB E

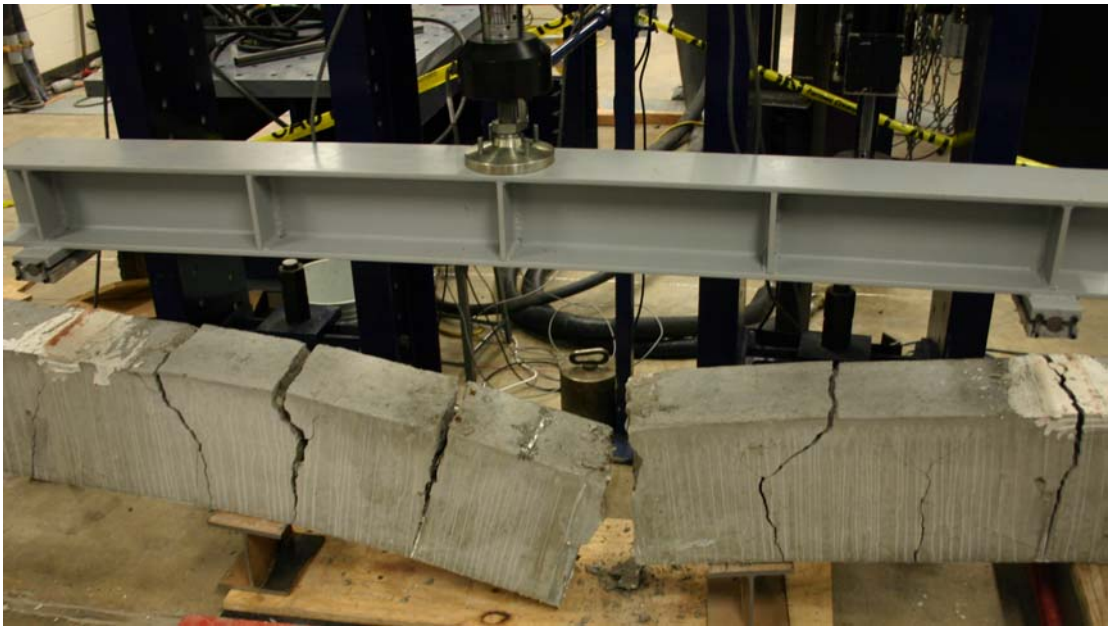

Figure 7.12 Failure of SSB E

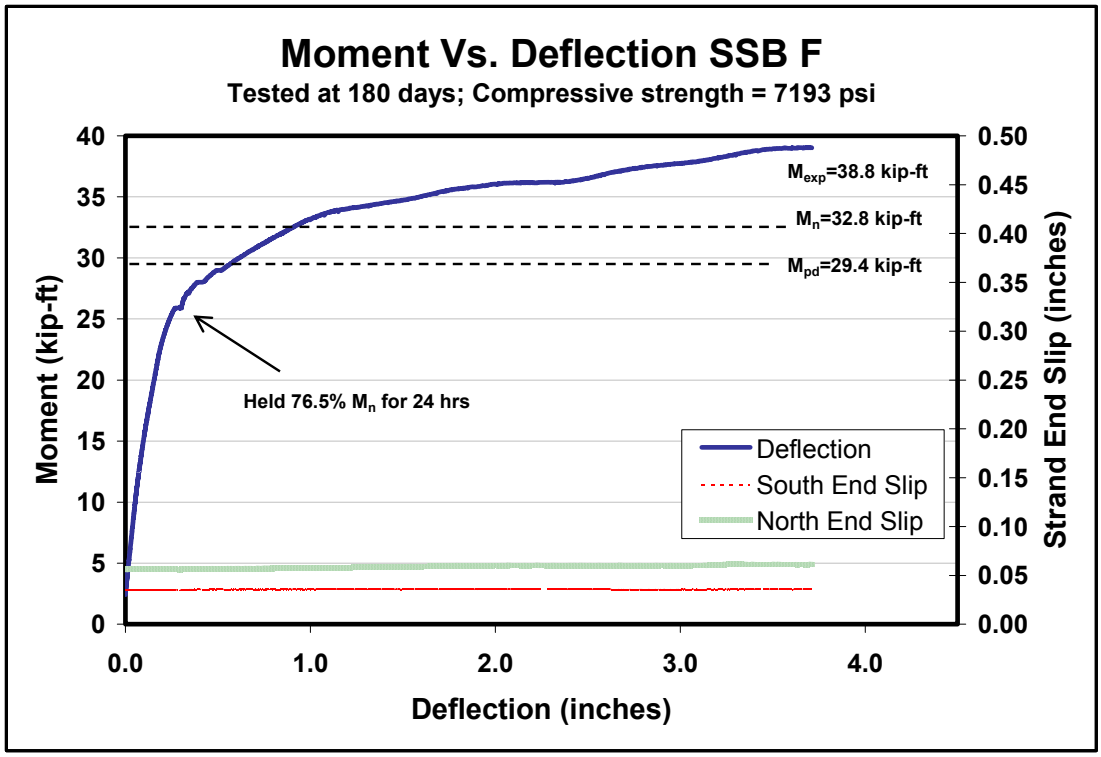

Figure 7.13 Moment versus deflection for SSB F

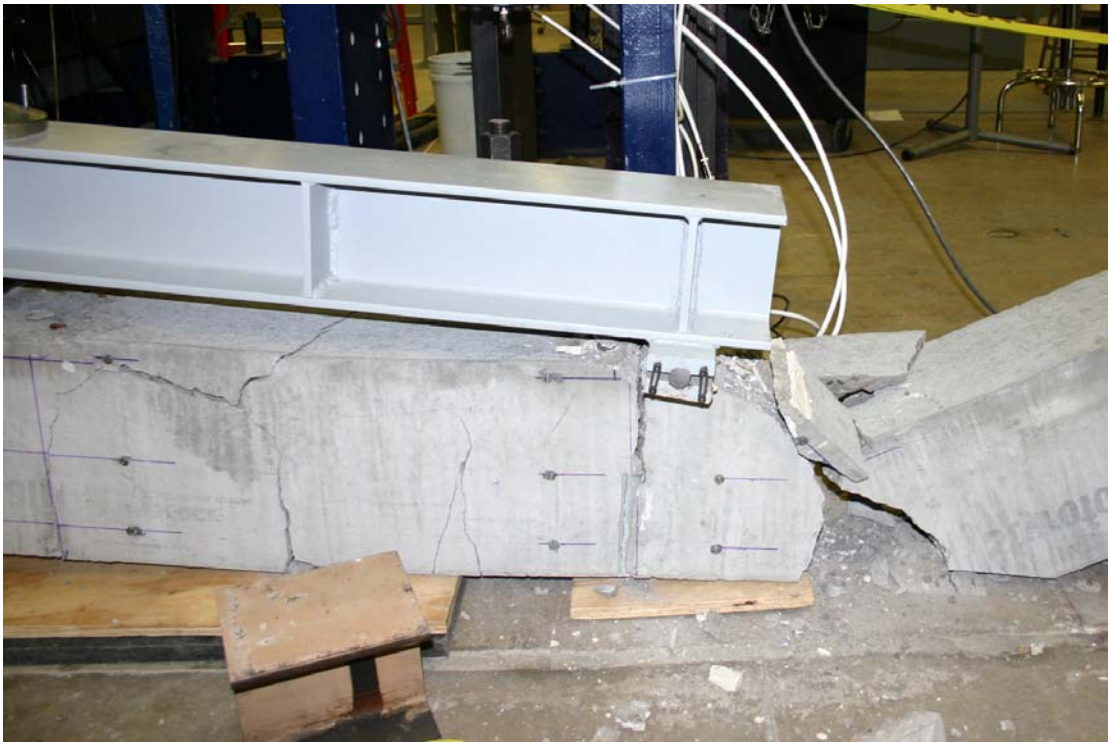

Figure 7.14 Failure of SSB F

7.3.2 TSB Specimen Flexural Results

A moment versus deflection graph for each TSB specimen shows that each one surpassed its nominal-moment capacity and failure by strand rupture, Figures 7.15 – 7.26. Also, end slip during loading is plotted for each specimen.

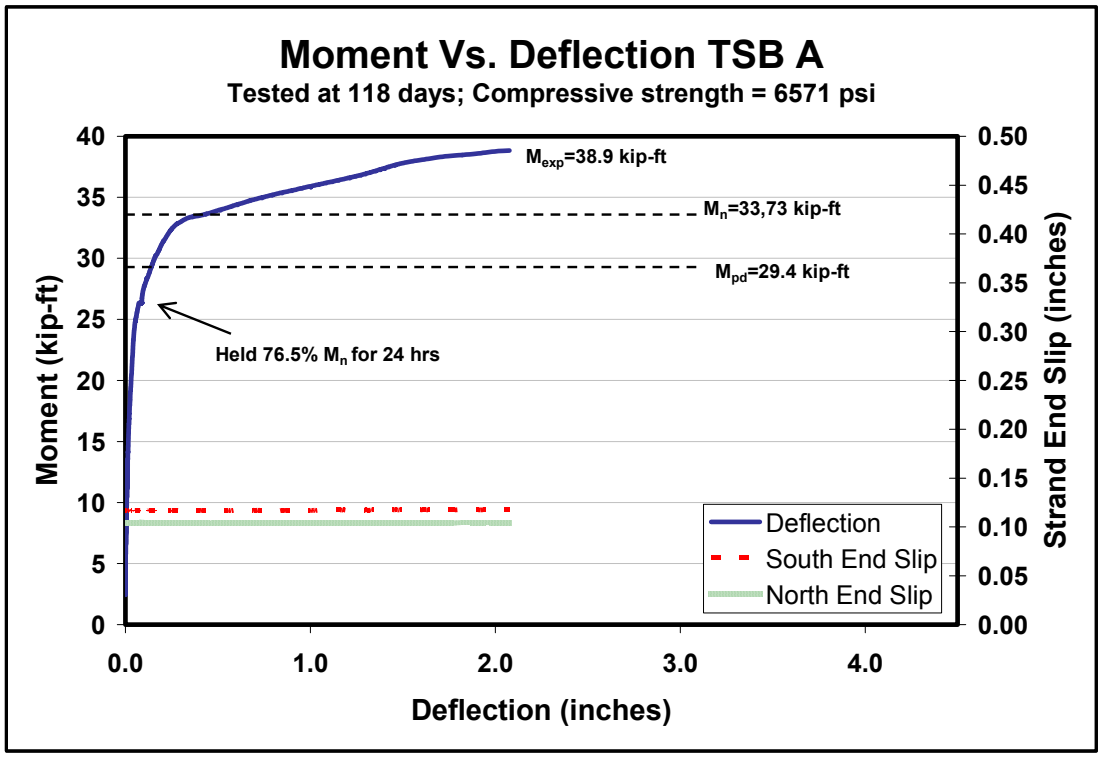

Figure 7.15 Moment versus deflection for TSB A

Figure 7.16 Failure of TSB A

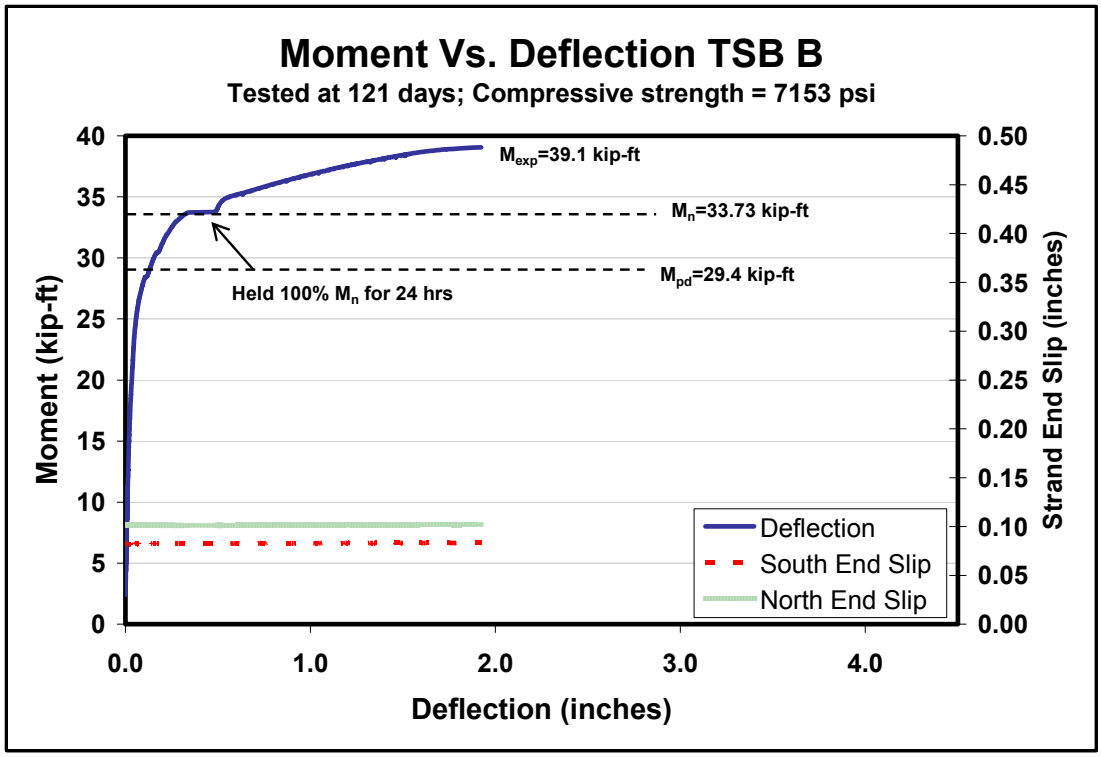

Figure 7.17 Moment versus deflection for TSB B

Figure 7.18 Failure of TSB B

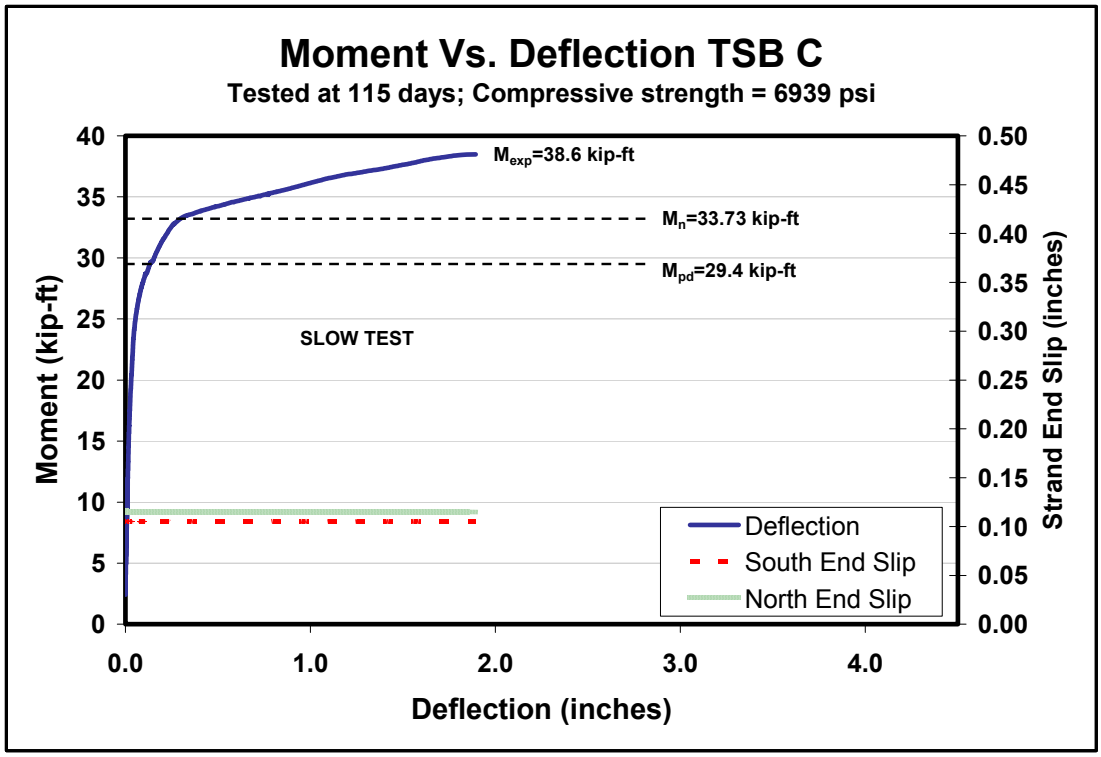

Figure 7.19 Moment versus deflection for TSB C

Figure 7.20 Failure of TSB C

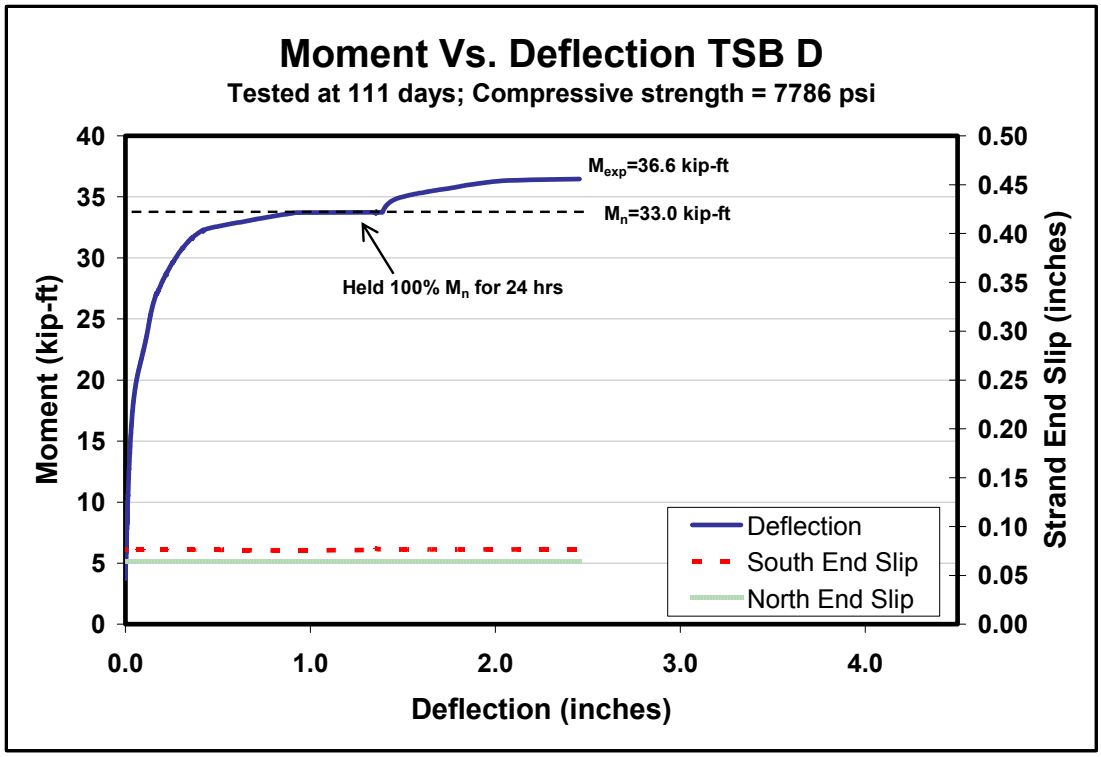

Figure 7.21 Moment versus deflection for TSB D

Figure 7.22 Failure of TSB D

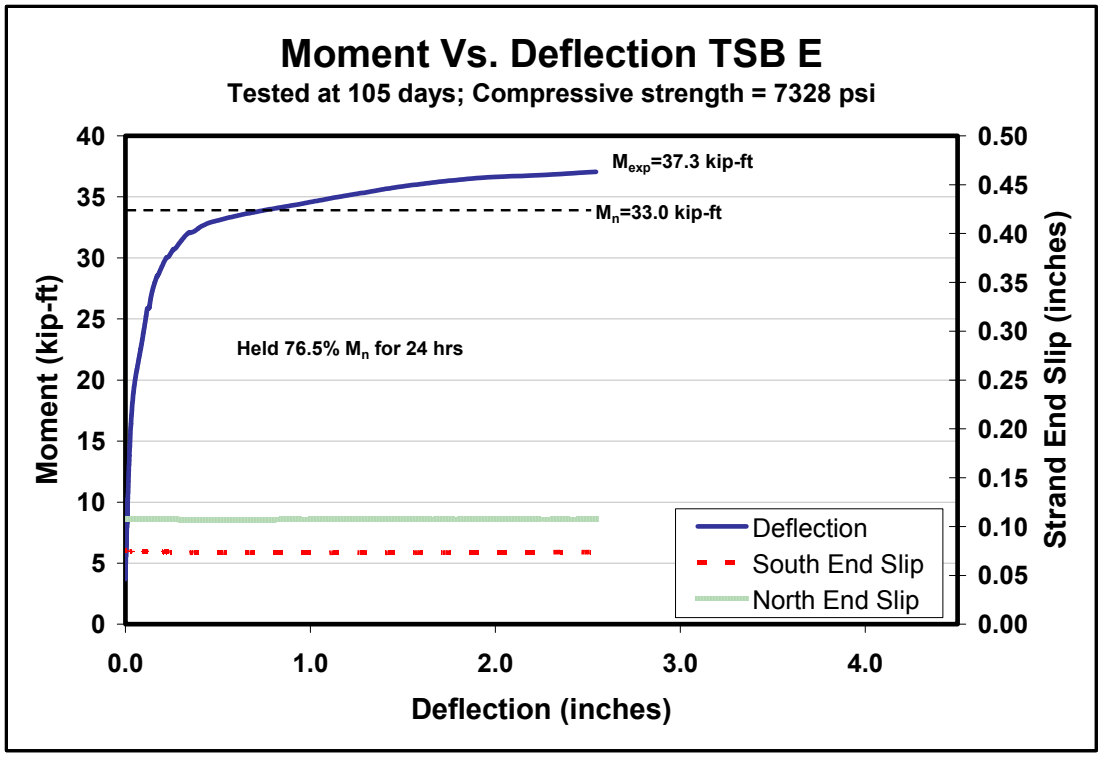

Figure 7.23 Moment versus deflection for TSB E

Figure 7.24 Failure of TSB E

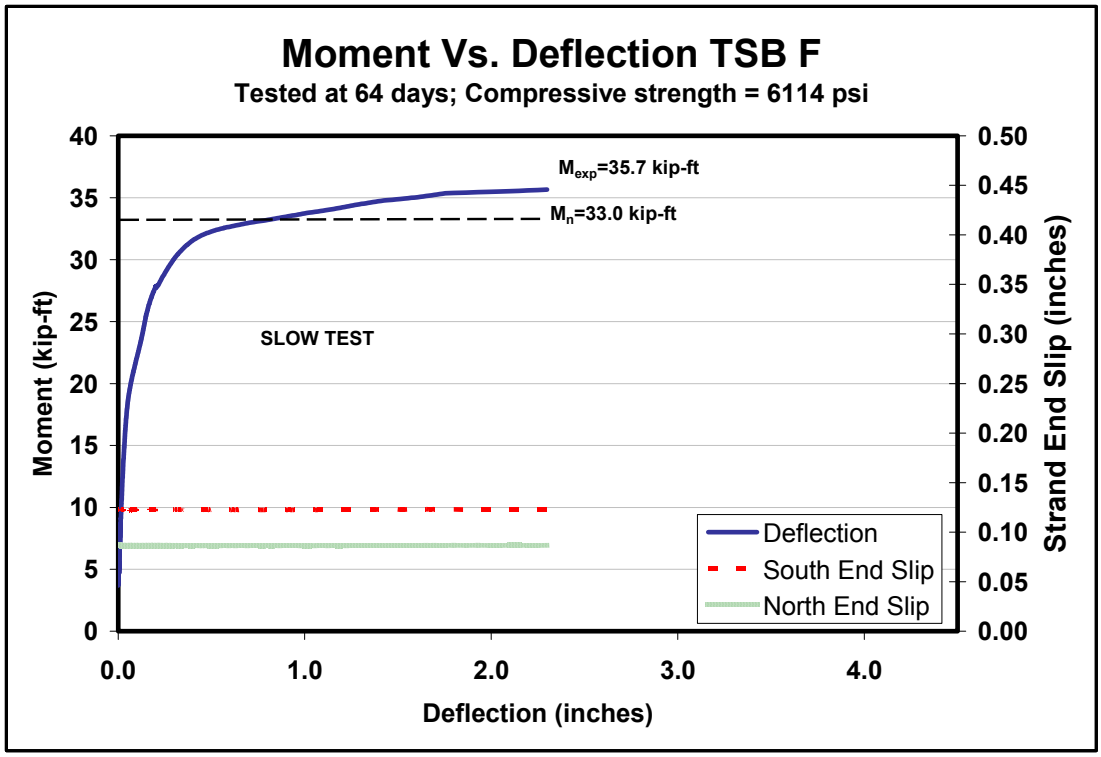

Figure 7.25 Moment versus deflection for TSB F

Figure 7.26 Failure of TSB F

7.3.3 TB Specimen Flexural Results

A moment versus deflection graph for each TB specimen shows that each one surpassed its nominal-moment capacity and failure by strand rupture, Figures 7.27 – 7.34. Also, end slip during loading is not shown as it was for the single-strand specimens because no additional end-slip occurred during the load test to failure.

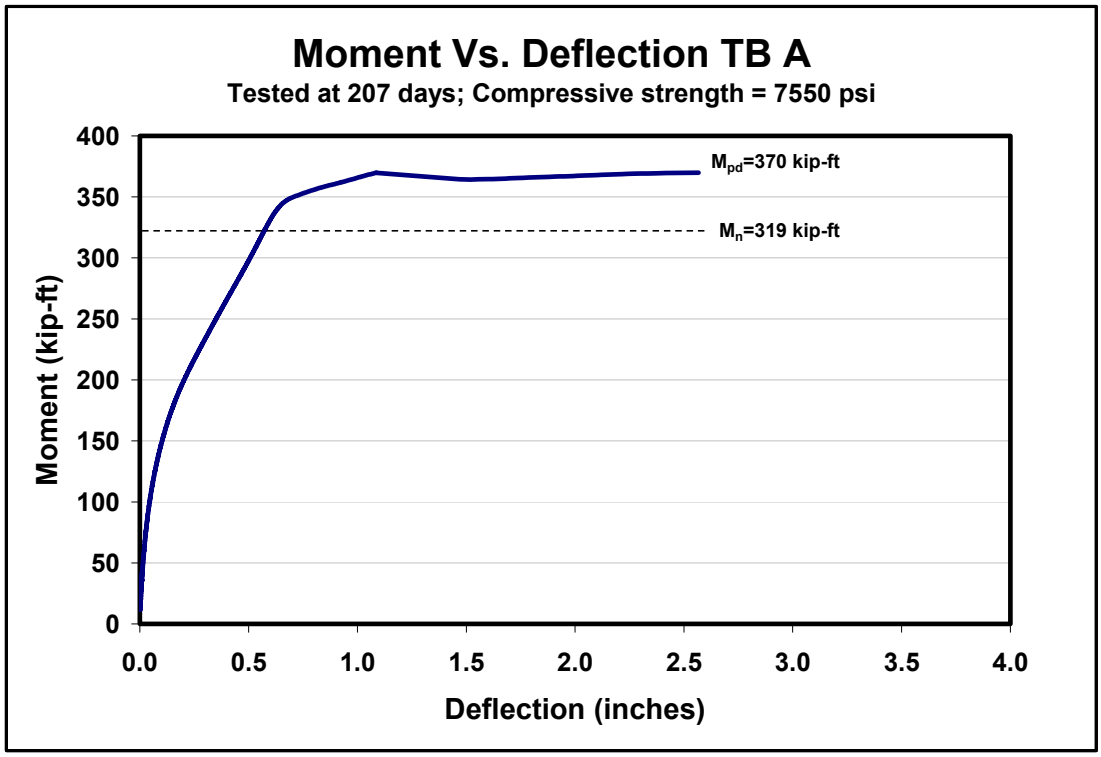

Figure 7.27 Moment versus deflection for specimen TB A

Figure 7.28 Failure of TB A

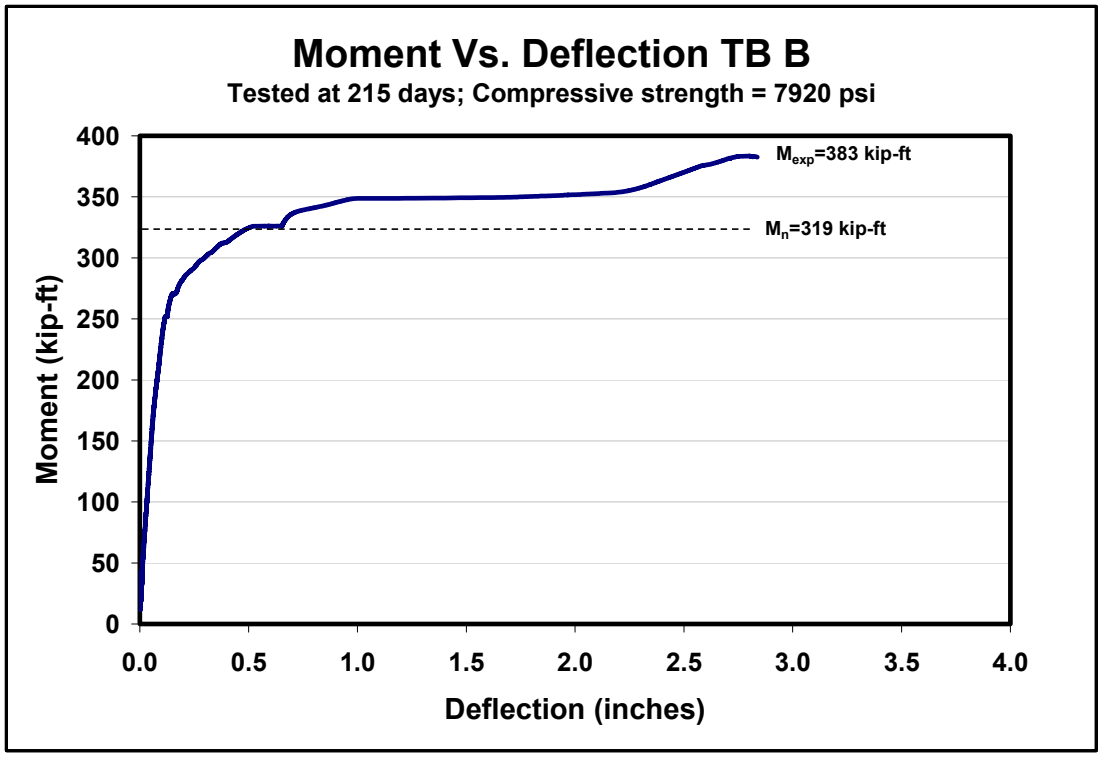

Figure 7.29 Moment versus deflection for specimen TB B

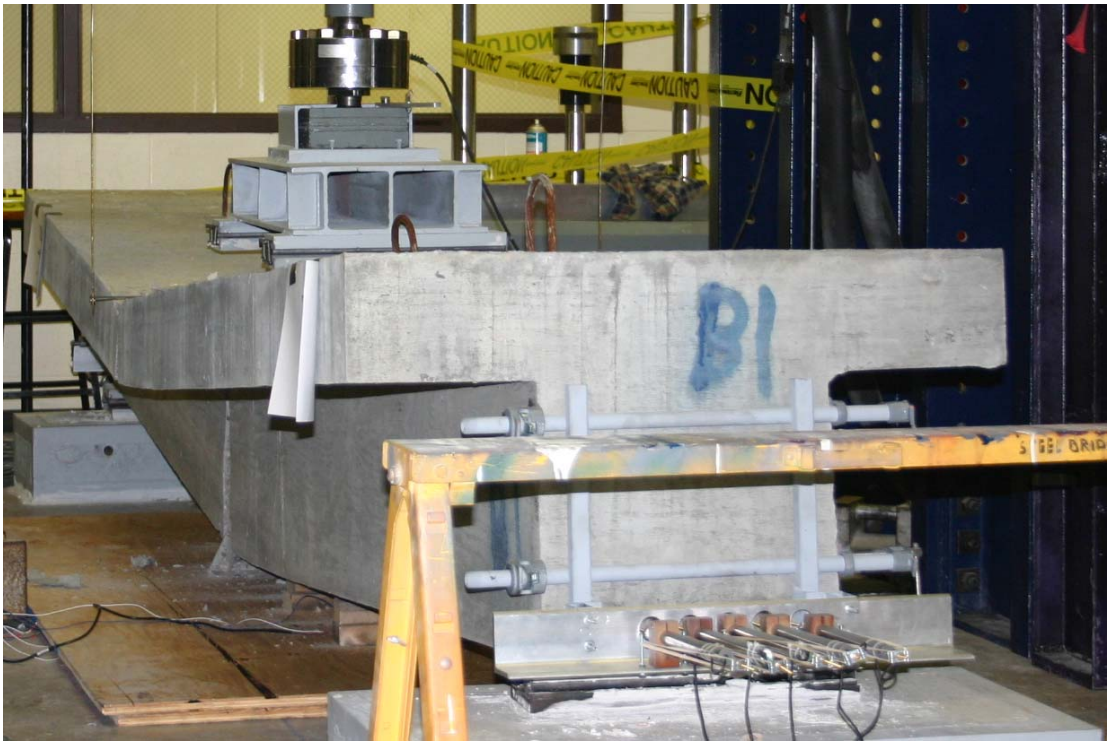

Figure 7.30 Failure of TB B

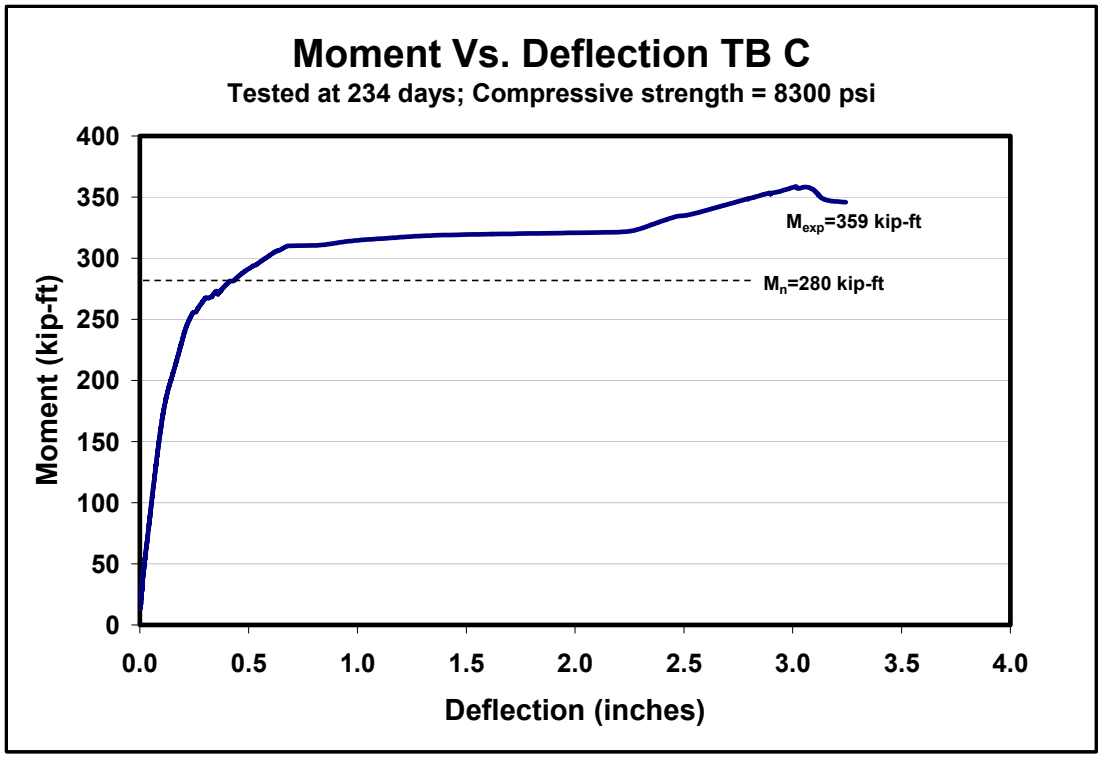

Figure 7.31 Moment versus deflection for specimen TB C

Figure 7.32 Failure of TB C

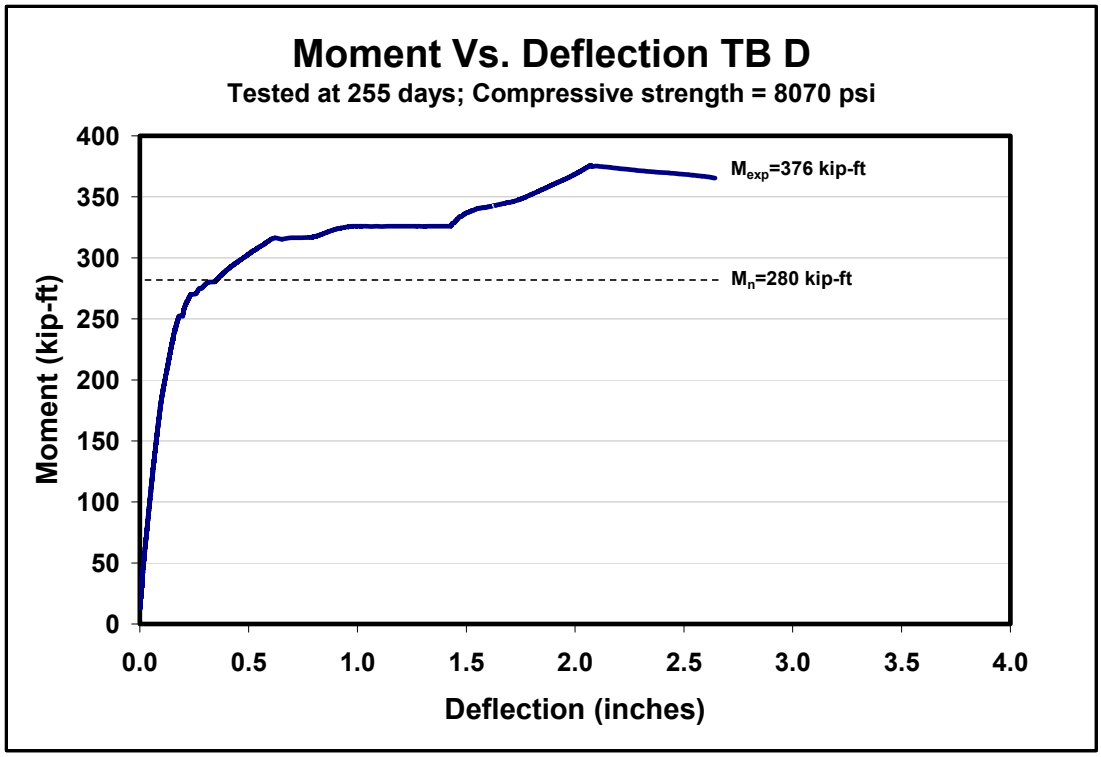

Figure 7.33 Moment versus deflection for specimen TB D

Figure 7.34 Failure of TB D

7.3.4 Comparison of Flexural Results

Figures 7.35 and 7.36 present the moment versus defection for the single-strand specimens tested at embedment lengths of 6'-1" and 4'-10", respectively. It can be seen that all specimens performed similar. Moment versus deflection curves for the T-beam specimens are shown in the same graph (Figure 7.37).

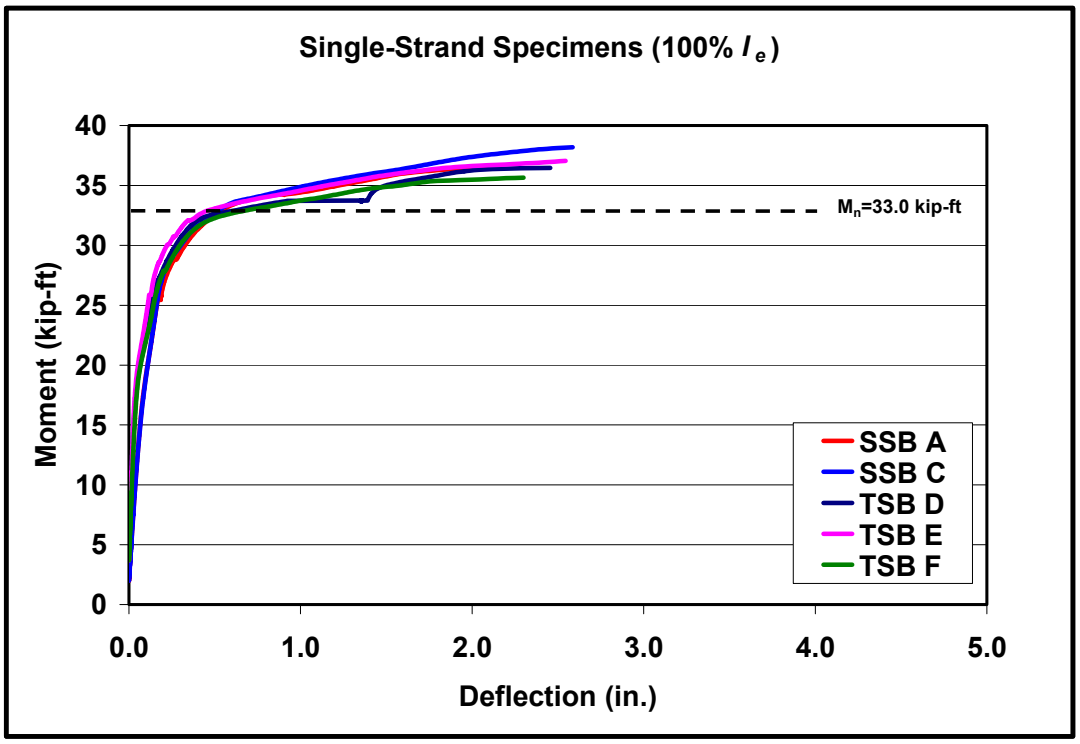

Figure 7.35 Moment versus deflection for all single strand specimens with 100% l_e

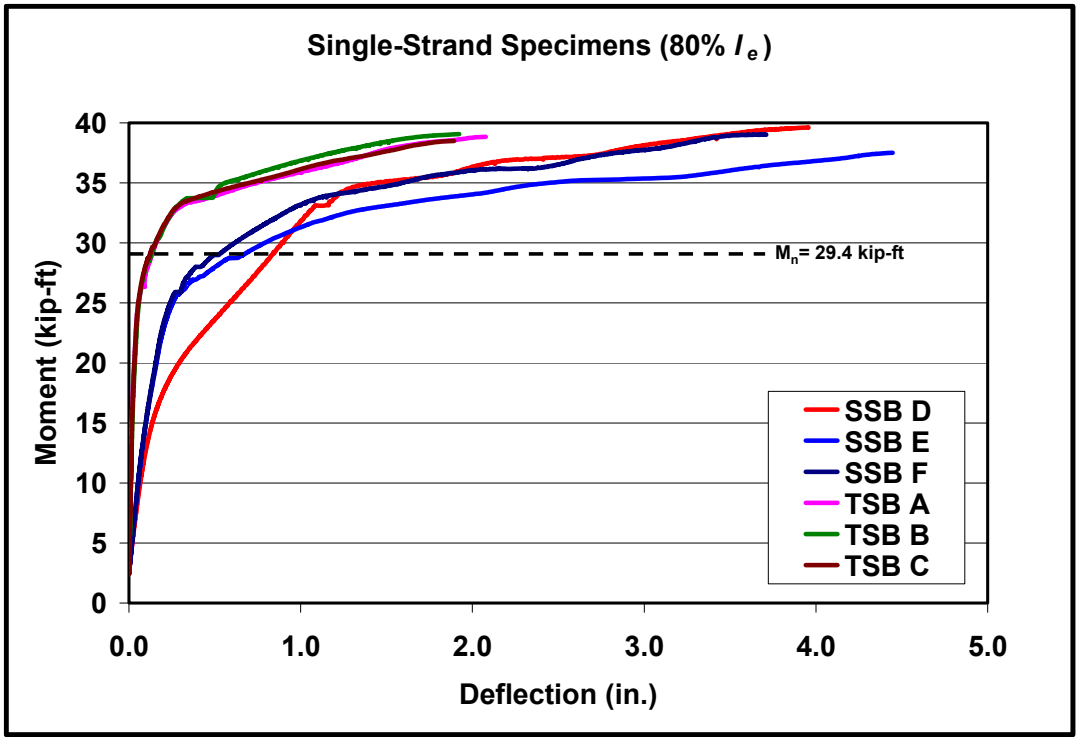

Figure 7.36 Moment versus deflection for all single strand specimens with 80% I_e

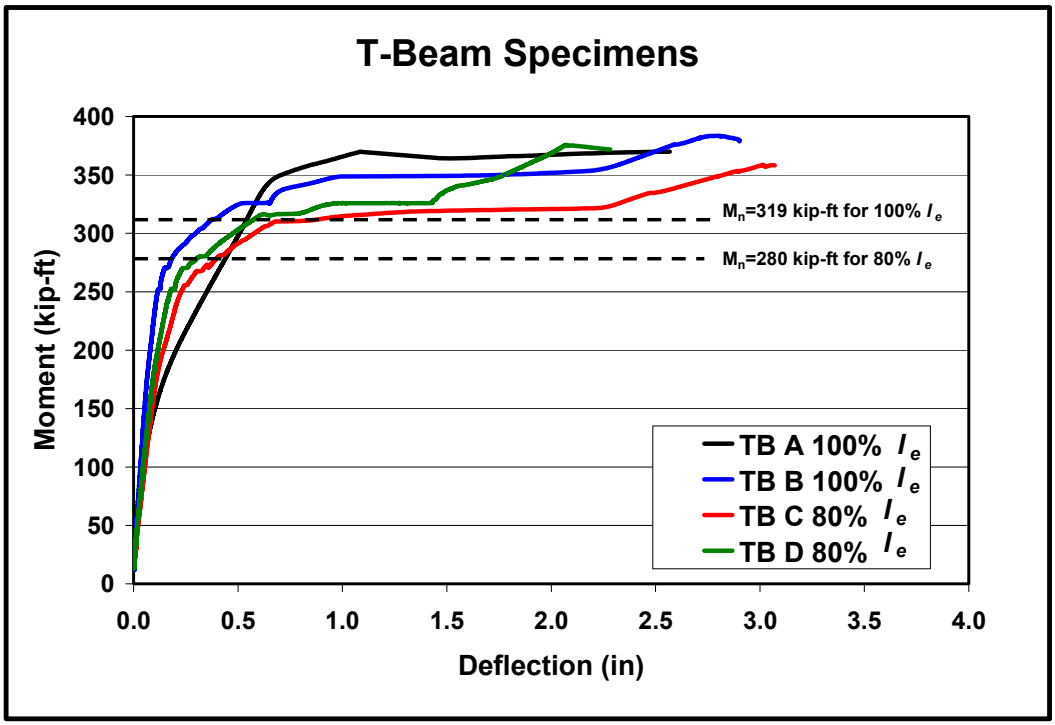

Figure 7.37 Moment versus deflection for all TB specimens

7.4 VWSG Results

As noted in a Chapter Six, VWSGs were embedded in three of the flexural specimens, SSB A, TSB D, and TB A. Gages were used to evaluate time-dependent deformations and compare with those predicted with code expressions. Prestress losses were calculated with the PCI method and the comparisons with experimental results can are shown in Tables 7.6-7.8. On average, the difference between the code predictions and experimental results are between 3-6 ksi.

Table 7.6 Comparison of prestress losses for SSB A

Time (Days)	PCI	Experimental
Release	196	198
2	196	197
8	191	194
17	189	193
23	189	190
35	188	191
55	187	190
84	186	189
111	185	188

all values in ksi

Table 7.7 Comparison of prestress losses for TSB D

Time (Days)	PCI	Experimental
Release	196	199
11	190	197
45	187	194
74	186	193
103	185	191
104	185	191
109	185	191

all values in ksi

Table 7.8 Comparison of prestress losses for TB A

Time (Days)	PCI	Experimental
Release	192	195
2	189	193
8	186	191
17	183	190
23	183	188
35	181	187
55	180	185
84	179	184
205	177	179

all values in ksi

CHAPTER EIGHT - DESIGN AND FABRICATION OF IT SPECIMENS

Inverted-T (IT)-shaped girders were cast in order to determine the long-term prestress losses of prestressed members cast with the proposed SCC mixture. Creep and shrinkage were isolated from one another and time-dependent losses of both these factors were determined.

8.1 IT Properties

Four ITs, twelve feet in length, were cast in order to determine the time-dependent losses of bridge girders with SCC. A twelve-foot length was considered to be adequate for this SCC mixture because previous tests concluded that a six-foot development length was more than adequate to achieve full bond. The girder type used for this part of the project was the IT600. The name is a metric designation and the 600 refers to the girder cross section being 600 mm in width at the bottom and 600 mm in height. The cross section for the IT600 can be seen in Figure 8.1. Table 8.1 presents geometric properties and other useful properties of the IT600. Since the cast specimens differed slightly from the dimensions on the plans, actual dimensions of the specimens were measured and then used for all calculations.

Of the four girders cast, two had the prestressing strand stressed to 75% of the guaranteed ultimate tensile stress (f_{pu}). These two specimens were designated as FT #1 and FT #2, where FT stands for fully tensioned. FT #1 and FT #2 were used to determine the combined long-term effects of creep, shrinkage, and relaxation. Elastic shortening, which is determined just after detensioning, was also determined from these specimens.

In addition, the two fully tensioned specimens were used to evaluate transfer lengths by the method discussed in Chapter 5.

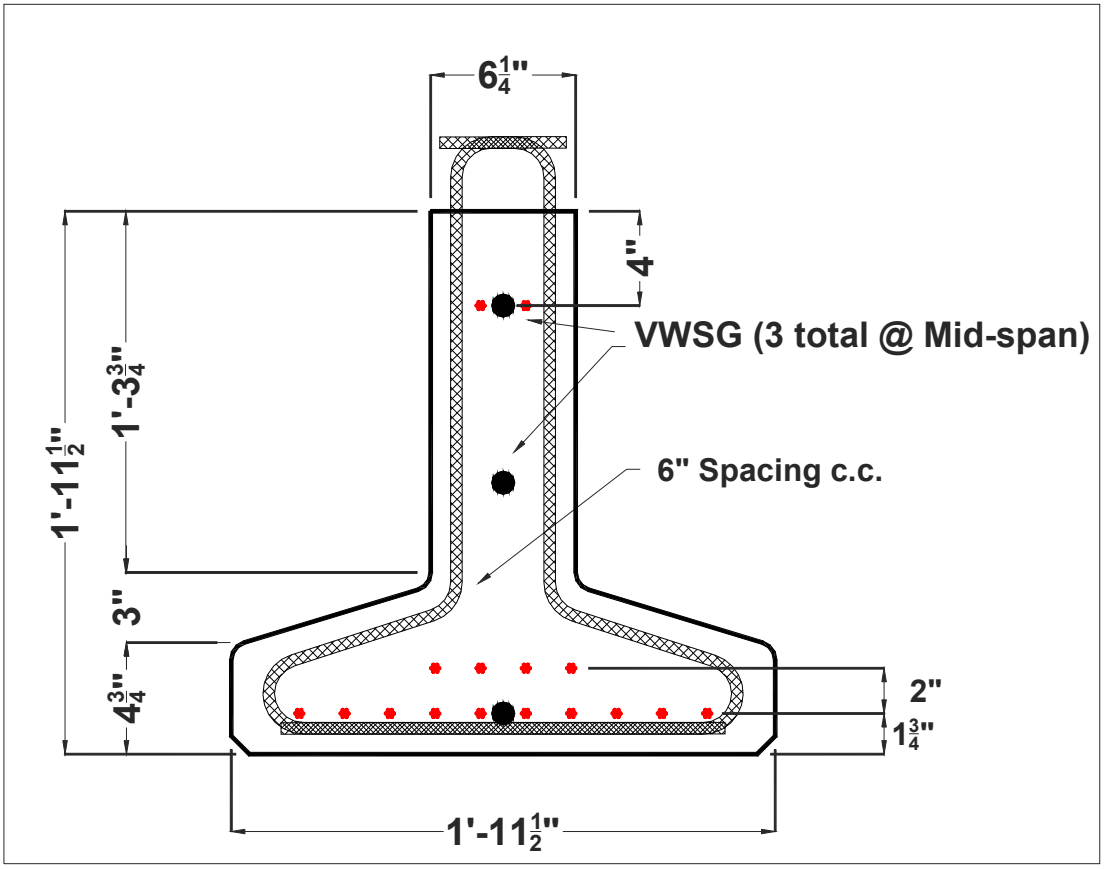

Figure 8.1 Cross section of IT600

Table 8.1 Geometric properties of IT600

A =	256	$inch^2$	I =	12,822	$inch^4$
E_{ci} =	3,600	ksi	E_c =	5,300	ksi
f_{ci} =	6,280	psi	f_c =	7,880	psi
Y_{bot} =	8.45	inch	*e* =	3.86	inch
H =	23.5	inch	L =	12	feet
M_{sw} =	4.41	kip-ft	V/S =	2.87	inch
f_{pj} =	198	ksi	A_{ps} =	2.448	$inch^2$
E_{ps} =	28,500	ksi	RH =	65	%

The remaining two specimens, used to determine the effect of shrinkage alone, had the prestressing strand tensioned to a "hand-tight" condition. Designations of these specimens were UT #1 and UT #2, where UT stands for untensioned. The same number of strands were used in the untensioned specimens as in the fully tensioned specimens so that both specimen types had identical transformed section properties.

Long-term strains were recorded by use of embedded, vibrating-wire strain gages (VWSGs), Figure 8.2. The strain gages selected were the Model VCE-4200 Vibrating Wire-Embedded Strain Gage, manufactured by Geokon, Inc., Lebanon, New Hampshire. The manufacturer recommended this gage type for this project for its long-term strain and temperature-measuring capabilities of the concrete. Strains were measured using the vibrating-wire principle: a length of steel wire is tensioned between two end blocks that are embedded directly in the concrete. Deformations of the concrete mass will cause the two end blocks to move relative to one another, thus altering the tension in the steel wire. The tension is measured by plucking the wire and measuring its resonant frequency of vibration using an electromagnetic coil.[46] The gages are connected to a data-acquisition system, and strain and temperature recordings are taken periodically. A correction calculation is needed to convert the strain reading into a true mechanical strain.[40]

$$\mu_{actual} = (R_1 - R_0)B + (T_1 - T_0)(C_1) \tag{7.1}$$

where

μ_{actual} = actual strain (in/in);
R_0 = initial strain reading (in/in);
R_1 = next strain reading (in/in);
B = batch calibration factor given by manufacturer;
T_0 = initial temperature reading (^oC);
T_1 = next temperature reading (^oC); and
C_1 = coefficient of expansion of steel (wire) $(12.2\ \mu\varepsilon/^oC)$.

Three VWSGs were placed at mid span of each specimen. One was placed at a depth of four inches from the top (location of the top strands), another at 8.25 inches from the bottom (neutral axis of the cross section), and the final one at two inches from the bottom (location of bottom layer of strands), Figure 8.3. Strains from the gage at the bottom strand height were converted to stress and used for comparison purposes with code expressions. The other two gages were used to make sure the strains in the section remained linear and the bottom gage was reading correctly. To determine the stress from the corrected strain values, Hooke's Law was used.

$$\sigma = E_{ps}\varepsilon \tag{7.2}$$

where

E_{ps} = modulus of elasticity of prestressing strand (ksi) and
ε = corrected strain value (in/in).

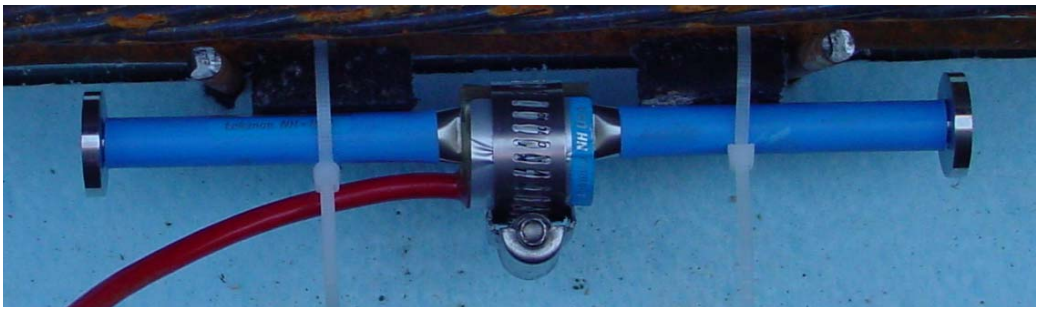

Figure 8.2 VWSG closeup

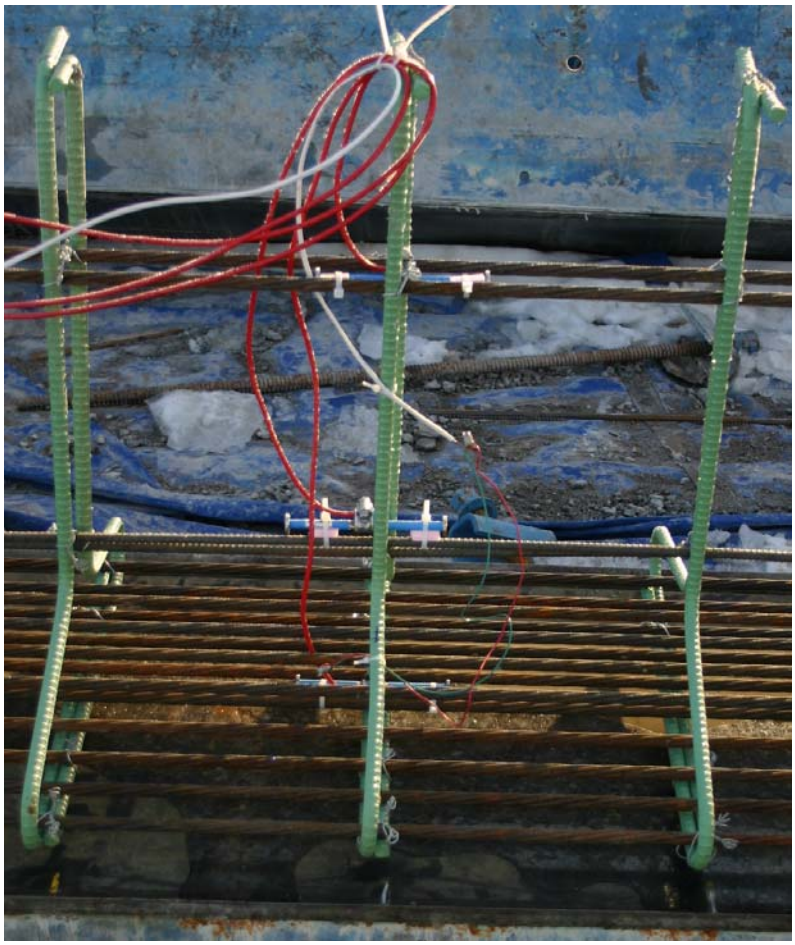

Figure 8.3 VWSGs at mid span

A load cell was placed at the "dead" end of the prestressing bed, Figure 8.4, in order to get an exact tensile force of the prestressing strand after jacking. The nominal value of the jacking stress, f_{pj}, was calculated to be 202.5 ksi. However, experimentally it was found to be 198 ksi and this value will be used as the jacking stress (f_{pj}) for all comparison calculations against code expressions. Strains were zeroed just prior to detensioning. Therefore, subsequent strain changes were due to prestress losses and not the concrete hardening during the setting process.

Figure 8.4 Load cell at dead end

Elastic shortening losses occur at the time the prestress force is transferred to the concrete and can be eliminated from long-term calculations. With use of low-relaxation prestressing strands, the increase in relaxation losses from transfer to final losses is very small compared to creep and shrinkage losses. Hence, individual relaxation losses were not isolated experimentally. Values for relaxation losses were calculated using code expressions. Elastic shortening losses were determined using two fully tensioned specimens and taking the change in stress at the center of gravity of the prestressing strands from just prior to detensioning to just after detensioning.

Long-term, time-dependent prestress losses (creep and shrinkage) were determined by use of both sets of specimens. Prestress loss due to shrinkage was obtained from the two untensioned specimens. Losses due to creep were determined by taking the losses of the fully tensioned specimens and subtracting the abovenoted

shrinkage loss in the untensioned specimens, the elastic shortening loss, and the calculated relaxation loss.

To compare experimental results with design code estimates, intermediate losses needed to be calculated. Most common methods (ACI, PCI, AASHTO) only calculate losses at transfer and at the end of the service life of the member. In order to estimate creep and shrinkage values for periods less than two years, the expression by Corley and Sozen[47] was used. The following equation made it possible to compare creep and shrinkage values for periods less than two years.

$$R = 0.13 \ln(t+1) \tag{7.3}$$

where

R = the total time-dependent proportion and
t = time (days).

This equation made it possible to calculate losses the member was experiencing at different selected days. Other more complex models could have been used to estimate creep and shrinkage values at intermediate time steps. However, since the applicability of these models to SCC has not been established, the general expression as shown in the previous equation 8.3 was chosen.

8.2 IT Fabrication

Fabrication of all IT specimens was performed at Prestressed Concrete Inc., Newton, Kansas. They were cast in the afternoon on February 10, 2005, and detensioned the next morning, February 11, 2005. As was the case with the flexural specimens, inverted-slump flow (spread), VSI, J-Ring, and L-Box tests were performed at the time of casting. The two fully tensioned specimens were cast on the rollaway bed (Figure 8.5)

and the two untensioned specimens (Figure 8.6) on a utility bed. After all internal shear reinforcement was tied into place, the VWSGs were tied into place. After that, the side walls were folded into place, Figure 8.7. Concrete was then poured into the forms, and no internal or external vibration was used on the SCC, Figure 8.8. The following morning, the walls were removed (Figure 8.9) and Whittemoe points (Figure 8.10) were glued onto the concrete two inches from the bottom. Once all the Whittemore points were installed and initial readings were taken, the strands were detensioned by flame cutting, Figure 8.11. Post-detensioning readings were taken and the specimens were placed on a flat bed trailer and shipped to Manhattan, Kansas. They were then monitored for their time-dependent deformations.

Figure 8.5 Tensioned IT specimen

Figure 8.6 Untensioned IT600 specimen

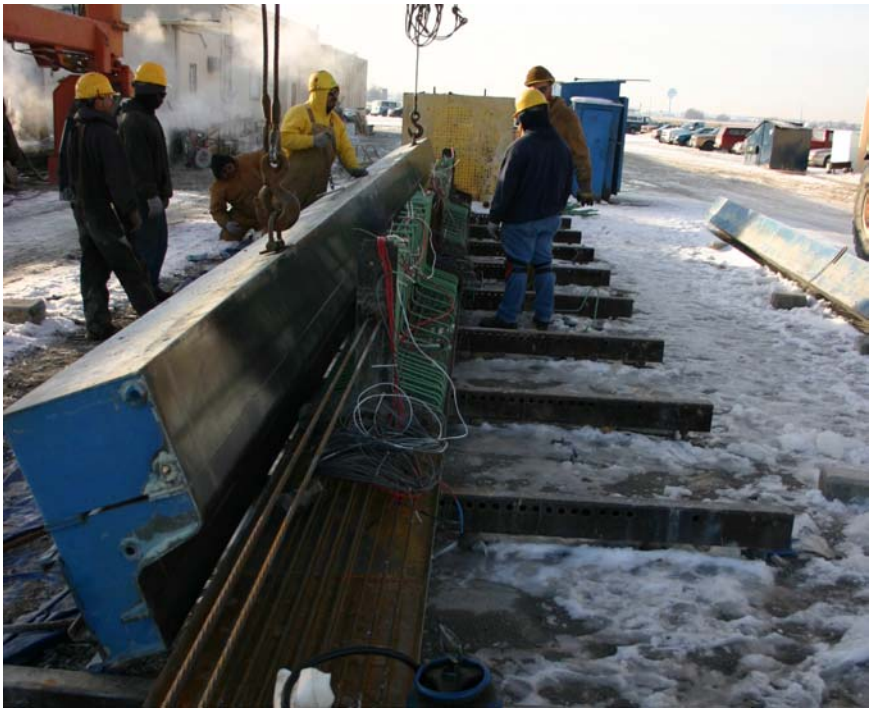

Figure 8.7 Side-form placement for IT600

Figure 8.8 Placement of SCC

Figure 8.9 Side-form removal

Figure 8.10 Application of Whittemore points

Figure 8.11 Flame cutting of strands

CHAPTER NINE - IT SPECIMEN RESULTS

9.1 Material Properties

Inverted-slump flow (spread), VSI, J-Ring, and L-Box tests were performed before the casting of all IT specimens. Also, cylinder breaks that were matched-cured until detensioning were completed at the time of prestress release and at 28 days. Values for compressive strengths and modulus of elasticity for the SCC mixture can be seen in Table 8.1. The inverted-slump flow was measured to be 24 inches, J-Ring 22 inches, and the ratio of h_2/h_1 for the L-Box was 0.85. The VSI was determined by the author to be 0.

9.2 Transfer Length Results

Transfer lengths of the IT specimens were determined by use of concrete surface strains. The procedure for this method is detailed in section 5.2. The concrete strain profile versus specimen length for both FT #1 and FT #2 was plotted to determine transfer lengths. FT #1, Figure 9.1, had transfer lengths of 32 inches on one end and 23 inches on the other end. FT #2, Figure 9.2, had transfer lengths of 24 inches on one end and 28 inches on the other. Ends of the specimens with the greatest transfer lengths were both flame cut at detensioning, while ends with the smaller values underwent a gradual release during detensioning. Transfer length, as predicted by equation 1.1, was 24 inches. The value of 145 ksi was used for f_{se} (calculation shown in A.8). Using the expression for shear design for ACI (50-strand diameters as described in section 11.4.3 of the ACI Building Code), transfer length is 25 inches and 30 inches when using 60-strand diameters as stated by the AASHTO code (eq 5.11.4.1). Experimental values for transfer length were all in general accordance with the values recommended by code equations.

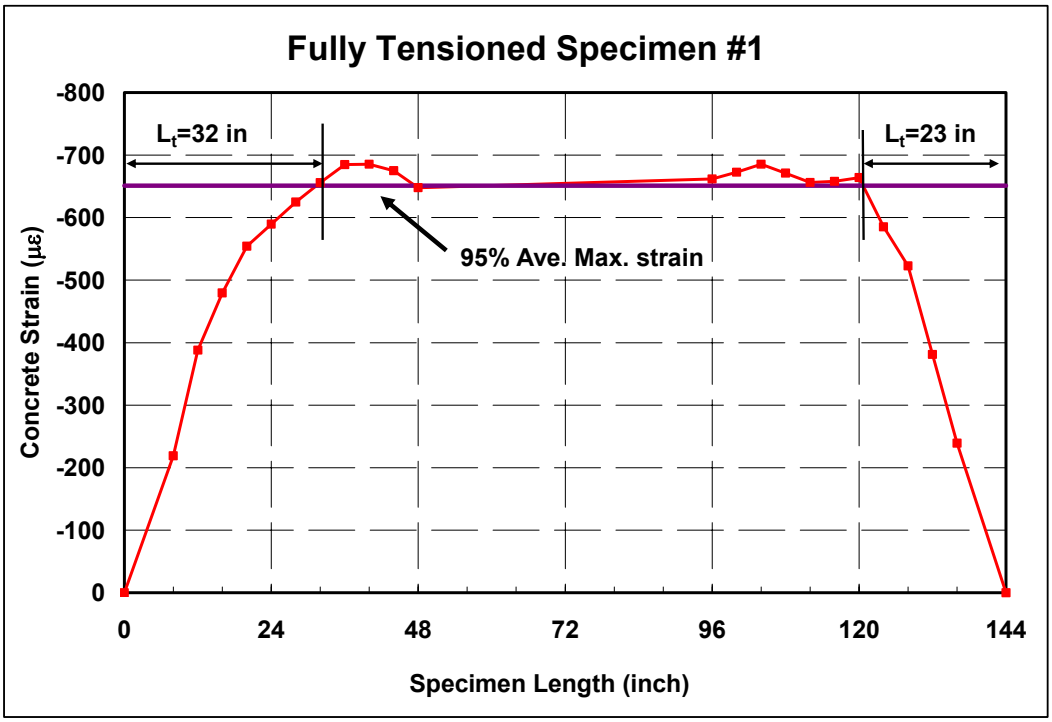

Figure 9.1 Concrete strain versus specimen length for FT #1

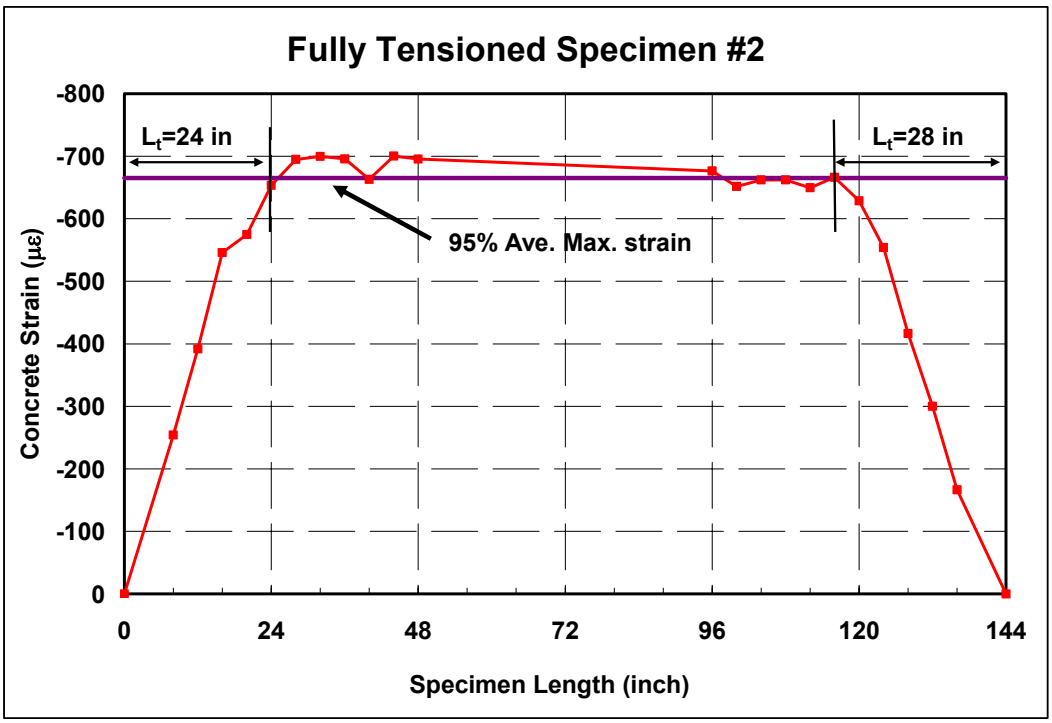

Figure 9.2 Concrete strain versus specimen length for FT #2

9.3 Prestress Loss Results

Using methods for determining prestress losses as described in Chapter Two and presented in section A.8, all values for elastic shortening, creep, shrinkage, and relaxation were calculated, see Table 9.1. Experimental results for modulus of elasticity for the concrete (E_{ci} & E_c) were used for calculations using code expressions. Experimental values recorded from the two fully tensioned IT specimens are also presented. (The average of the two specimens is given.) It was found that ACI and PCI methods gave the same results; therefore, they are presented in the same row. Experimental values for elastic shortening, creep, shrinkage, and relaxation are also given.

Table 9.1 Summary of time-dependent losses

Method	Elastic Shortening	Creep	Shrinkage	Relaxation	Effective Prestress Stress
AASHTO	19.3	29.3	7.3	1.5	141
ACI/PCI	17.3	23.6	6.8	3.1	147
KDOT	18.9	29.3	7.3	1.3	141
Experimental*	18.8	23.5	0.7	--	155

all values in ksi
* Data recorded at 514 days

Strains have been recorded throughout the life of the specimens. By using equation 8.3, time-dependent losses were estimated at several intermediate days and compared to the experimentally determined values. Results are shown in Table 9.2 and Figure 9.3 in graphical form.

Table 9.2 Strand stress predictions at various days

Time (Days)	AASHTO	ACI/PCI	KDOT	Experimental
Transfer	175	176	175	180
25	162	165	162	170
50	159	162	159	166
75	157	161	157	163
96	156	160	156	162
120	155	159	155	161
144	153	158	154	158
200	152	157	153	158
240	151	156	152	157
340	149	155	150	156
450	148	154	149	156
514	148	153	148	155
Long Term	141	147	141	--

all values in ksi

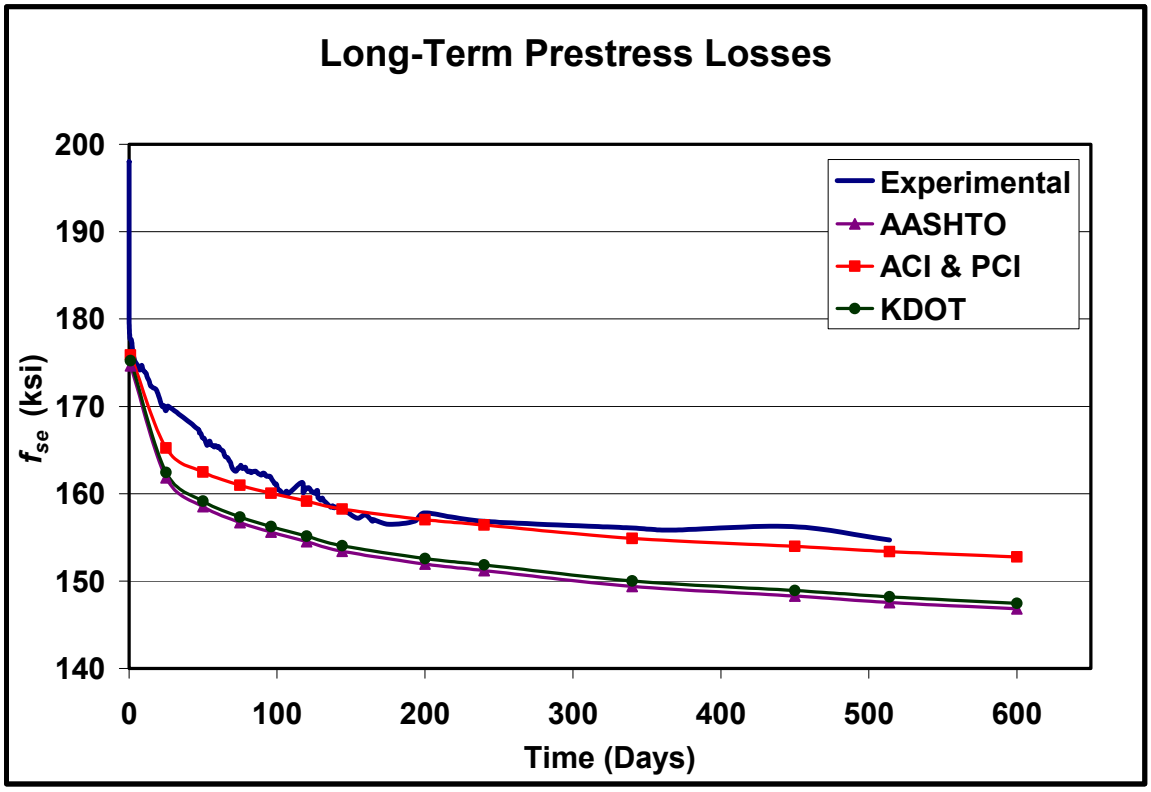

Figure 9.3 Strand stress predictions at various days

It can be seen from Table 9.1 that the experimental specimens did not experience as much of the prestress loss due to shrinkage as predicted by code equations. The two untensioned specimens were used to isolate the shrinkage loss, and the resulting values along with the PCI predicted values can be seen in Figure 9.4 (average of both specimens are shown). The maximum range for shrinkage was 3 ksi, but 0.7 ksi was used at 514 days because that was the present value. The erratic nature of the experimental results is due to the fact that the specimens were kept in the open and were able to experience more moisture and sunlight than normal bridge girders.

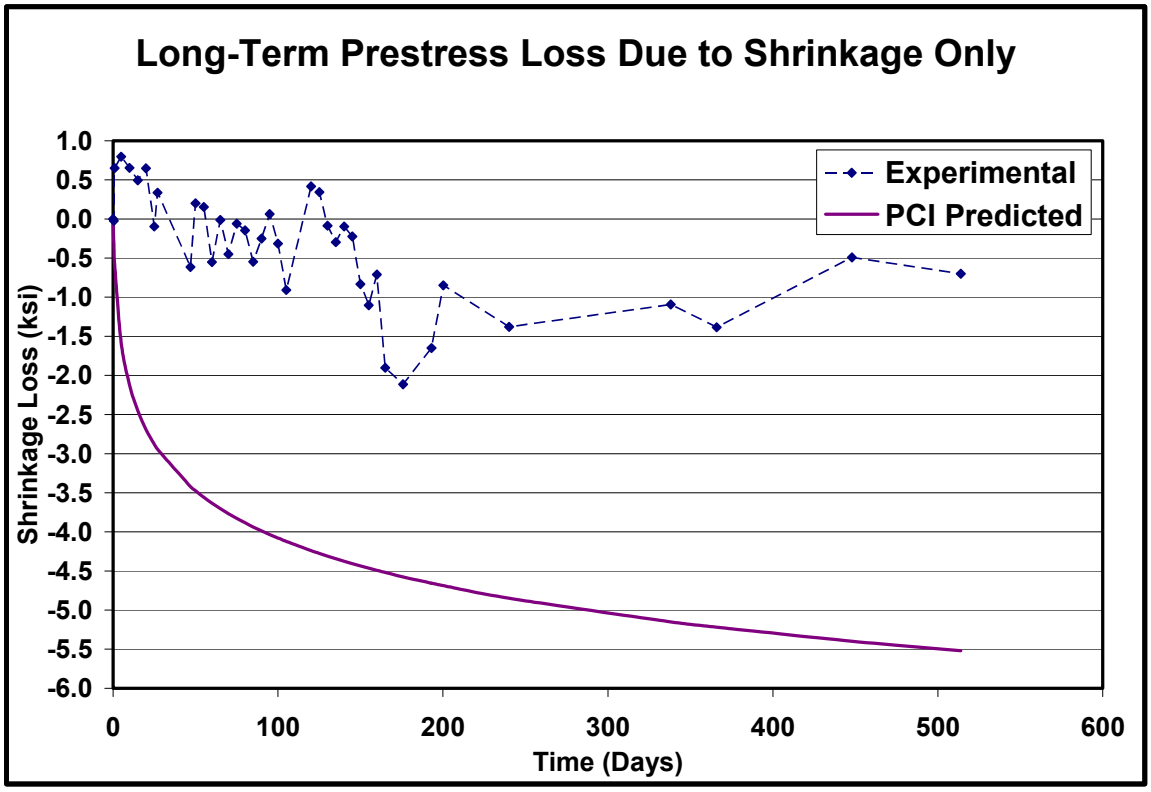

Figure 9.4 Prestress loss due to shrinkage only

Since three VWSGs were placed at mid span of the specimens at varying depths the concrete strains versus depth for both fully tensioned specimens could be plotted. From Figures 9.5 and 9.6, it can be seen that the strains remained linear throughout the life of the specimens, as expected.

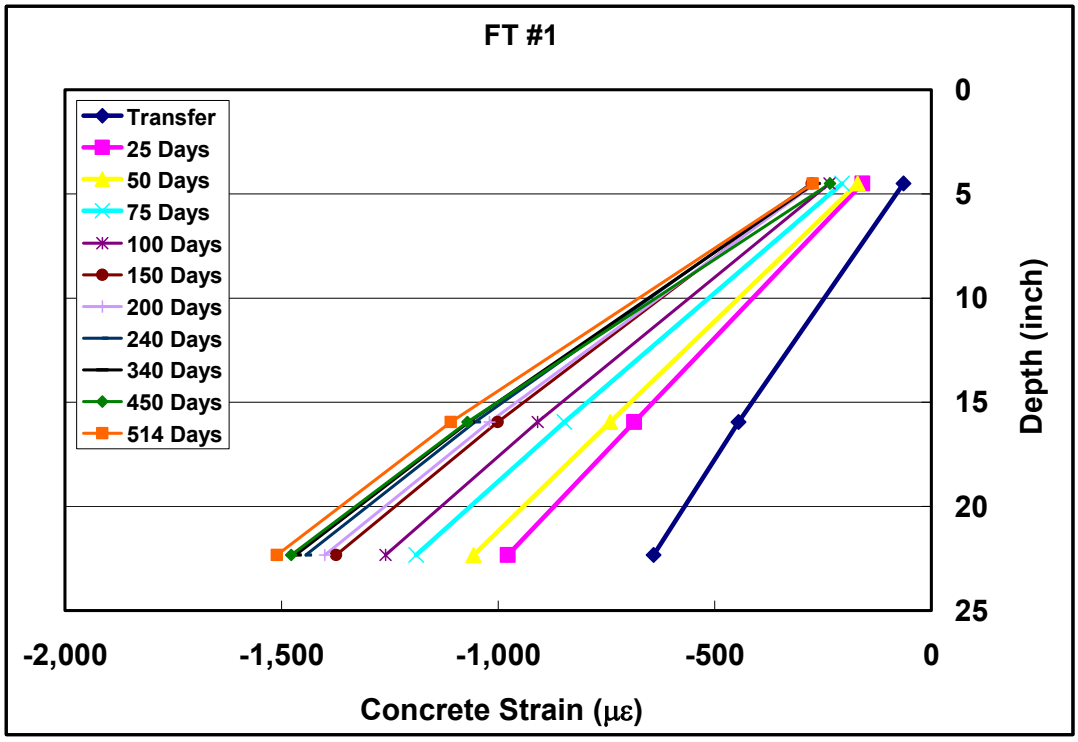

Figure 9.5 Concrete strain versus depth for FT #1

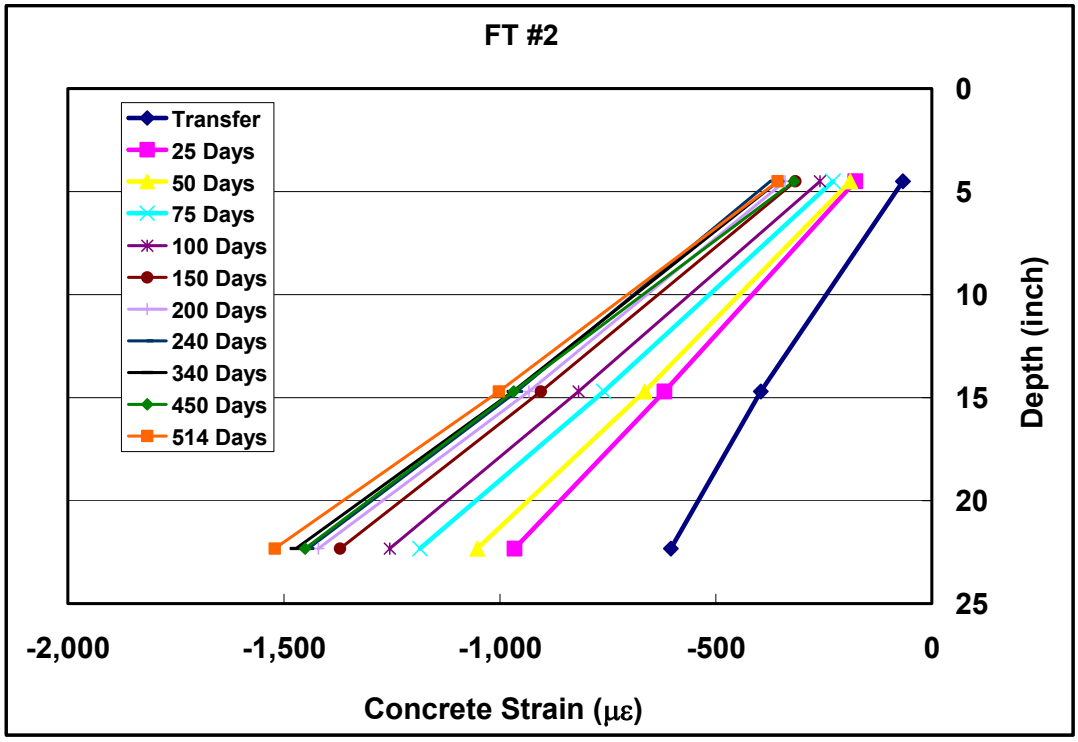

Figure 9.6 Concrete strain versus depth for FT #2

CHAPTER TEN - CREEP AND SHRINKAGE PRISMS

Creep and shrinkage are important factors in determining time-dependent deformations of precast members. ACI Committee 209 released a report which presented a unified approach to predicting the effect of moisture changes, sustained loading, and temperature on prestressed concrete structures. Creep is defined as the time-dependent deformation of hardened concrete subjected to sustained stress.[48] Creep values are obtained by subtracting from the total measured strain of a loaded specimen the sum of the initial instantaneous (elastic) strain due to the sustained stress and shrinkage strain in an identical load-free specimen, which is subjected to the same relative humidity and temperature conditions. Shrinkage is defined as the contraction of concrete due to drying and physiochemical changes, dependent on time but not on stresses induced by external loading.[48] Shrinkage is expressed as a dimensionless strain (inch/inch) under steady conditions of relative humidity and temperature. There are three types of shrinkage: drying shrinkage, autogenous shrinkage, and carbonation shrinkage.[10] Drying shrinkage is due to moisture loss in the concrete. Autogenous shrinkage is caused by the hydration of cement. Carbonation shrinkage results as various cement hydration products are carbonated in the presence of CO.

10.1 ACI 209 Creep Model

ACI Committee 209[10] presents the following equation for predicting the creep coefficient (ratio of creep strain to initial elastic strain) of concrete at any time

$$v_t = \frac{t^{\Psi}}{d + t^{\Psi}} v_u \qquad (9.1)$$

where

v_t = creep coefficient at any time t;
t = time in days after loading;
Ψ = constant, $(0.40 < \Psi < 0.80)$;
d = constant, $(6 < d\ 30$ days); and
v_u = ultimate creep coefficient, $(1.30 < v_u < 4.15)$.

Creep tests were conducted as outlined in ASTM C512, Standard Test Method for Creep of Concrete in Compression.[49] Specimens measuring four inches x four inches x 24 inches (square specimens) and 4.5 inches diameter x 24 inches (cylindrical specimens) were used in determining the ultimate creep coefficient. Ends of each specimen were capped with a sulfur-based, high-strength capping compound. The specimens were then loaded into the creep frame (Figure 10.1) and loaded to 40 percent of the compressive strength. Three specimens with four-inch x four-inch ends, along with one specimen with a 4.5-inch-diameter end were loaded to 40% of the compressive (release) strength while the specimens were one-day old. Four of the four-inch x four-inch ends were then loaded at 28 days to a stress of 40% of the 28-day compressive strength. The four specimens that were loaded at 28 days were kept in a moist room. Surface strains of the concrete were measured using Whittemore locating points (Figure 10.2 for square specimens and Figure 10.3 for cylindrical specimens). Each specimen had six strain measurements taken, three on each side. For the duration of the test, strain measurements of the creep specimens were measured and recorded periodically. In the 4.5-inch-diameter specimen and one of the specimens loaded at 28 days, a VWSG was embedded in the center to also measure creep strain. Values of Ψ, d, and v_u can be determined by fitting the data obtained from the tests performed.

Figure 10.1 Specimen loaded in creep apparatus

Figure 10.2 Square specimen for creep and shrinkage

Figure 10.3 Cylindrical specimen for creep and shrinkage

10.2 ACI 209 Shrinkage Model

ACI Committee 209[10] presents the following equation for predicting shrinkage strain of concrete at any time:

$$\left(\varepsilon_{sh}\right)_t = \frac{t^{\alpha}}{f + t^{\alpha}}\left(\varepsilon_{sh}\right)_u \tag{9.2}$$

where

$\left(\varepsilon_{sh}\right)_t$ = shrinkage strain at any time t;
t = time in days after loading;
α = constant $(0.90 < \alpha < 1.10)$;
f = constant $(20 < f < 130$ days); and
$\left(\varepsilon_{sh}\right)_u$ = ultimate shrinkage strain $(415\,x10^{-6} < \left(\varepsilon_{sh}\right)_u < 1070\,x10^{-6})$.

Companion shrinkage specimens were cast at the same time as the creep specimens were made. To provide the same exposed surface area as the creep specimens, the shrinkage specimens were also capped. This prevented the shrinkage specimens from exchanging moisture with the environment through their ends. Four, four-inch x four-inch x 24-inch and one 4.5-inch-diameter by 24-inch specimens were used to measure shrinkage strains. Shrinkage specimens were stored in the vertical position, similar to the creep specimens. Identical to the creep specimens, surface strains were recorded using a Whittemore gage. Similar to the creep specimens, a VWSG was embedded into one of the four-inch x four-inch and one 4.5-inch-diameter end specimen. Both creep and shrinkage specimens were stored in the laboratory where the temperature was close to 75 degrees Fahrenheit with approximate 50% relative humidity. No controlled environment was provided to prevent fluctuation of the temperature and relative humidity.

CHAPTER ELEVEN - CREEP AND SHRINKAGE PRISM RESULTS

11.1 Creep

Creep tests were conducted for a duration of more than 500 days for the proposed SCC mixture. Immediately after loading, the initial deformation, representing the elastic response, was measured. Creep strains were then calculated by subtracting from the total strain, the initial elastic strain, and the average shrinkage of the unloaded companion specimens.

The experimental creep coefficient was found by the procedure described in ACI 209. the coefficient was found by deducting the initial elastic strain and also the shrinkage strains from the measured value and dividing by the initial elastic strain. Adjusting the parameters in equation 10.1, the ultimate creep coefficient can be determined by plotting the experimental data against the values obtained from equation 10.1. This adjustment was implemented to match the predicted curve with the experimental curve. Using this trial-and-error approach, the creep parameters for the square specimens were determined to be 0.7 for Ψ, 16 for d, and 1.75 for v_u for the specimens loaded at day one; and 0.6 for Ψ, 24 for d, and 2.00 for v_u for the specimens loaded at 28 days; for the SCC mixture. Values of the constants determined were all within the given ranges suggested by ACI 209. Results of the square specimens can be seen in Figures 11.1 and 11.2 for both “different loading days” cases.

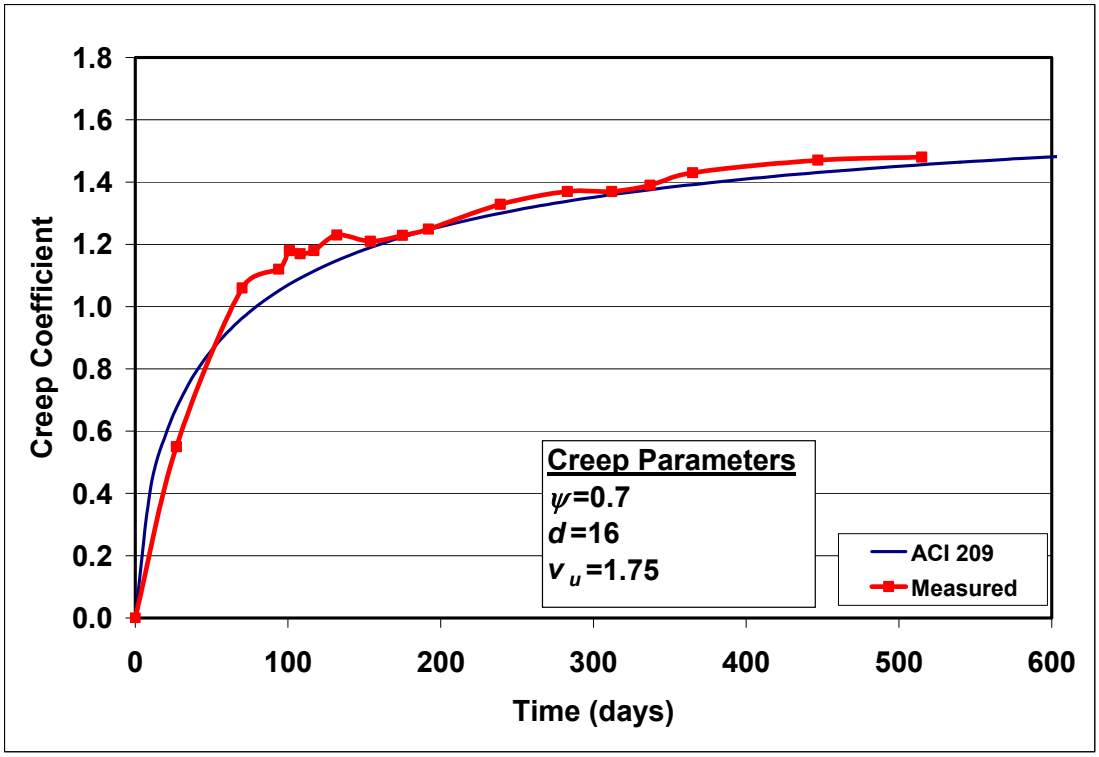

Figure 11.1 Creep coefficient for square specimens loaded at day one

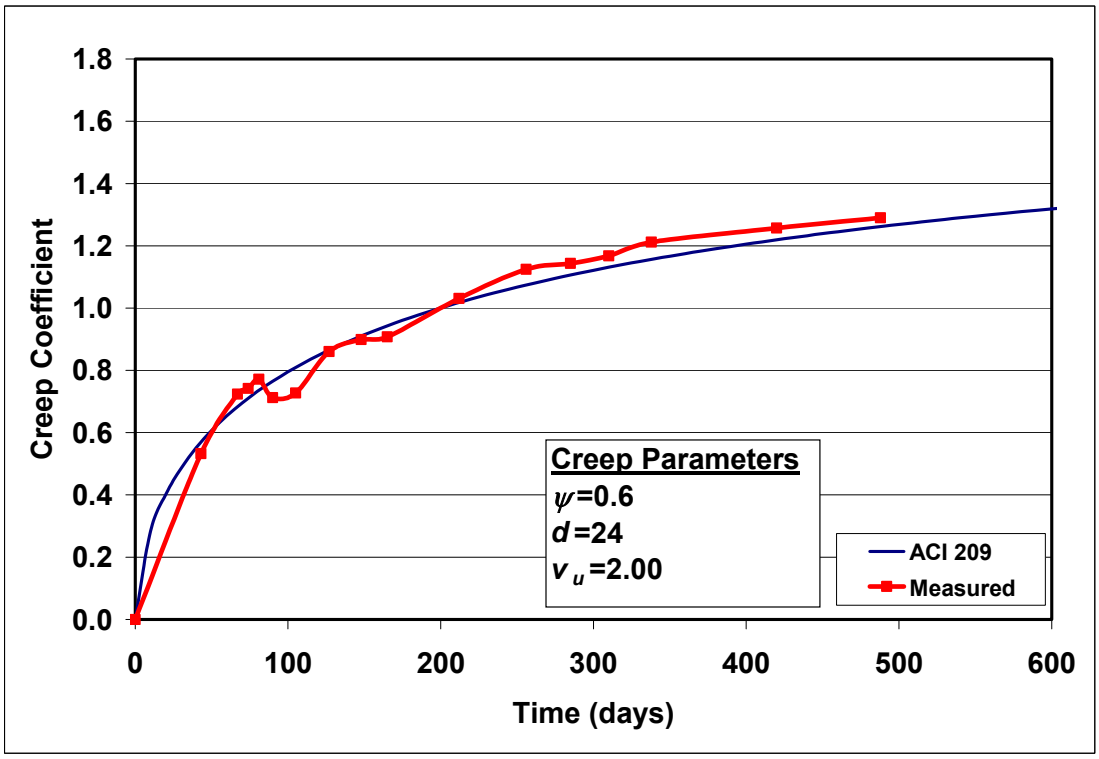

Figure 11.2 Creep coefficient for square specimens loaded at day 28

Figure 11.3 compares the creep coefficient predicted by ACI 209, to the experimental values measured for square, cylindrical, and cylindrical specimen with an embedded VWSG, all for a "day-one loaded" case. Figure 11.4 is an identical comparison for a "day-28 loaded" case. It can be seen in both cases that the specimen with the VWSG in the center had a larger creep coefficient. This can be attributed to the fact that the center of the specimen was experiencing more of the creep effect than the surface of the specimen.

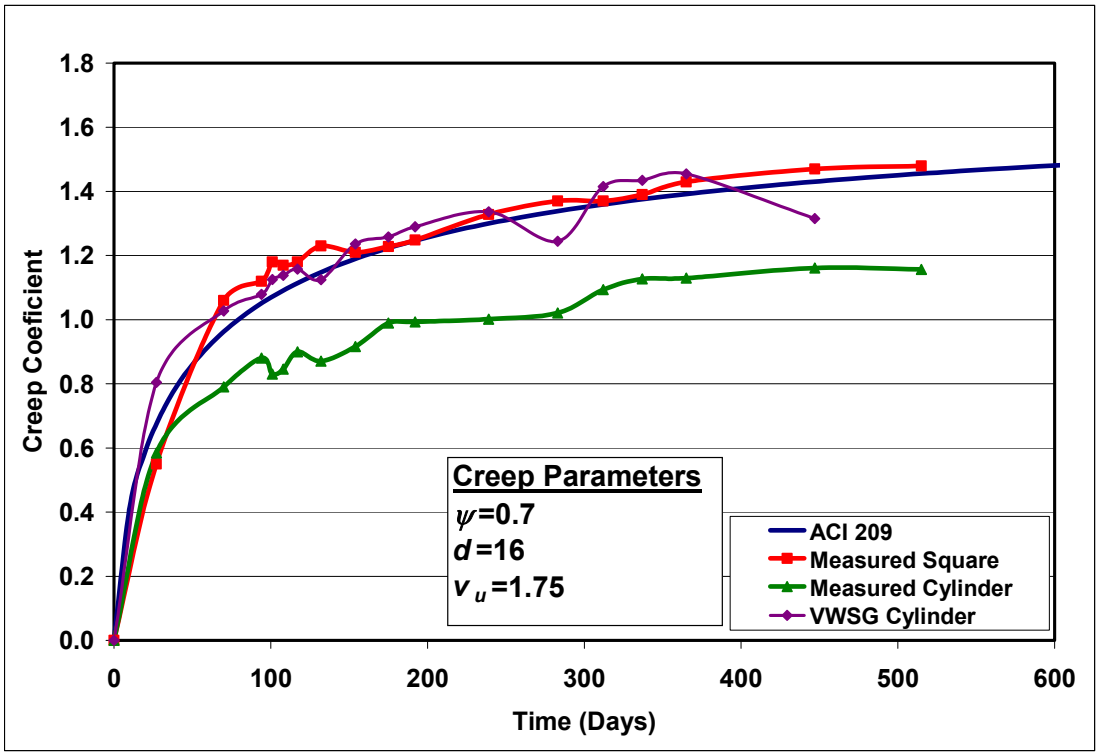

Figure 11.3 Creep coefficient for square and cylindrical (+VWSG) specimens loaded at day one

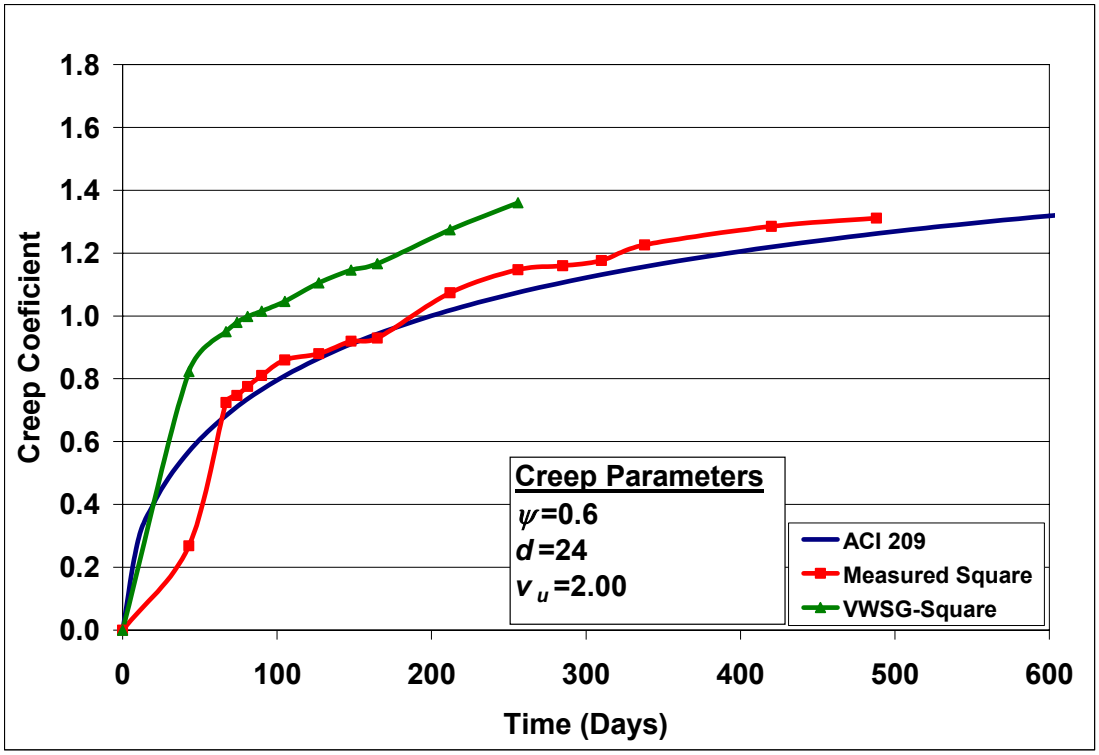

Figure 11.4 Creep coefficient for square (+VWSG) specimens at day 28

11.2 Shrinkage

Figure 11.5 shows the measured shrinkage strains of the square specimens with respect to time for the proposed SCC mixture. Predicted shrinkage strains are calculated from equation 10.2. Along with the predicted ACI 209 value and measured strains, the strain results of an embedded VWSG are also shown. It can be seen that the dip in strain values occurred for the strains measured with both the Whittemore points and the VWSG. This suggests that temperature and relative humidity changed during this portion. Shrinkage specimen parameters used in determining the predicted curve were 1.0 for α, 20 for f, and 550 x 10^6, for the ultimate shrinkage value $(\varepsilon_{sh})_u$. Figure 11.6 shows the measured shrinkage strains of the cylindrical specimen with respect to time for the

proposed SCC mixture. The predicted shrinkage strains are calculated from equation 10.2. Along with the strains measured and predicted by ACI-209 strains recorded by the embedded VWSG are presented in Figure 11.5. Shrinkage specimen parameters used in determining the predicted curve were 1.0 for α, 20 for f, and 600 x 10^6, for the ultimate shrinkage value $(\varepsilon_{sh})_u$. Figures 11.5 and 11.6 show that the surface of the specimens experienced more shrinkage than center of the specimens.

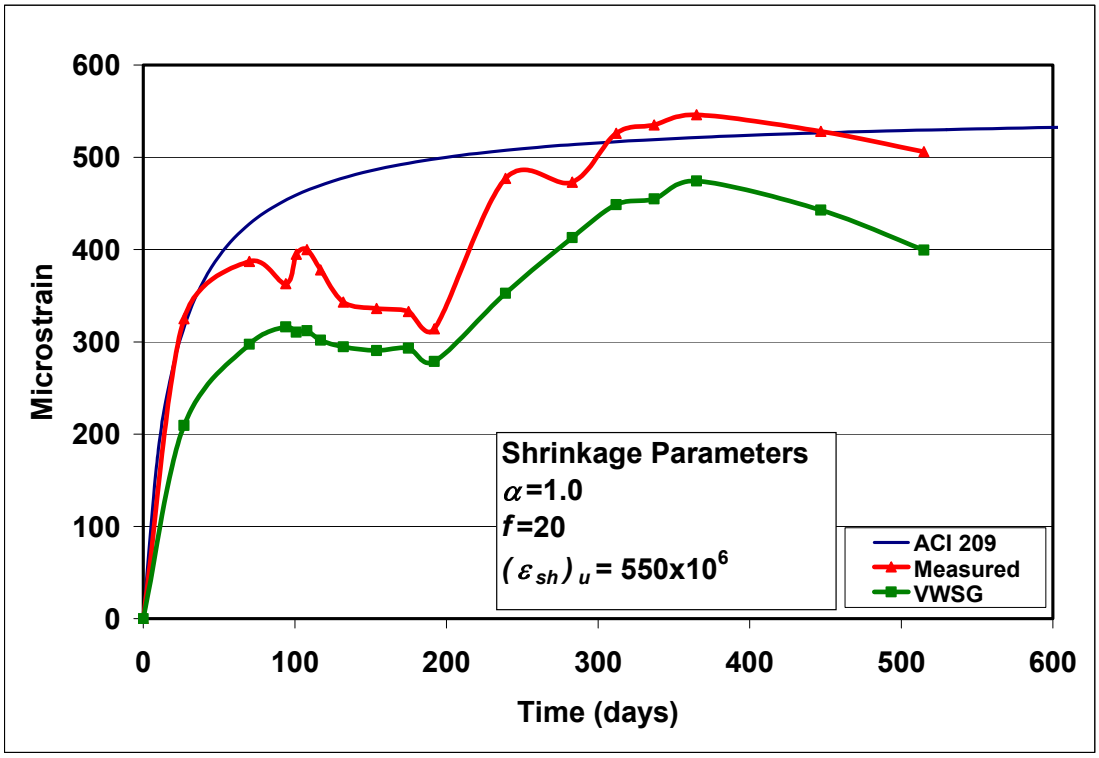

Figure 11.5 Shrinkage strains for square (+VWSG) specimens

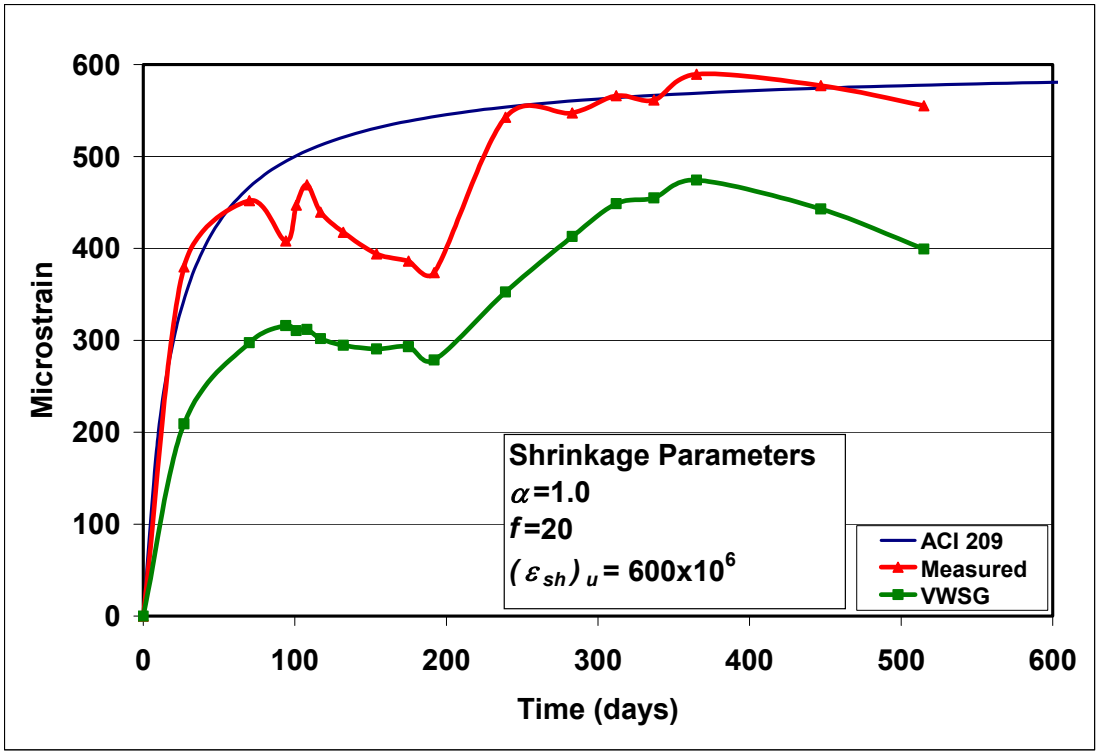

Figure 11.6 Shrinkage strains for cylindrical (+VWSG) specimens

Figure 11.7 shows the comparison of shrinkage strains for the square and cylindrical specimens. The cylindrical specimen experienced slightly larger strains than the square specimens. This was unexpected because the square specimens had a larger surface-to-volume ratio than the cylindrical specimens.

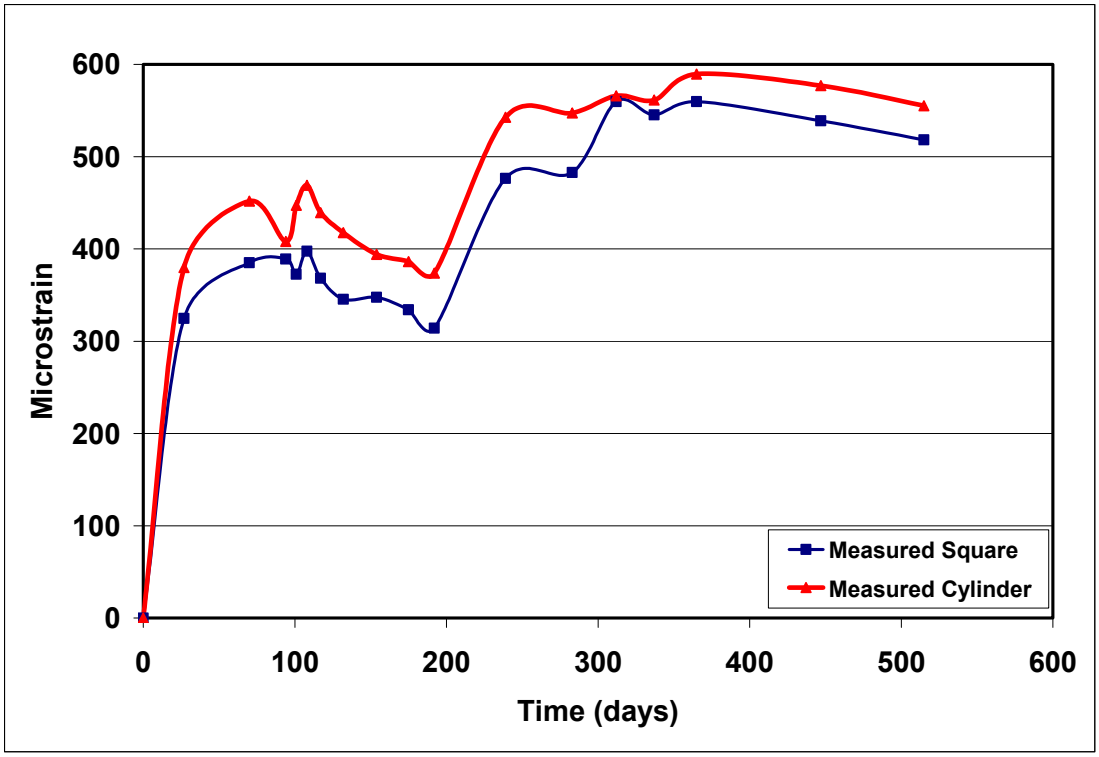

Figure 11.7 Comparison of square versus cylindrical specimen shrinkage strains

11.3 Comparison of ACI 209 Prestress Loss Predictions

The ACI 209 document, shown in section A.9, also has a procedure for calculating time-dependent losses. The creep and shrinkage loss terms utilize the creep coefficient (one day) and shrinkage strains that were determined in the previous sections. By using the results obtained from equations 10.1 and 10.2, the effective prestress was determined using the ACI 209 method (Table 11.1 and Figure 11.8) and compared to the experimental results of the IT specimens. It can be seen that the overall losses are fairly close to that of the experimental results. However, if each individual term is calculated separately, the creep predictions by ACI-209 will be much lower than the experimental results, and the shrinkage predictions will be much higher than the experimental results. Table 11.2 shows this, along with the values predicted by the PCI method.

Table 11.1 Prestress loss predictions using ACI-209 method

Day	Elastic Shortening	Creep	Shrinkage	Relaxation	Total Losses	ACI 209 Predicted	Experimental Stress
Release	19.9	0.0	0.0	1.2	21.1	176.9	180.0
25	19.9	11.0	7.5	2.8	41.2	156.8	170.0
50	19.9	14.5	9.7	3.1	47.1	150.9	166.0
75	19.9	16.5	10.7	3.2	50.3	147.7	163.0
96	19.9	17.9	11.2	3.3	52.3	145.7	162.0
120	19.9	18.9	11.6	3.4	53.8	144.2	161.0
144	19.9	19.7	11.9	3.5	55.0	143.0	158.0
200	19.9	21.3	12.3	3.6	57.1	140.9	158.0
240	19.9	21.9	12.5	3.7	58.1	139.9	157.0
340	19.9	23.3	12.8	3.9	59.8	138.2	156.0
450	19.9	24.1	13.0	4.0	61.0	137.0	156.0
514	19.9	24.6	13.0	4.1	61.6	136.4	155.0
Ultimate	19.9	29.5	13.5	5.0	68.0	130.0	--

* all values reported in ksi

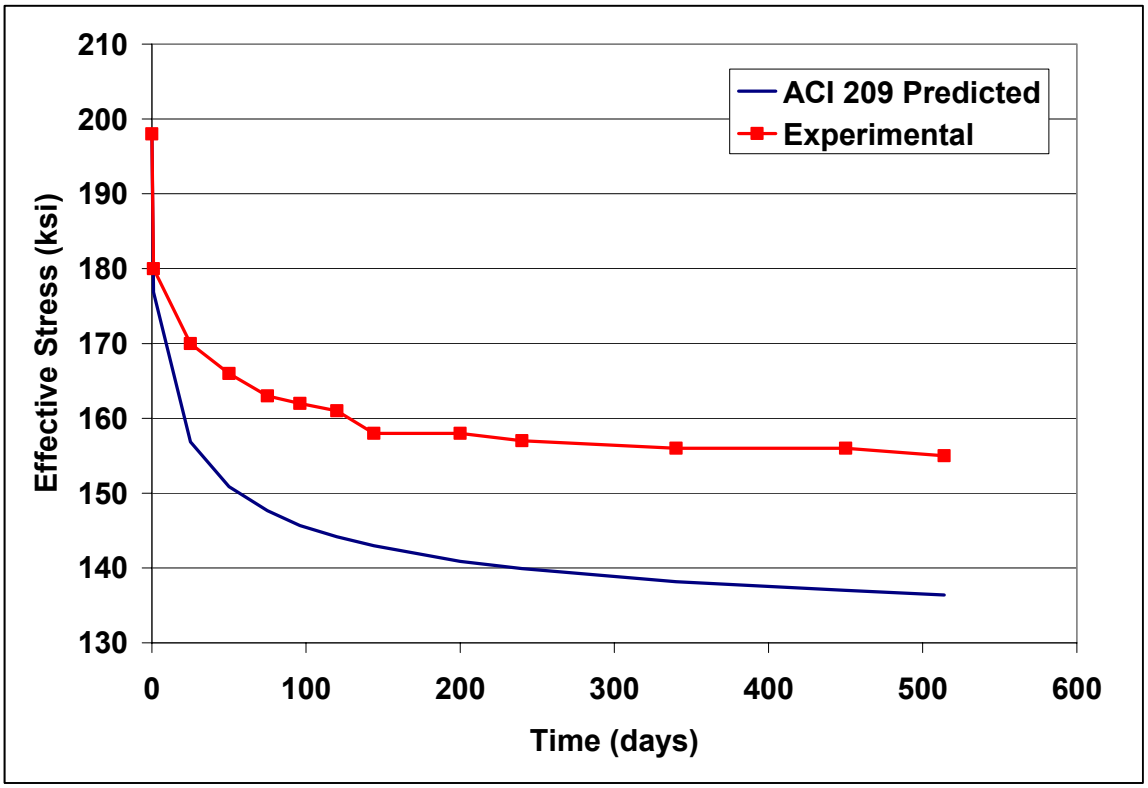

Figure 11.8 Effective stress versus time for ACI-209 prediction method

Table 11.2 Creep and shrinkage loss predictions using ACI-209 and PCI methods

Day	ACI-209 Creep	PCI Creep	Experimental Creep	ACI-209 Shrinkage	PCI Shrinkage	Experimental Shrinkage
Release	0.0	0.0	0.0	0.0	0.0	0.0
25	11.0	9.9	9.9	7.5	2.9	0.1
50	14.5	12.0	13.2	9.7	3.5	-0.2
75	16.5	13.2	16.1	10.7	3.8	-0.1
96	17.9	13.9	17.1	11.2	4.0	-0.1
120	18.9	14.6	19.4	11.6	4.2	-0.4
144	19.7	15.3	20.8	11.9	4.4	0.2
200	21.3	16.3	20.2	12.3	4.7	0.8
240	21.9	16.8	20.6	12.5	4.8	1.4
340	23.3	17.9	21.9	12.8	5.2	1.1
450	24.1	18.6	22.5	13.0	5.4	0.5
514	24.6	19.1	23.3	13.0	5.5	0.7
Ultimate	29.5	23.6	--	13.5	6.8	--

* all values reported in ksi

CHAPTER TWELVE - SCC BRIDGE MONITORING

A five-span bridge containing 35 girders was chosen to be instrumented, and long-term strain values were recorded. Of the 35 girders, 21 were cast with conventional concrete and the remaining 14 girders with SCC. The bridge was located on US Highway 160 in Cowley County just west of Winfield, Kansas. To determine the time-dependent losses, VWSGs were embedded into seven of the girders, four with conventional concrete and three with SCC. This was one of the first bridges with SCC to be monitored for long-term prestress losses. The girders used in this project were KDOT standard Type K3 girders, shown in Figure 12.1. Table 12.1 lists the geometric properties for this girder type.

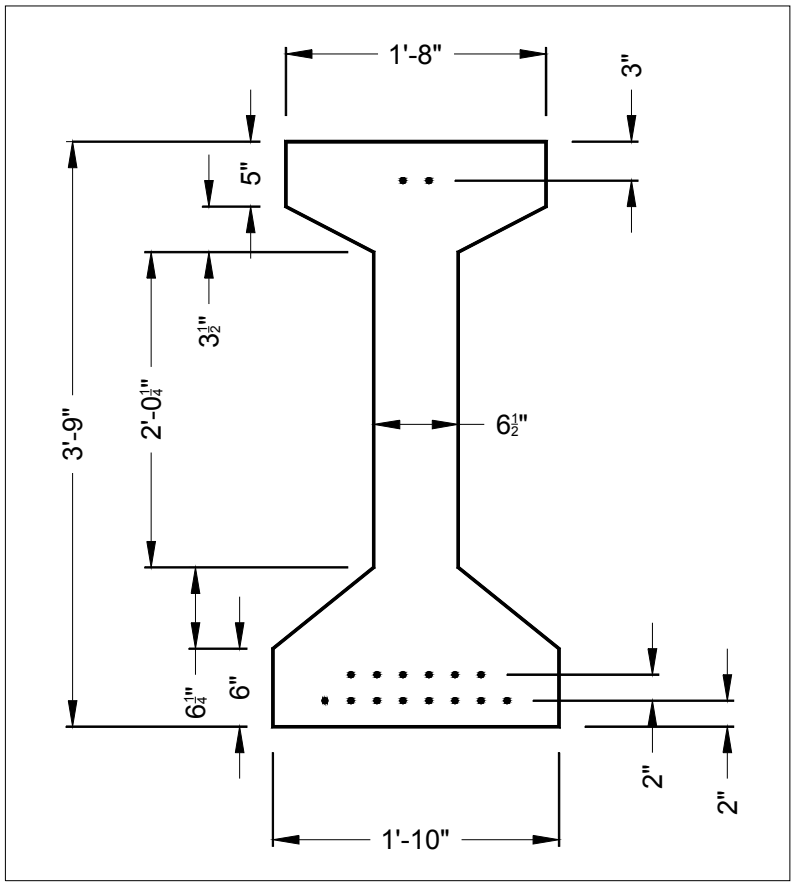

Figure 12.1 Cross section of K3 girder

Table 12.1 Geometric properties of K3 girder

A=	525	$inch^2$	I=	127,490	$inch^4$
Y_{bot}=	21	inch	*e* =	13.27	inch
H=	45	inch	L=	50	feet
w_o=	547	plf	V/S=	3.56	inch
f_{pj}=	202.5	ksi	A_{ps}=	2.448	$inch^2$
E_{ps}=	28,500	ksi	RH=	65	%

12.1 Girder Fabrication and Instrumentation

In order to determine the long-term strains experienced by the girders, VWSGs were selected for use in this project. Strain gages selected were the Model VCE-4200 Vibrating Wire-Embedded Strain Gage, identical to those used in the IT specimens.

Bridge instrumentation involved selecting seven girders and placing the VWSGs at various depths in each girder. Two different patterns of placing the gages at different depths were used. The first had three total gages embedded in the girder, with one being at the height of the top strand, one at 21 inches from the bottom (neutral axis of the section), and one at the bottom strand height, Figure 12.2. Girders with this depth pattern were A3, C3, and E3. The other gage pattern had six total gages embedded, one being at the height of the top strands, one at 21 inches from the bottom (neutral axis of the composite section, including the deck), one at 21 inches from the bottom (neutral axis of the section), one at four inches from the bottom, and two gages at the bottom strand height, Figure 12.2. The gage pattern was similar to the one used by Yang and Myers

(2005). Two gages were placed at the bottom in case one of the gages broke. All gages were placed at mid span of the seven selected girders.

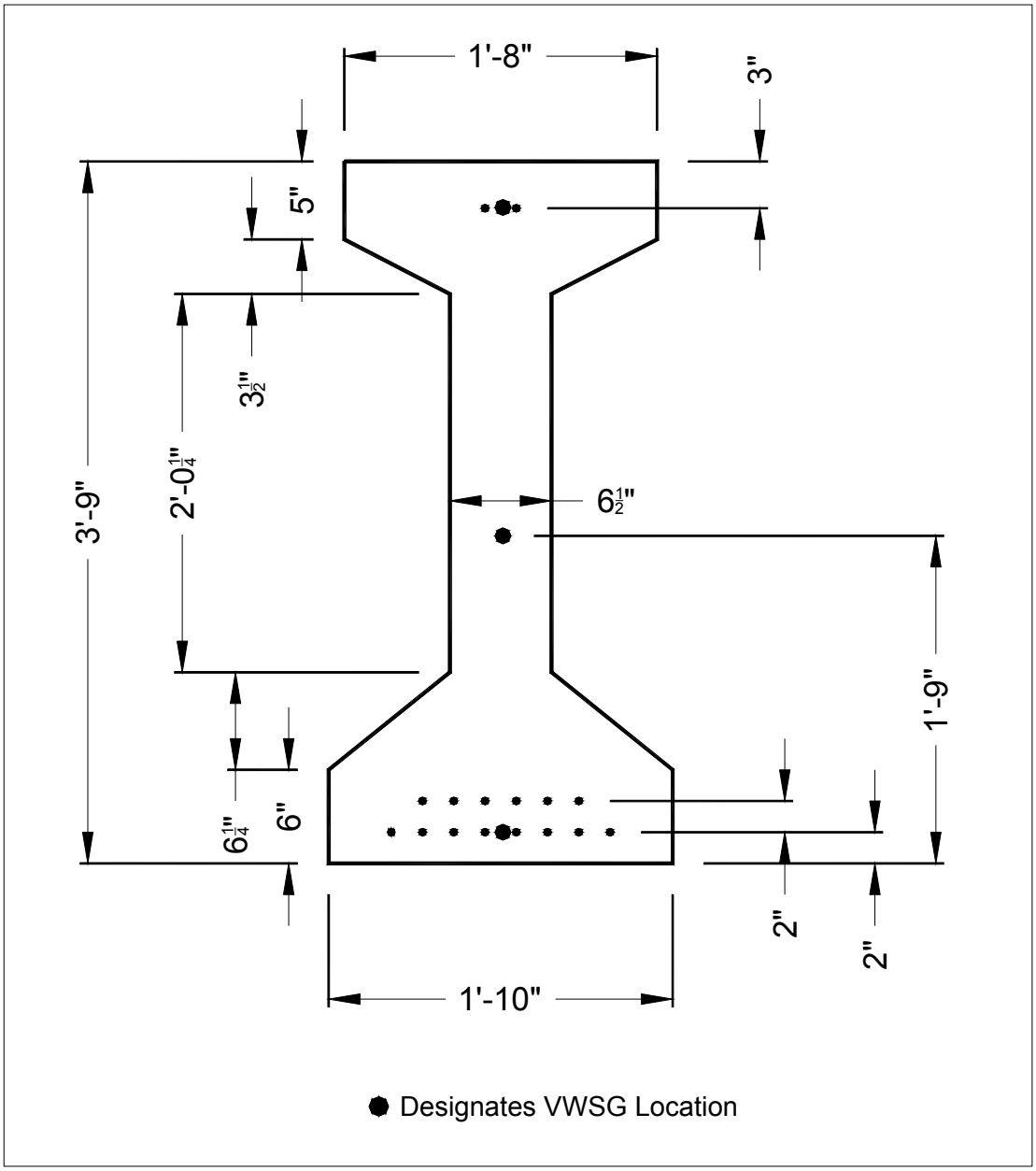

Figure 12.2 VWSG placement for girders with three gages

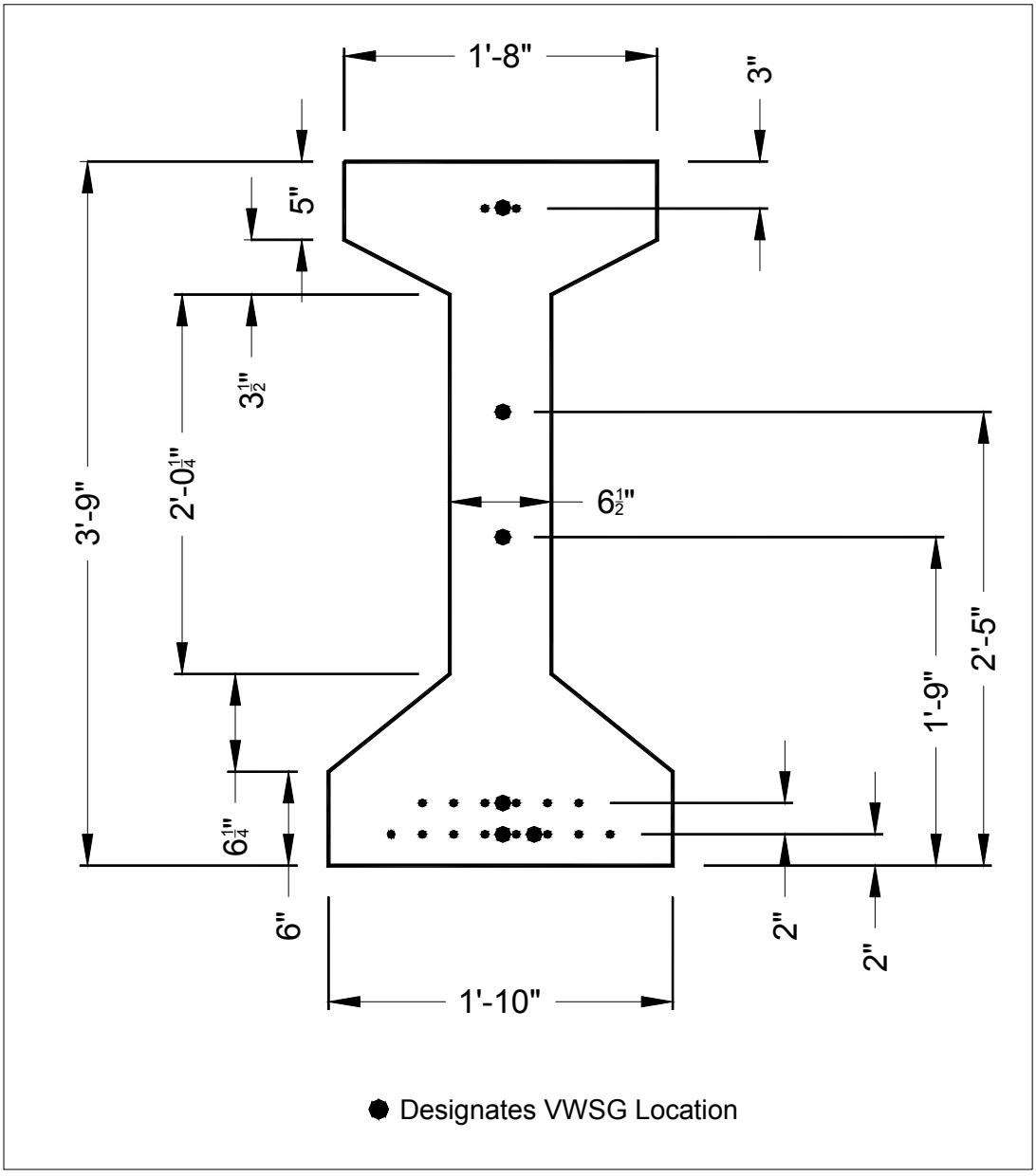

Figure 12.3 VWSG placement for girders with six gages

Figure 12.4 and 12.5 show the VWSGs tied to the internal rebar for the girders with three and six gages, respectively.

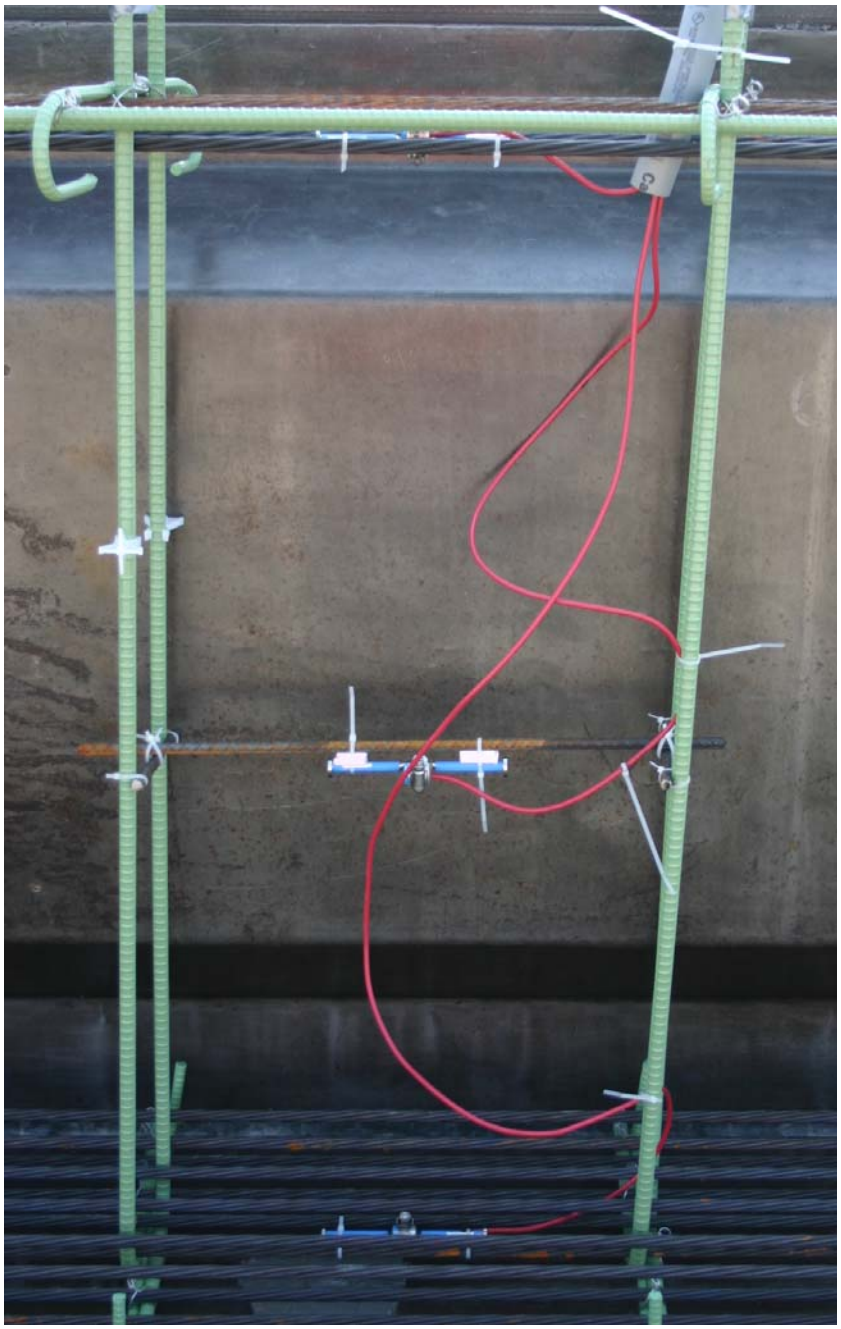

Figure 12.4 Location of VWSG's throughout cross-section

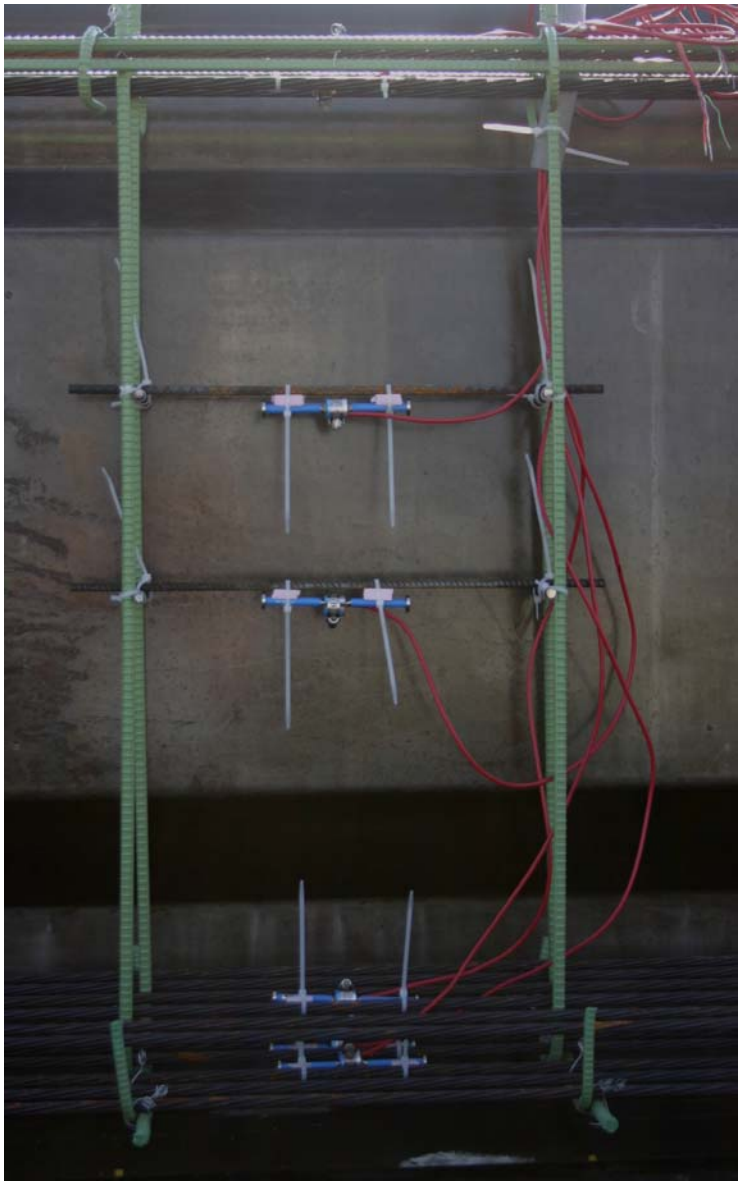

Figure 12.5 Location of VWSG's throughout cross-section

Casting of the K3 girders started August 3, 2005. Fabrication of all K3 girders was performed at Prestressed Concrete Inc., Newton, Kansas, the same precast plant where the flexural and IT specimens were cast. Forms at the precast plant allowed them to cast three girders at a time. Prestressing strand used in all the girders was 0.5-inch-diameter, Grade 270 ksi. Modulus of elasticity (E_{ps}) for the prestressing strand was reported as 28,500 ksi by the manufacturer. A straight-strand profile was used for every

girder. The procedure began with an empty prestressing bed, Figure 12.6. The prestressing strand was then pulled to 202.5 ksi and the internal shear stirrups were tied into place, Figure 12.7. Figure 12.8 shows the girders after all the steel had been tied into place and after one side wall had been put into place. The other form wall was then put into place (Figure 12.9) and concrete placement was ready to begin. Vibration was needed for the girders with conventional concrete, Figure 12.10. and girders with SCC did not require any vibration, Figure 12.11. Standard slump tests were performed on the conventional concrete mixture, Figure 12.12. Inverted-slump flow (spread) and L-Box tests were performed on the SCC mixtures, Figures 12.13 and 12.14, respectively. Figure 12.15 shows that the SCC mixture had good aggregate distribution and there was no large aggregate missing from the leading edge.

Figure 12.6 Empty prestressing bed

Figure 12.7 Tying of internal shear stirrups

Figure 12.8 Forms after one side wall has been set into place

Figure 12.9 Prestressing bed after walls have been set into place

Figure 12.10 Vibration of conventional concrete mixture

Figure 12.11 Laborers not having to vibrate SCC mixture

Figure 12.12 Slump test of conventional concrete mixture

Figure 12.13 Inverted-slump flow test for SCC mixture

Figure 12.14 L-Box test for SCC mixture

Figure 12.15 SCC mixture showing no excess paste and presence of aggregate on leading edge

The morning after casting concrete a set of three concrete cylinders were tested for compressive strength, the prestressing strand was detensioned as soon as the release strengths were achieved. To detension, the walls were removed and the strand was torched, Figure 12.16. The presence of "bug" holes can be seen in the girders with conventional concrete mixture, Figures 12.17 and 12.18 while the girders with the SCC mixture had a smooth exterior finish, Figures 12.19 and 12.20.

Figure 12.16 Detensioning of strands with a torch

Figure 12.17 Presence of "bug" holes in girder with conventional concrete

Figure 12.18 Closeup view of "bug" holes in girder with conventional concrete

Figure 12.19 Smooth exterior of SCC girder

Figure 12.20 Closeup of smooth SCC finish

12.2 Bridge Layout

As noted previously, the bridge consisted of 35 girders. The girder layout is shown in Figure 12.21. Spans A-C were all cast with conventional concrete, and spans D-E were cast with the proposed SCC mixture. The bridge was erected in two phases. All of the girders embedded with VWSGs, lines 1-3, were part of phase I. Girder lines 4-

7 were part of phase II. The girders with embedded VWSGs were A3, B1, B3, C3, D1, D3, and E3.

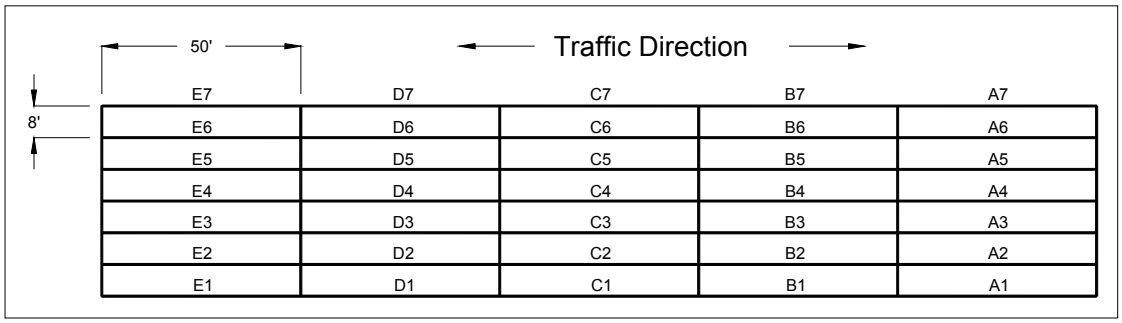

Figure 12.21 Layout and designation of bridge girders

12.3 Bridge Erection

The construction process at the bridge site started in mid July 2005. Having a 2-phase construction made it possible to keep one lane of traffic open during the whole process. Removal of the north half of the existing bridge was followed by construction of the first phase. After phase I was completed, the road was opened to traffic and the rest of the existing bridge was removed followed by the second construction phase. The entire bridge was opened to traffic after this phase.

As noted earlier, during construction of phase I, one lane of traffic remained open, Figure 12.22. Since the bridge had been altered, temporary support for the existing structure was needed, Figure 12.23. Once the old bridge had been removed, the first step was to drill new piles, Figure 12.24. Once the piles were in place, the abutment walls were cast, Figure 12.25. After all the supports were completed, it was time to set the girders into place. Figures 12.26, 12.27, and 12.28 show different views of the girders

after they had been set. Placing shoring for the deck construction was the next step, Figures 12.29 and 12.30. After all the shoring was in place, the deck steel was tied into place, Figures 12.31 and 12.32. During this time, wires from the VWSGs were hooked up to a multi-plexor, Figure 12.33, which were in turn connected to the data logger. Conduit was cast into the abutments to allow for the wires to run through them, Figure 12.34. Once all the wires were connected, casting of the deck started by using a concrete pump truck to pump the concrete to the bridge deck, Figure 12.35. The concrete was vibrated and finished, Figures 12.36 and 12.37.

Figure 12.22 One lane open to traffic during phase I construction

Figure 12.23 Temporary supports for existing bridge

Figure 12.24 Placement of cages for piles

Figure 12.25 Abutment wall

Figure 12.26 Placement of girders

Figure 12.27 Underneath view of placed girders

Figure 12.28 Underneath view of placed girders

Figure 12.29 Placement of shoring for deck casting

Figure 12.30 Placement of shoring for deck casting-II

Figure 12.31 Placement of deck reinforcement

Figure 12.32 Tying of deck reinforcement into place

Figure 12.33 Wires extending into multi-plexor

Figure 12.34 Wires extending through abutment wall

Figure 12.35 Pump truck for pumping concrete to bridge deck

Figure 12.36 Vibrating concrete

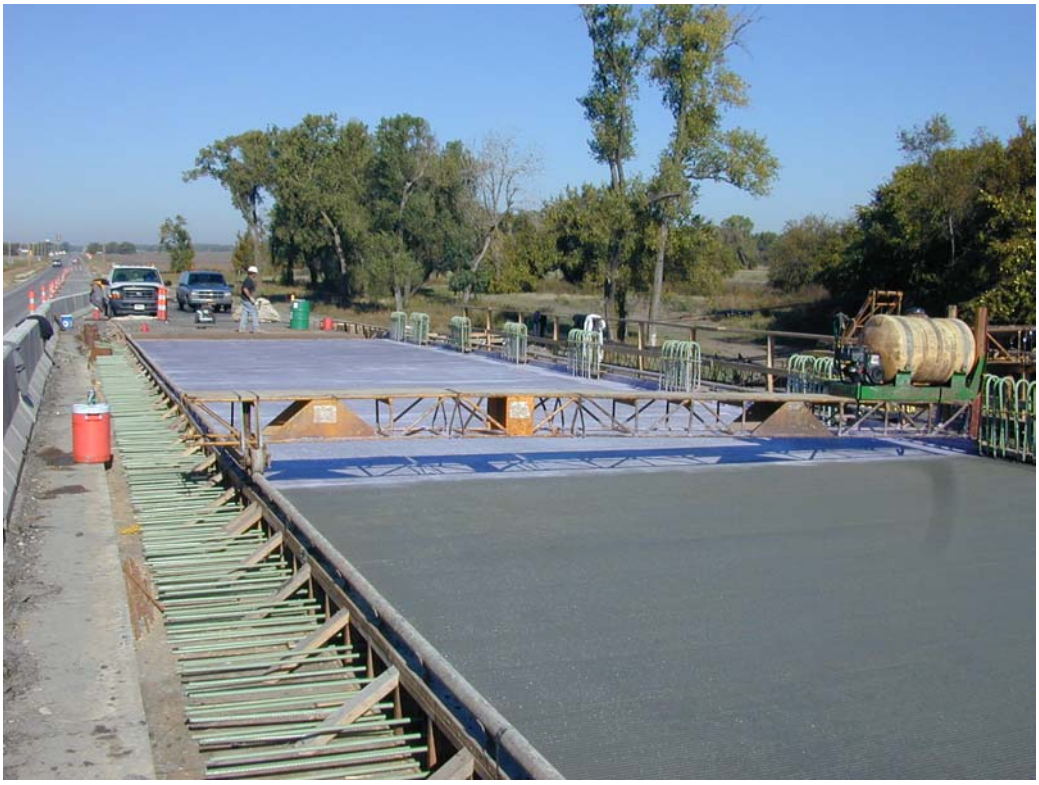

Figure 12.37 Finishing of concrete

Once the deck had cured, phase I was opened for traffic, Figure 12.38. The remaining part of the existing bridge was removed and construction on phase II began, Figure 12.39. After the girders of phase II were set into place, shoring for the deck was erected, Figure 12.40. Once the shoring and deck steel were all in place, the deck was cast, Figure 12.41. All remaining tasks were finished and traffic in both directions was opened in early April 2006, Figure 12.42. Restoration around the site was completed (Figure 12.43) and a solar panel was installed on the side rail to provide power to the data logger, Figure 12.44. A side view of the completed bridge is shown in Figure 12.45.

Figure 12.38 Opened lane of phase I and beginning of phase II

Figure 12.39 Groundwork for phase II

Figure 12.40 Shoring for phase II

Figure 12.41 Deck completion of phase II

Figure 12.42 Finished bridge and approach

Figure 12.43 Side restoration

Figure 12.44 Solar panel on side railing

Figure 12.45 Side view of completed project

CHAPTER THIRTEEN - PRESTRESS LOSS RESULTS OF SCC BRIDGE

13.1 Material Properties

13.1.1 Girder Properties

As noted earlier, conventional and self-consolidating concrete, as two separate concrete mixtures, were used in the bridge girders. The hardened concrete properties were different for these two mixtures. This difference plays an important role when comparing experimental results to code predictions. Figure 13.1 shows the measured modulus of elasticity for release and 28-day modulus for both mixes. Figure 13.1 shows the measured compressive strength for release and 28-day strength for both mixes. At the time of casting for the SCC girders with the VWSGs, the release strengths were lower than normal. However, the average release strengths of the remaining ungaged girders with SCC were much higher than those girders with conventional concrete, Figure 13.3. This figure shows the release compressive strength for all the girders containing SCC and conventional concrete for all 35 girders cast. The lower modulus of elasticity for the SCC mixture was expected due to more "fines" in the mixture. For the girders with the SCC mixture, the slump flow ranged from 24 inches to 29 inches. The slumps ranged from 4.5 inches to nine inches for the girders with the conventional concrete mixture. Currently KDOT recommends a three to nine-inch slump for conventional concrete in bridge girders and does not have a range for girders with SCC.

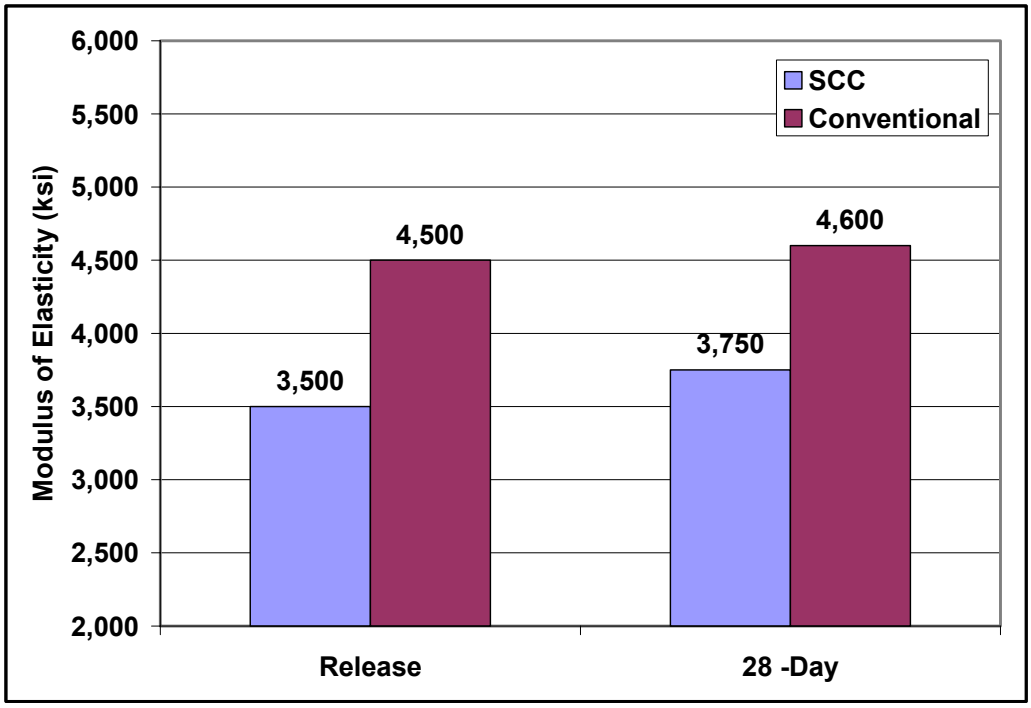

Figure 13.1 Modulus of elasticity for girders gaged with VWSGs

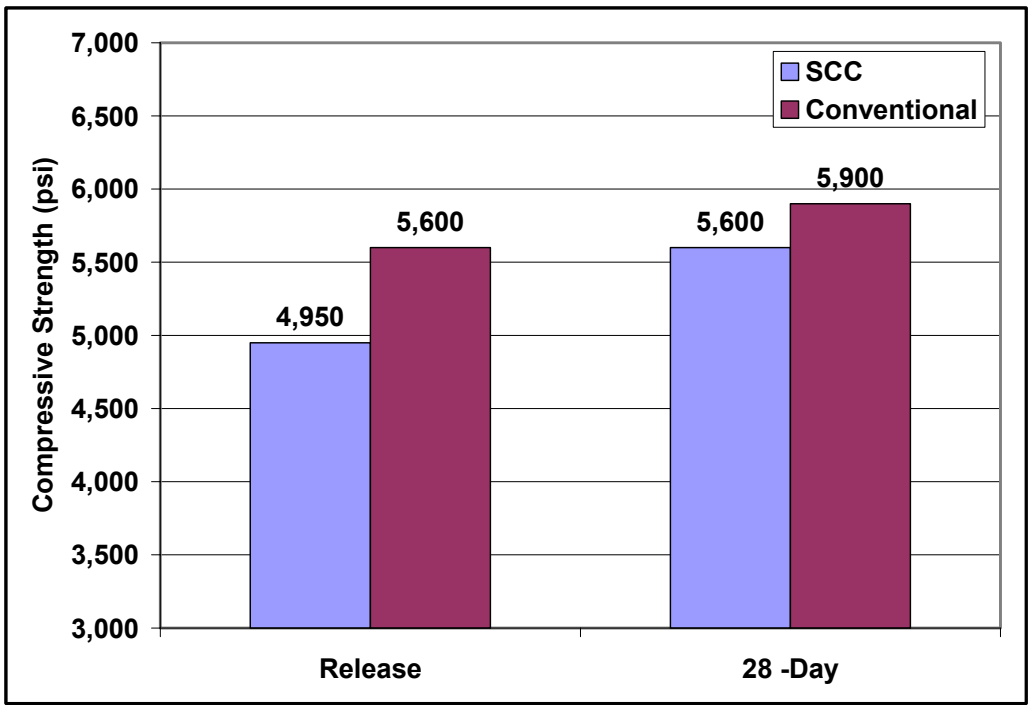

Figure 13.2 Compressive strength for girders gaged with VWSGs

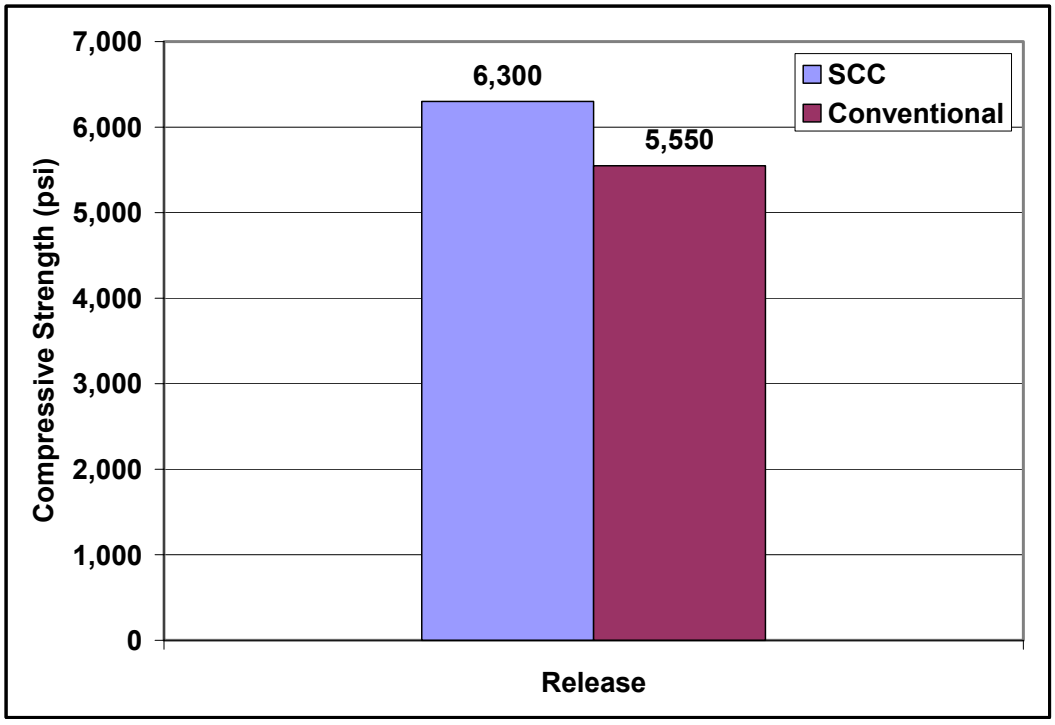

Figure 13.3 Release compressive stregnth for all girders cast

13.1.2 Deck Properties

The deck for phase I was cast on October 18, 2005. The 28-day compressive strength was found to be 4,500 psi with a modulus of elasticity of 5,150 ksi. Split-cylinder tests were also performed at 28 days and tensile strength was found to be 350 psi. The deck thickness was 8.5-inches.

13.2 Experimental Stress Results

The VWSGs yielded results in strain. To compare these values with the code equations, the strain values were converted to stress. Equation 8.2 was used for this calculation. The code equations computed the prestress loss values at the center of

gravity of the prestressing strands. Hence, strain values located at the level of the bottom strand height were used for direct comparison. The total time-dependent losses as predicted by the PCI method, yielded 173 ksi and 168 ksi for the girders with conventional concrete and SCC, respectively. The calculations can be seen in section A.10. The major difference between these two values was the elastic shortening loss which was impacted by the modulus of elasticity of the concrete at release.

13.2.1 Girders with Conventional Concrete

Figures 13.4–13..7 shows the effective stress versus time for the girders cast with conventional concrete. Figures 13.8—13.10 present the strains in concrete versus depth. It must be noted that a strain versus depth profile was not available for girder B3, due to a problem with some of the gages. The strains however did remain linear with depth.

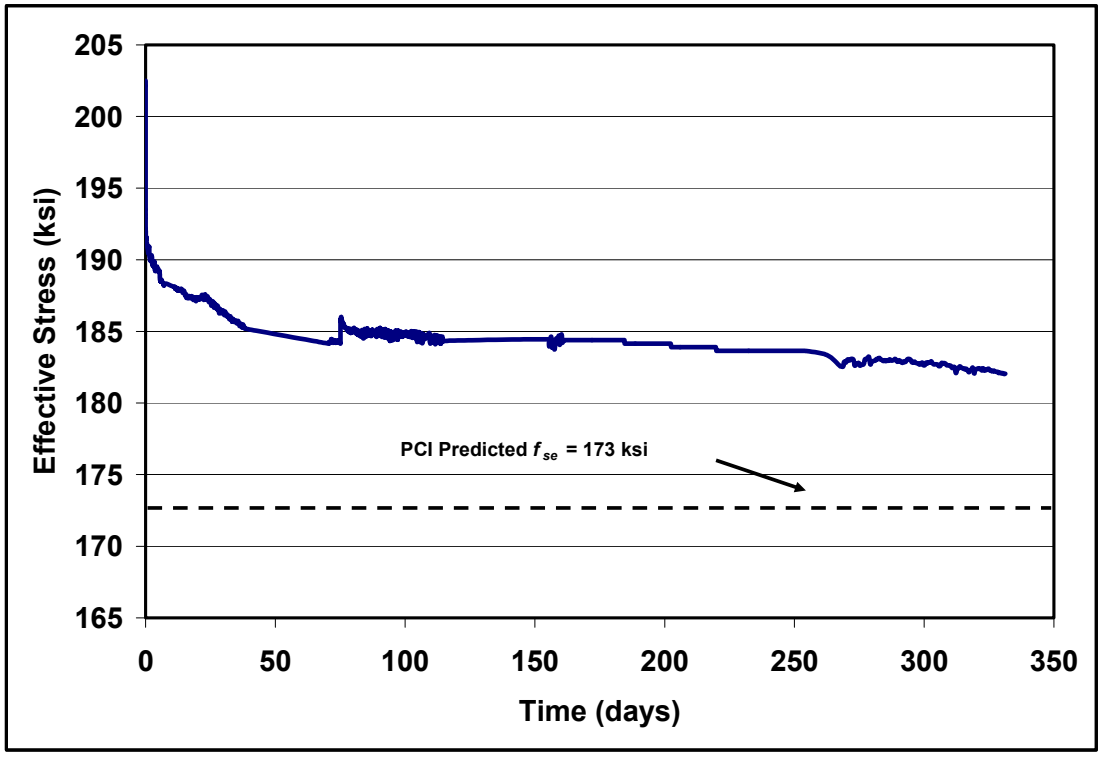

Figure 13.4 Effective stress for girder A3

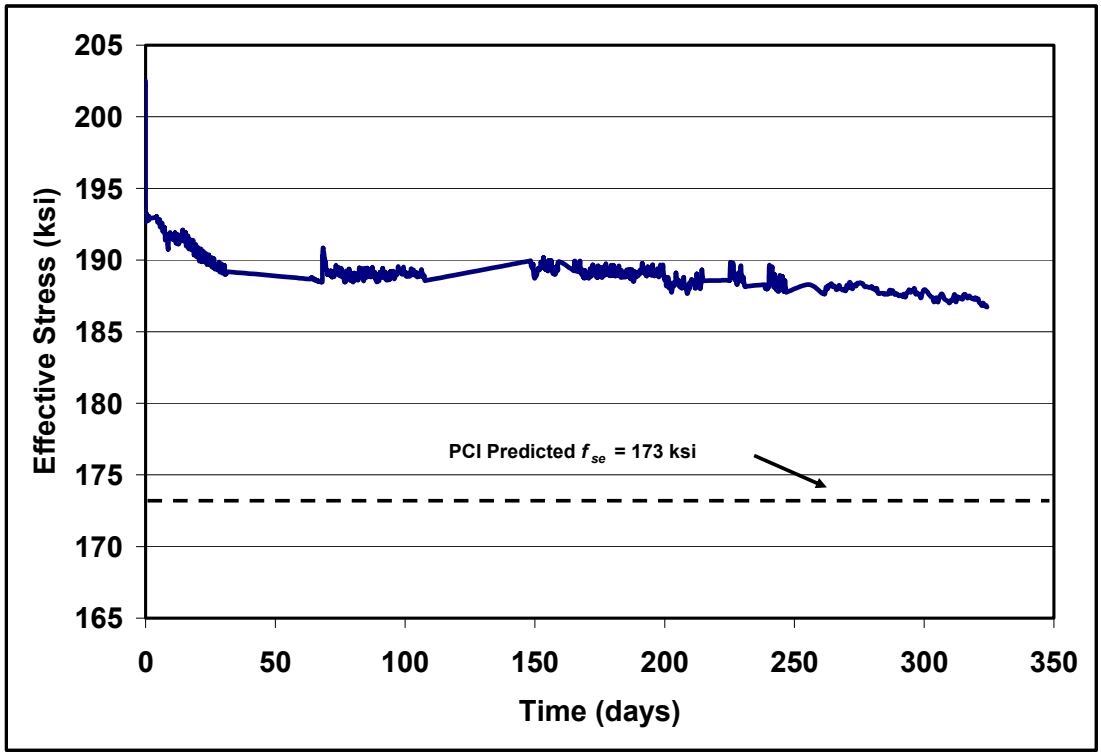

Figure 13.5 Effective stress for girder B1

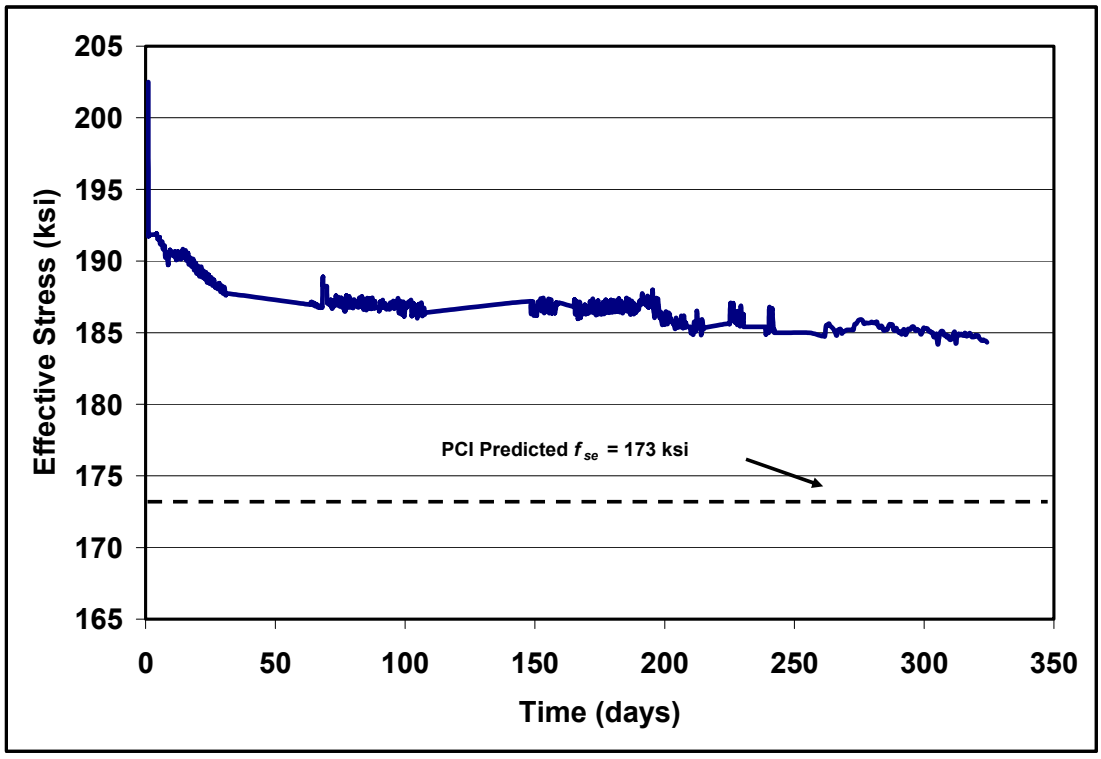

Figure 13.6 Effective stress for girder B3

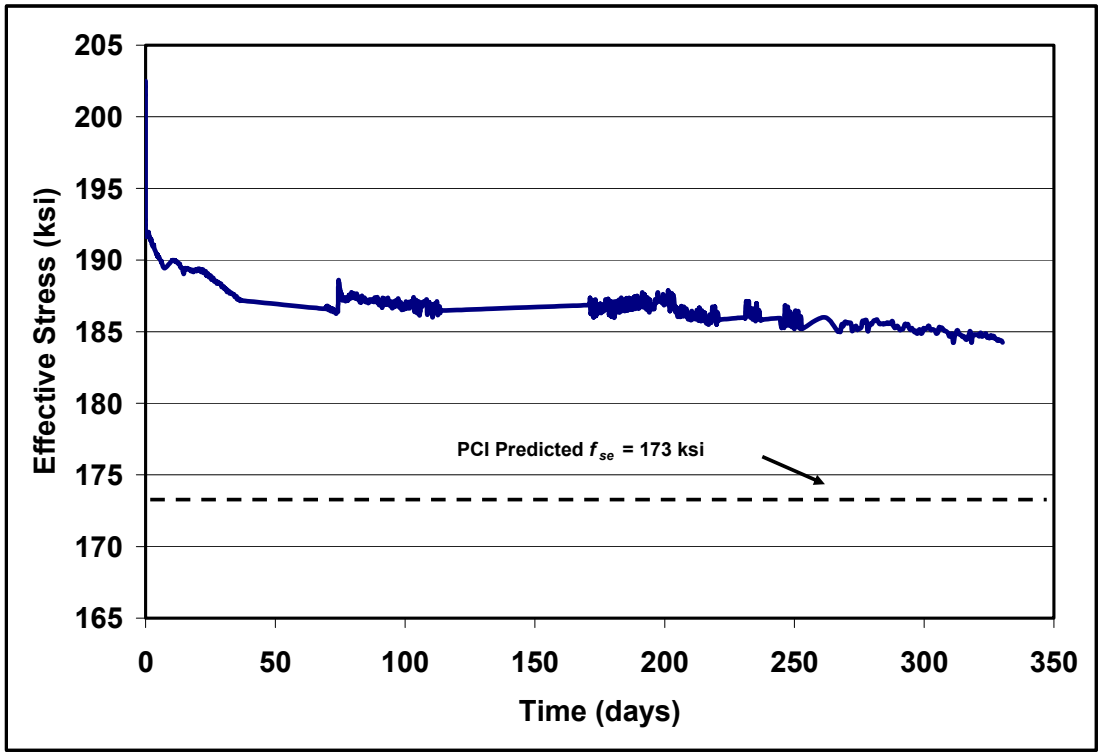

Figure 13.7 Effective stress for girder C3

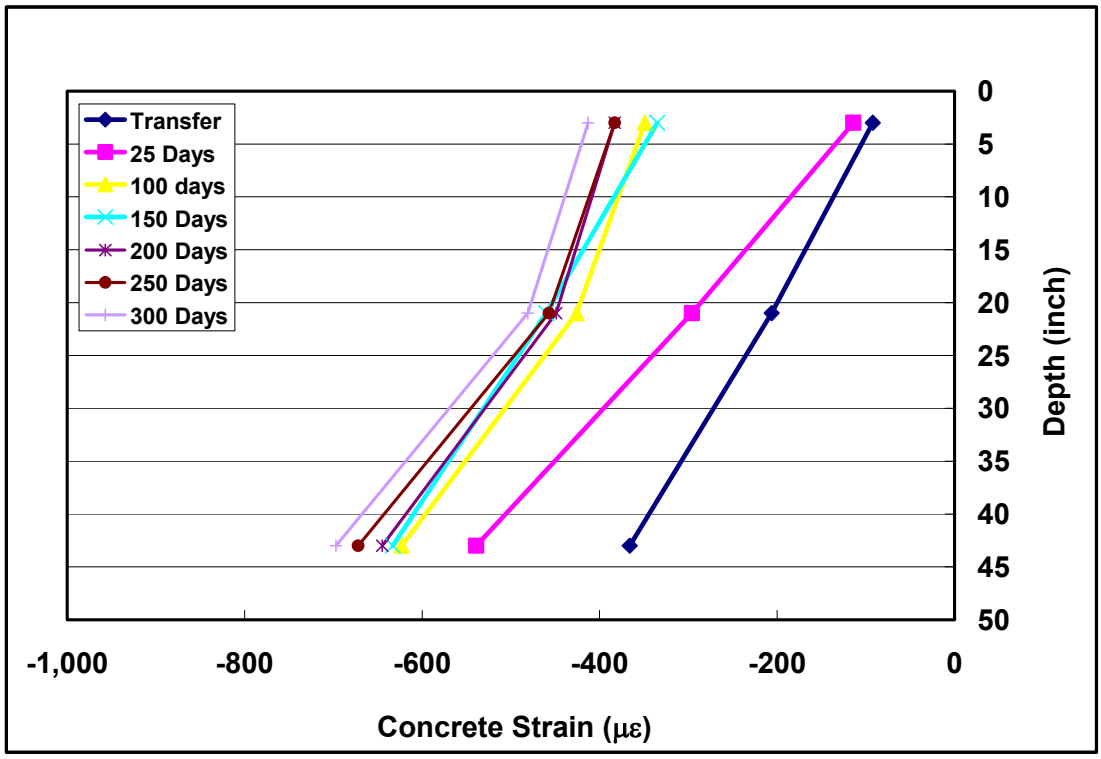

Figure 13.8 Concrete versus depth for girder A3

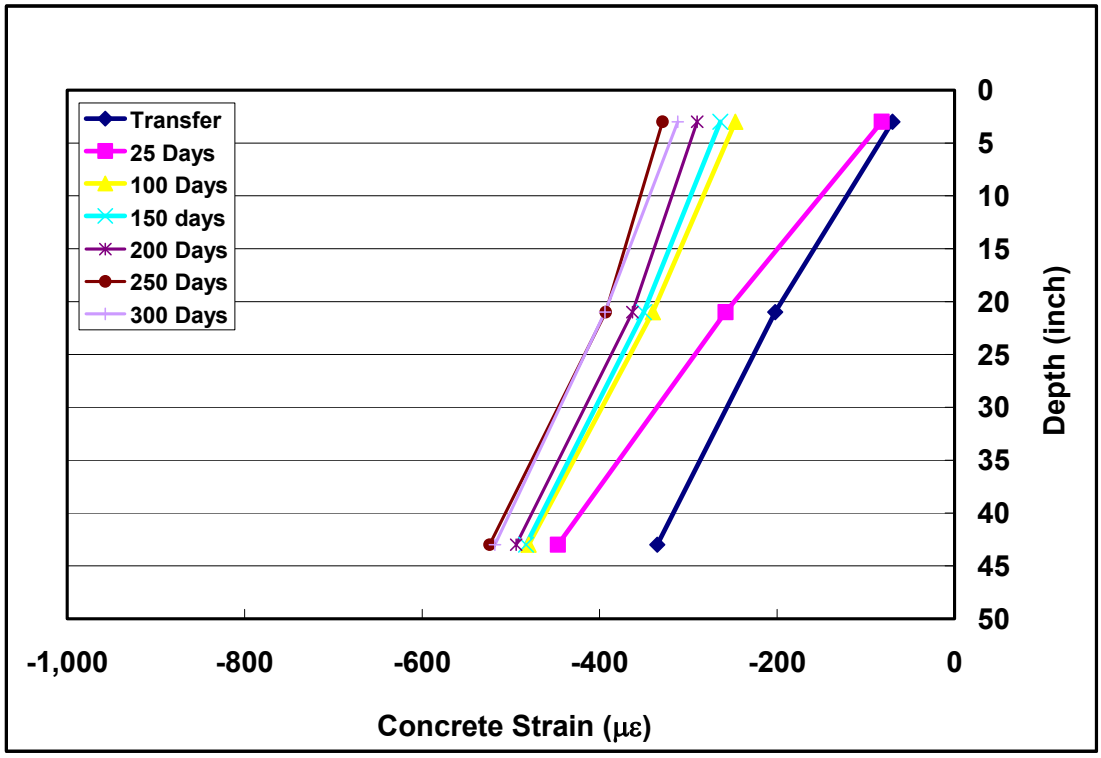

Figure 13.9 Concrete versus depth for girder B1

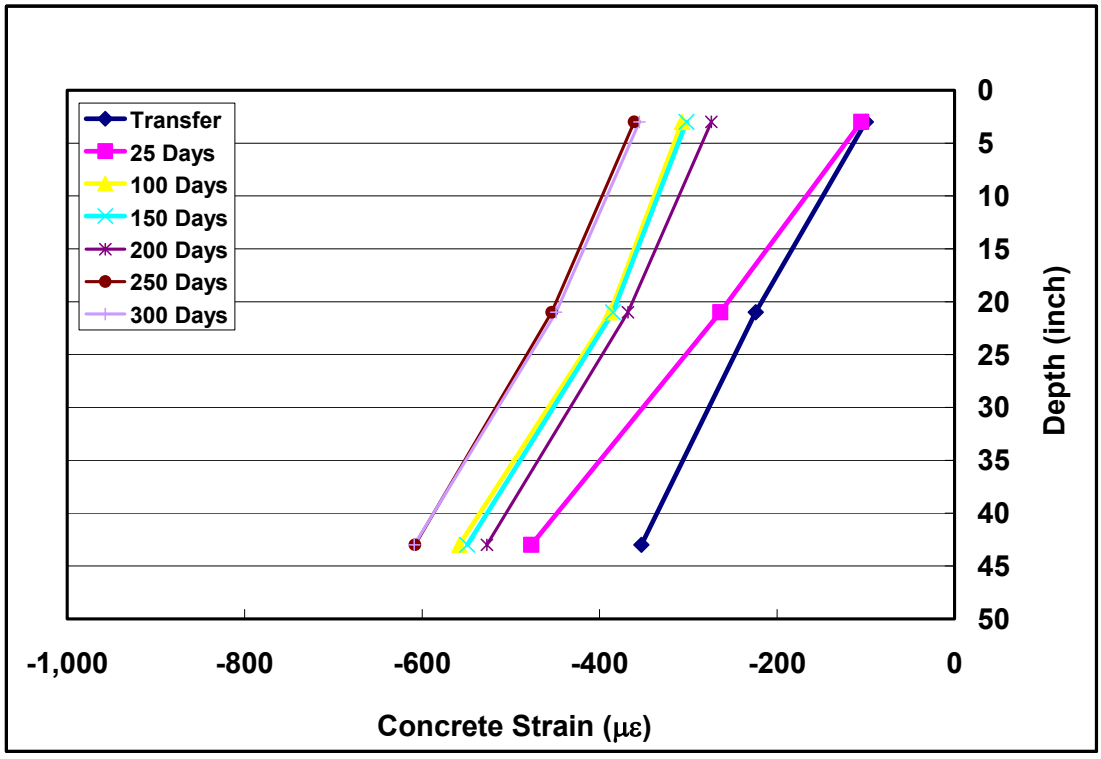

Figure 13.10 Concrete versus depth for girder C3

13.2.2 Girders with Self-Consolidating Concrete

Figures 13.11–13.13 show the effective stress versus time for the girders cast with self-consolidating concrete. Figures 13.14—13.16 present the strains in the concrete versus the depth.

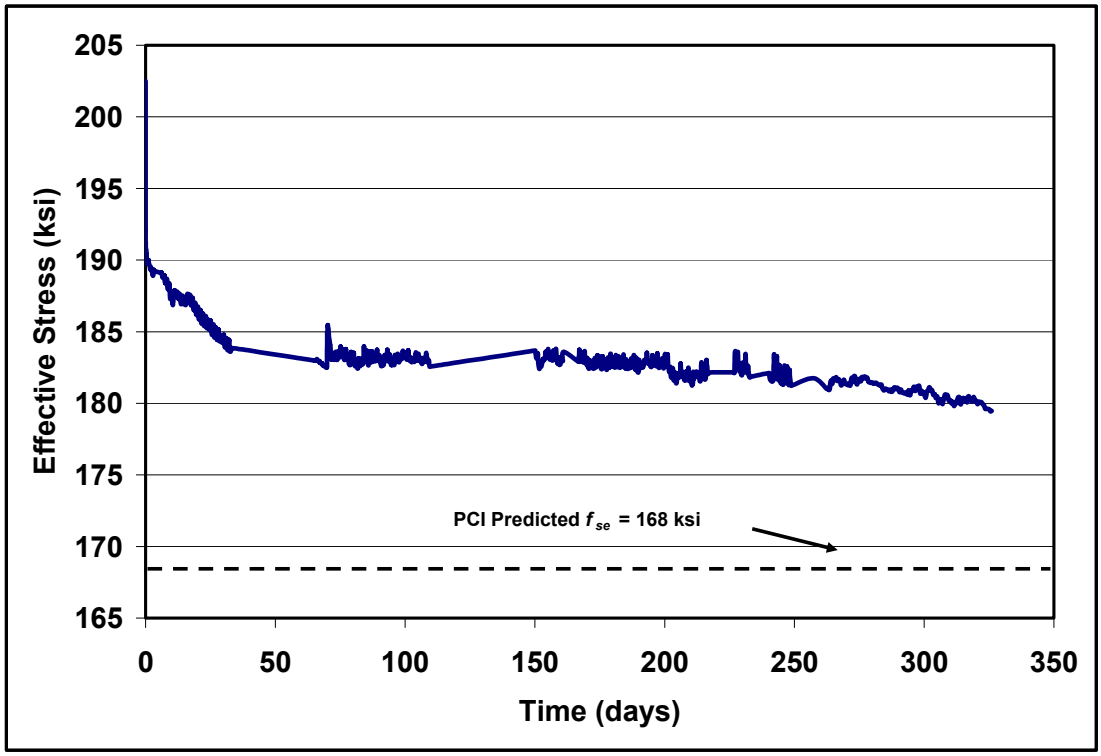

Figure 13.11 Effective stress for girder D1

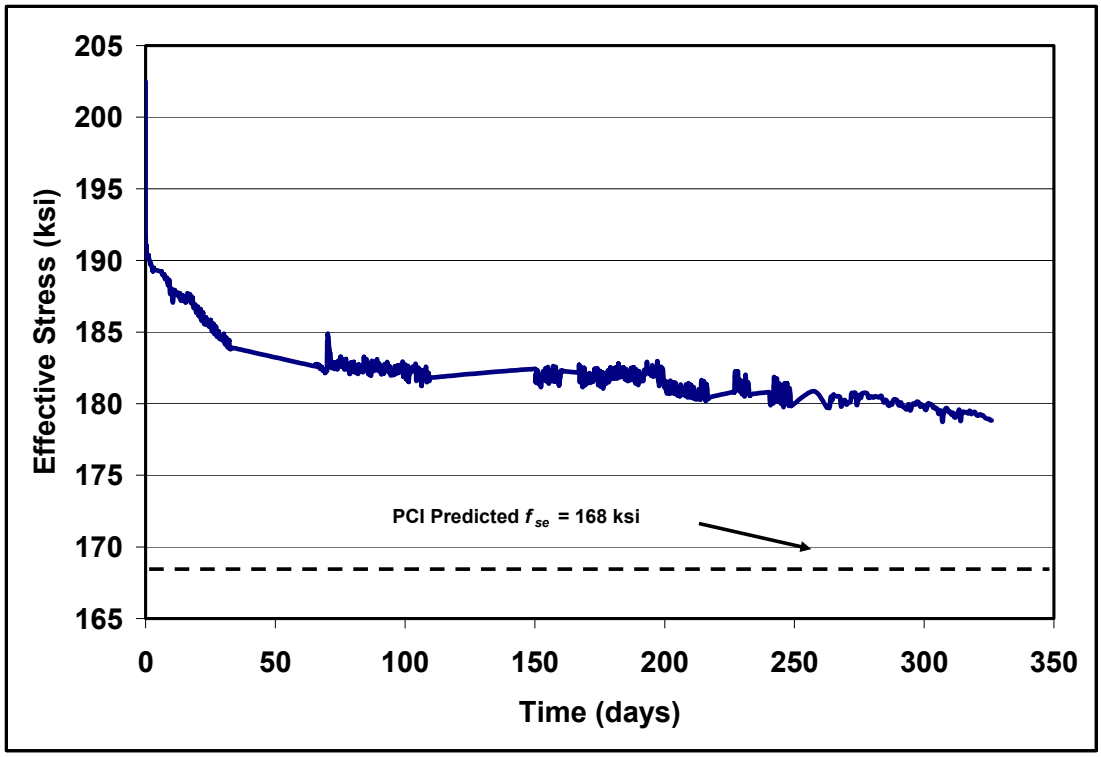

Figure 13.12 Effective stress for girder D3

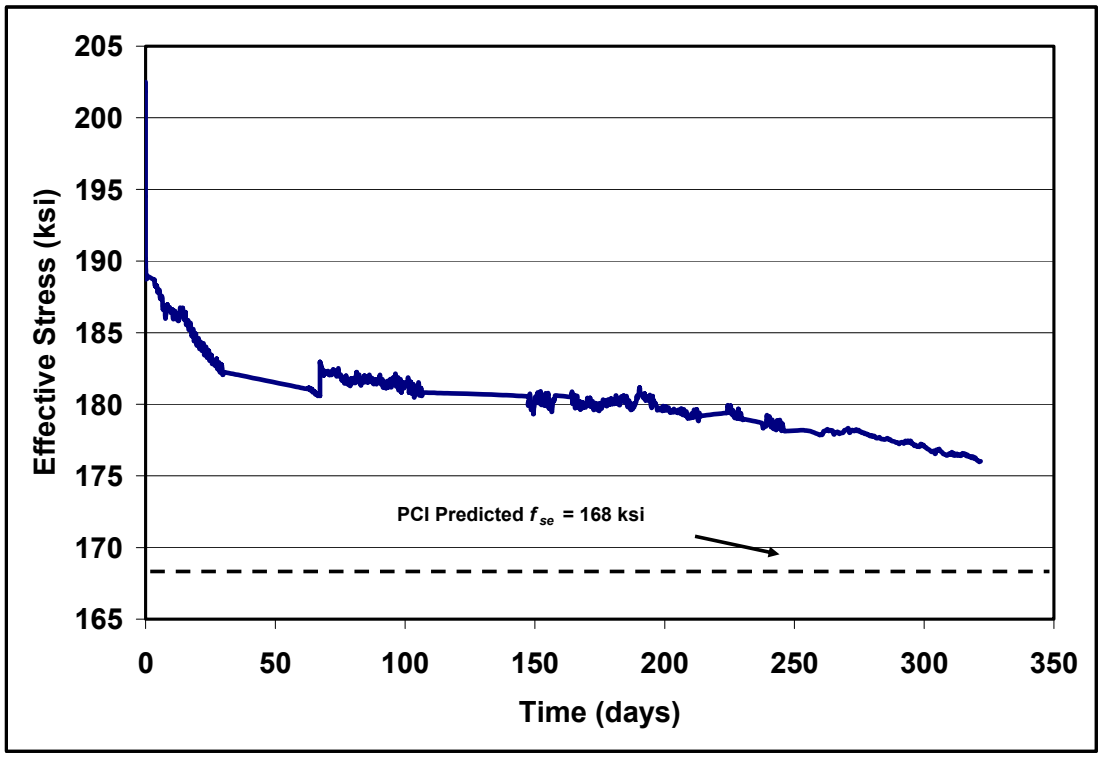

Figure 13.13 Effective stress for girder E3

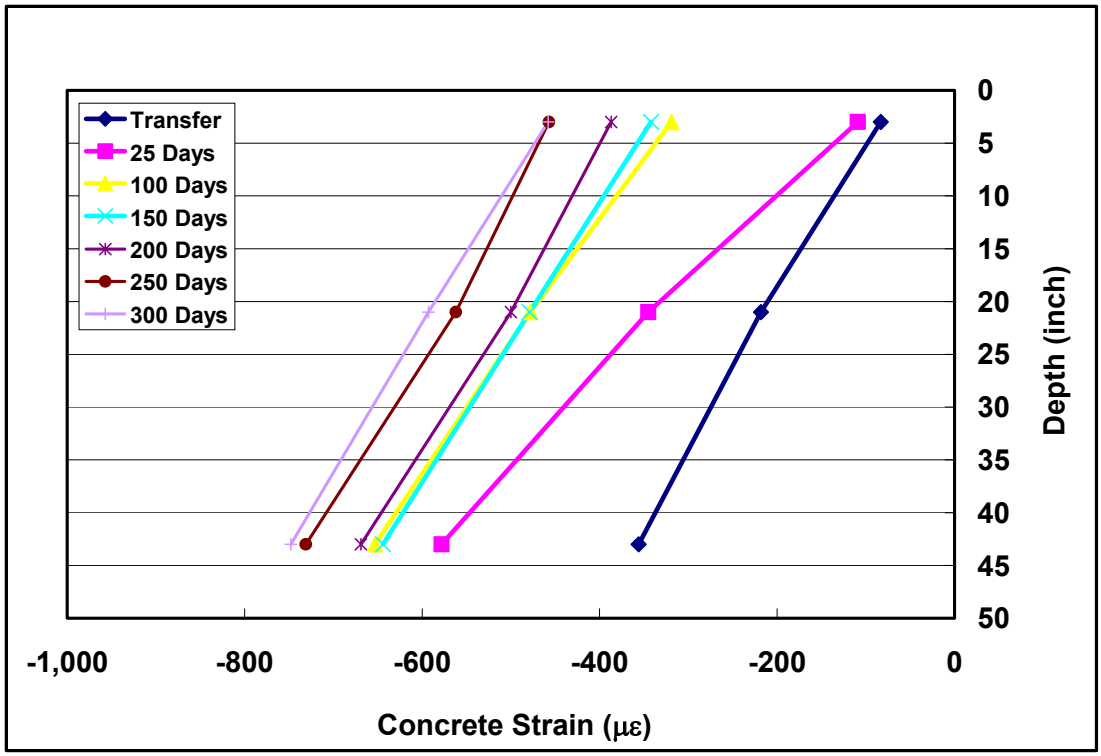

Figure 13.14 Strain versus depth for girder D1

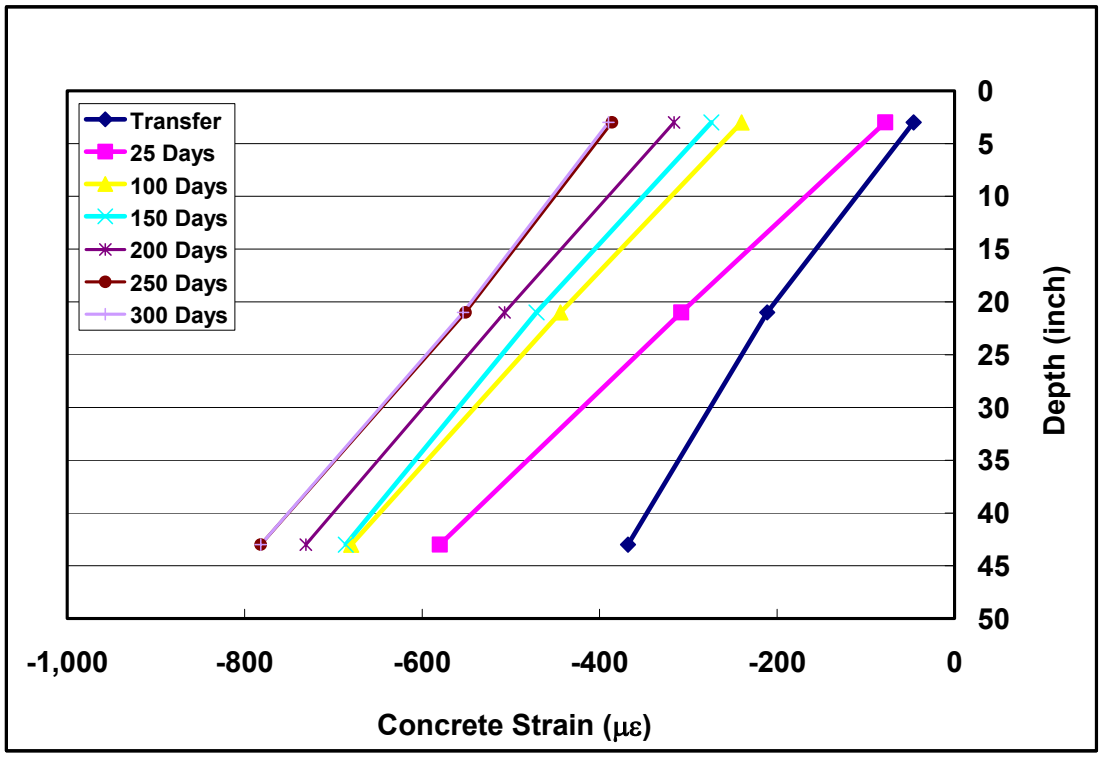

Figure 13.15 Strain versus depth for girder D3

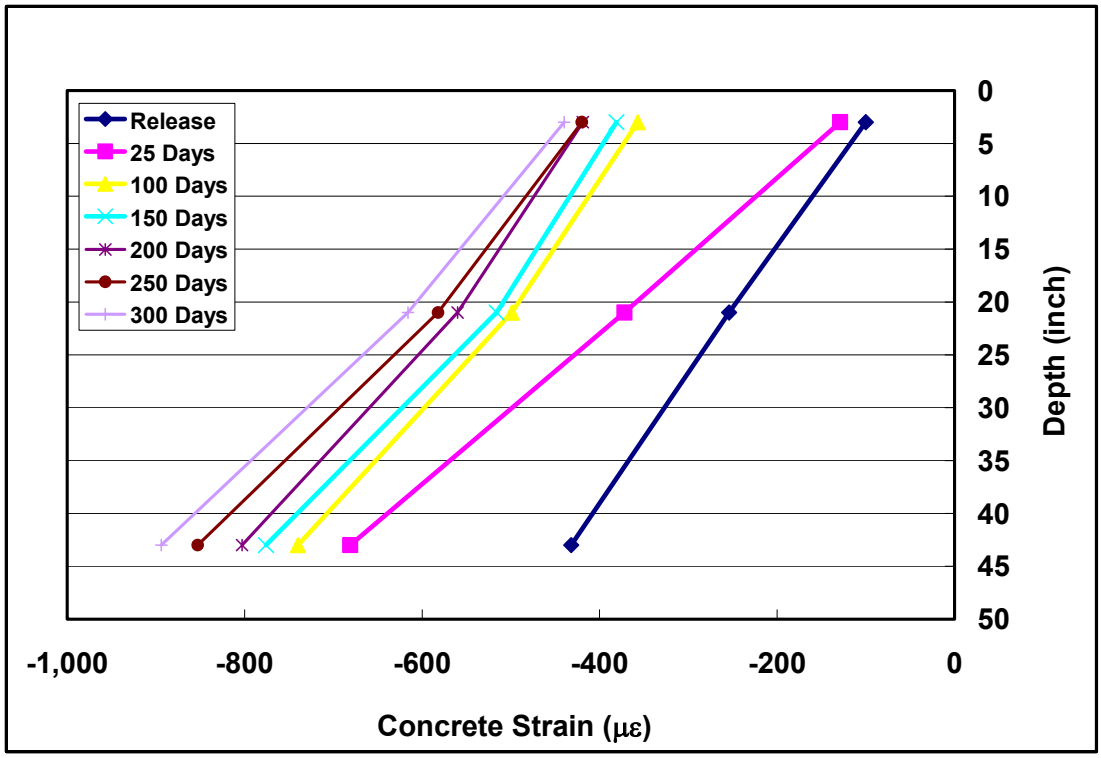

Figure 13.16 Strain versus depth for girder E3

13.3 Comparison with Code Expressions

This section compares experimental stress results with code predictions. Figure 13.17 compares the average effective stress for girders with SCC against those with conventional concrete. It can be seen that girders with conventional concrete have experienced less prestress loss than those with SCC. This can be attributed mainly to differences in the elastic shortening term. Also the creep effect may be larger due to the lower modulus of elasticity of the concrete.

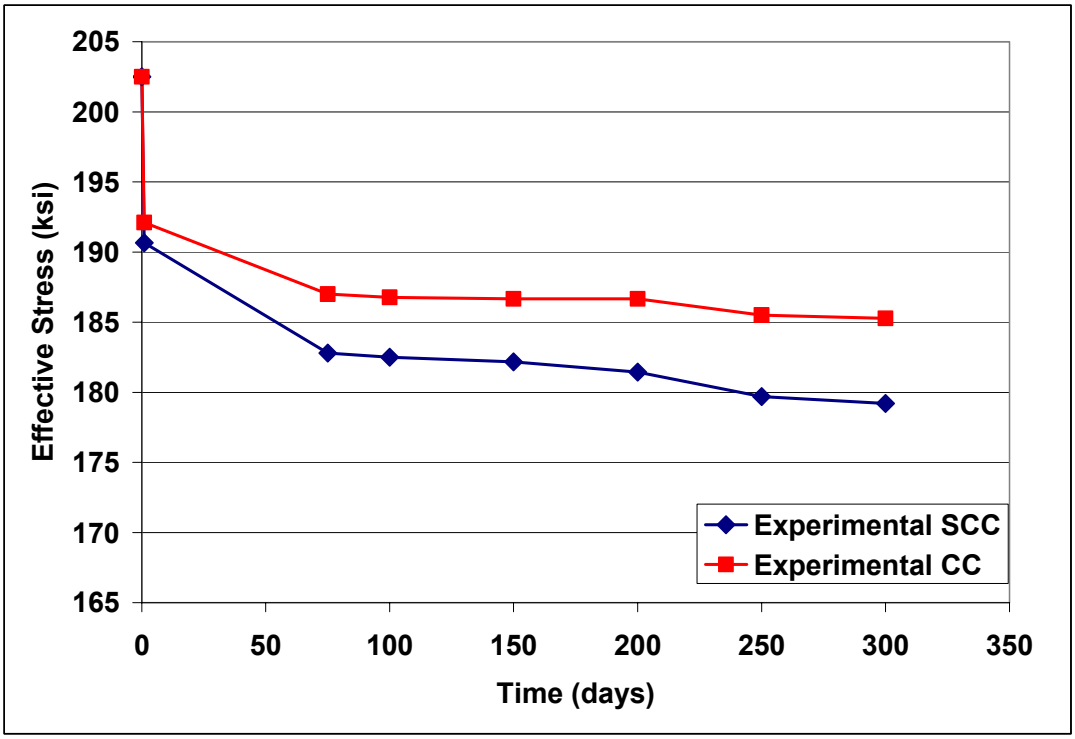

Figure 13.17 Comparison of SCC versus conventional concrete effective stress results

Code predictions were calculated using five different methods. Each method is outlined in section A.2 and calculations are in A.10. The five different methods used were ACI[4], PCI[9], AASHTO[5], KDOT[8], and ACI-209.[10] (It must be noted the ACI and PCI methods give very similar results and they will be presented together.) Resulting values from the first four methods are shown in Table 13.1. Effective stress values for both conventional concrete and SCC girders are shown. Tables 13.2 – 13.7 show the breakdown of each individual prestress loss term for the different methods used. Figures 13.18 and 13.19 present conventional concrete and SCC code predictions versus experimental results. Equation 8.3 was used to calculate loss predictions at intermediate days.

Table 13.1 Predicted effective stress values

Day	Conventional				SCC			
	ACI[4]/PCI[9]	AASHTO[5]	KDOT[8]	Experimental Stress	ACI[4]/PCI[9]	AASHTO[5]	KDOT[8]	Experimental Stress
Release	193.0	191.7	192.1	192.1	190.7	189.2	189.6	190.7
75	180.9	177.5	178.3	187.0	177.3	175.3	176.0	182.8
100	180.2	176.7	177.5	186.8	176.5	174.5	175.2	182.5
150	179.3	175.6	176.4	186.7	175.5	173.4	174.1	182.2
200	178.6	174.8	175.6	186.7	174.7	172.6	173.3	181.4
250	178.1	174.1	174.9	185.5	174.1	171.9	172.6	179.7
300	177.7	173.6	174.4	185.3	173.6	171.4	172.1	179.2
Ultimate	173.1	168.0	168.8	--	168.4	165.8	166.5	--

* all values reported in ksi

Table 13.2 Prestress loss using ACI/PCI method for conventional concrete girders

Day	Elastic Shortening	Creep	Shrinkage	Relaxation	Total Losses	ACI/PCI	Experimental Stress-CC
Release	7.9	0.0	0.0	1.6	9.5	193.0	192.1
75	7.9	6.4	3.6	3.7	21.6	180.9	187.0
100	7.9	6.8	3.9	3.7	22.3	180.2	186.8
150	7.9	7.4	4.2	3.7	23.2	179.3	186.7
200	7.9	7.9	4.4	3.7	23.9	178.6	186.7
250	7.9	8.2	4.6	3.7	24.4	178.1	185.5
300	7.9	8.5	4.8	3.7	24.8	177.7	185.3
Ultimate	7.9	11.4	6.4	3.7	29.4	173.1	--

* all values reported in ksi

Table 13.3 Prestress loss using AASHTO method for conventional concrete girders

Day	Elastic Shortening	Creep	Shrinkage	Relaxation	Total Losses	AASHTO	Experimental Stress-CC
Release	9.0	0.0	0.0	1.8	10.8	191.7	192.1
75	9.0	8.3	4.1	3.6	25.0	177.5	187.0
100	9.0	8.8	4.3	3.6	25.8	176.7	186.8
150	9.0	9.6	4.7	3.6	26.9	175.6	186.7
200	9.0	10.1	5.0	3.6	27.7	174.8	186.7
250	9.0	10.6	5.2	3.6	28.4	174.1	185.5
300	9.0	10.9	5.4	3.6	28.9	173.6	185.3
Ultimate	9.0	14.7	7.3	3.6	34.6	168.0	--

* all values reported in ksi

Table 13.4 Prestress loss method using KDOT method for conventional concrete girders

Day	Elastic Shortening	Creep	Shrinkage	Relaxation	Total Losses	KDOT	Experimental Stress-CC
Release	8.8	0.0	0.0	1.6	10.4	192.1	192.1
75	8.8	8.3	4.1	3.0	24.2	178.3	187.0
100	8.8	8.8	4.3	3.0	25.0	177.5	186.8
150	8.8	9.6	4.7	3.0	26.1	176.4	186.7
200	8.8	10.1	5.0	3.0	26.9	175.6	186.7
250	8.8	10.6	5.2	3.0	27.6	174.9	185.5
300	8.8	10.9	5.4	3.0	28.1	174.4	185.3
Ultimate	8.8	14.7	7.3	3.0	33.8	168.8	--

* all values reported in ksi

Table 13.5 Prestress loss method using ACI/PCI method for SCC girders

Day	Elastic Shortening	Creep	Shrinkage	Relaxation	Total Losses	ACI/PCI	Experimental Stress-SCC
Release	10.2	0.0	0.0	1.6	11.8	190.7	190.7
75	10.2	7.9	3.6	3.5	25.2	177.3	182.8
100	10.2	8.4	3.9	3.5	26.0	176.5	182.5
150	10.2	9.1	4.2	3.5	27.0	175.5	182.2
200	10.2	9.7	4.4	3.5	27.8	174.7	181.4
250	10.2	10.1	4.6	3.5	28.4	174.1	179.7
300	10.2	10.4	4.8	3.5	28.9	173.6	179.2
Ultimate	10.2	14.0	6.4	3.5	34.1	168.4	--

* all values reported in ksi

Table 13.6 Prestress loss method using AASHTO method for SCC girders

Day	Elastic Shortening	Creep	Shrinkage	Relaxation	Total Losses	AASHTO	Experimental Stress-SCC
Release	11.5	0.0	0.0	1.8	13.3	189.2	190.7
75	11.5	8.3	4.1	3.3	27.2	175.3	182.8
100	11.5	8.8	4.3	3.3	28.0	174.5	182.5
150	11.5	9.6	4.7	3.3	29.1	173.4	182.2
200	11.5	10.1	5.0	3.3	29.9	172.6	181.4
250	11.5	10.6	5.2	3.3	30.6	171.9	179.7
300	11.5	10.9	5.4	3.3	31.1	171.4	179.2
Ultimate	11.5	14.7	7.3	3.3	36.8	165.8	--

* all values reported in ksi

Table 13.7 Prestress loss method using KDOT method for SCC girders

Day	Elastic Shortening	Creep	Shrinkage	Relaxation	Total Losses	KDOT	Experimental Stress-SCC
Release	11.3	0.0	0.0	1.6	12.9	189.6	190.7
75	11.3	8.3	4.1	2.8	26.5	176.0	182.8
100	11.3	8.8	4.3	2.8	27.3	175.2	182.5
150	11.3	9.6	4.7	2.8	28.4	174.1	182.2
200	11.3	10.1	5.0	2.8	29.2	173.3	181.4
250	11.3	10.6	5.2	2.8	29.9	172.6	179.7
300	11.3	10.9	5.4	2.8	30.4	172.1	179.2
Ultimate	11.3	14.7	7.3	2.8	36.1	166.5	--

* all values reported in ksi

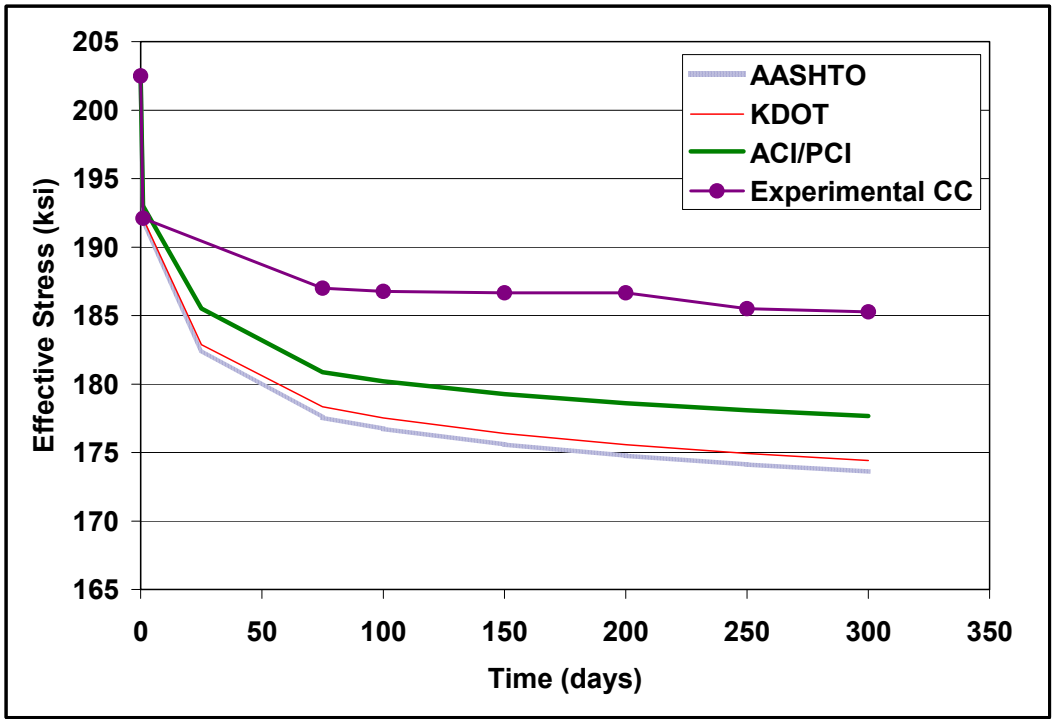

Figure 13.18 Effective stress calculations for conventional concrete girders

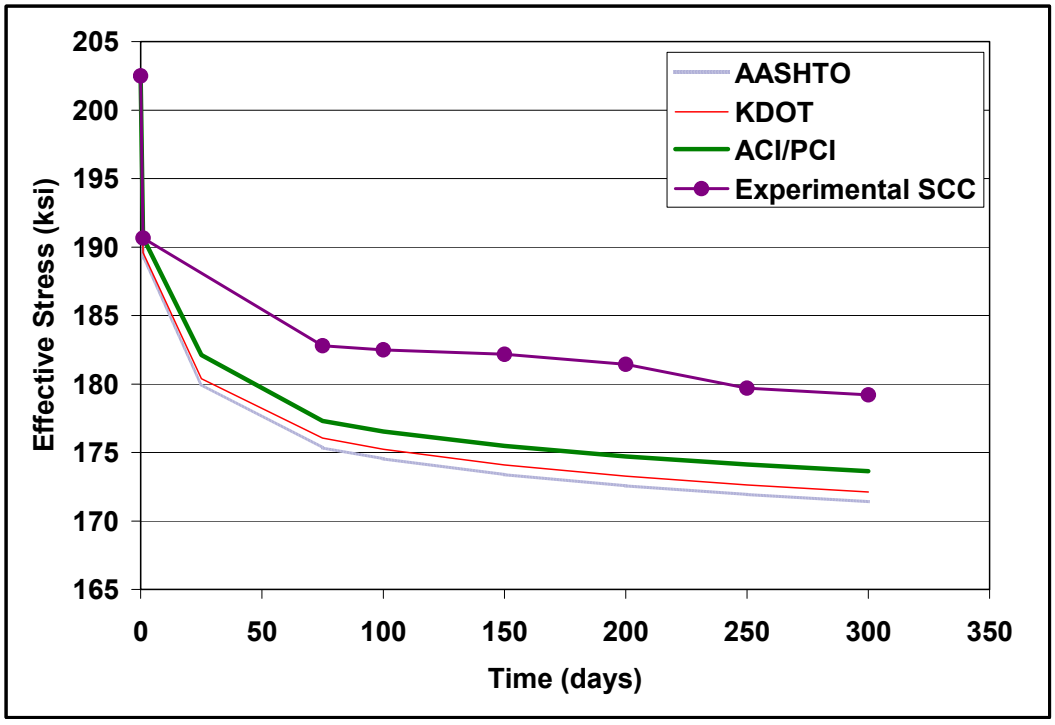

Figure 13.19 Effective stress calculations for girders with SCC

The ACI-209 method for predicting prestress loss was also used for the girders with SCC. Figure 13.20 presents these results. It can be seen that the ACI 209 method is much more conservative than predictions made by using the other four methods. A major difference is the prediction for shrinkage loss. It can be seen in Table 13.8 that the shrinkage loss prediction, using the ACI 209 method, is much greater than that of the other four methods. With a more accurate prediction of shrinkage loss for the ACI 209 method, it is assumed that predicted and experimental values would be much closer.

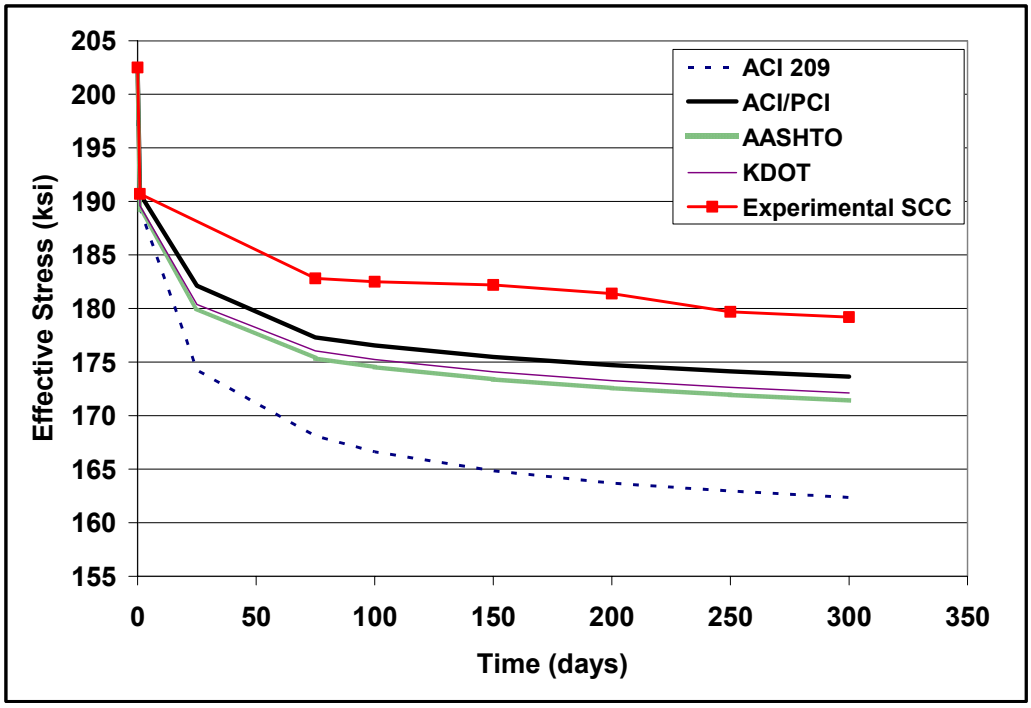

Figure 13.20 Effective stress comparison with all five methods for girders with SCC

Table 13.8 Shrinkage predictions using all five methods

Day	ACI-209	ACI/PCI	AASHTO	KDOT
Release	0.0	0.0	0.0	0.0
75	12.0	3.6	4.1	4.1
100	12.6	3.9	4.3	4.3
150	13.4	4.2	4.7	4.7
200	13.8	4.4	5.0	5.0
250	14.0	4.6	5.2	5.2
300	14.2	4.8	5.4	5.4
Ultimate	15.2	6.4	7.3	7.3

* all values reported in ksi

CHAPTER FOURTEEN - CONCLUSIONS AND RECOMMENDATIONS

14.1 Introduction

A three-phase comprehensive experimental and analytical research program was conducted to evaluate a proposed self-consolidating concrete (SCC) mixture in prestressed bridge applications. Phase I consisted of analyzing transfer lengths and development lengths of flexural specimens. Phase II evaluated the transfer length of an IT specimen by use of concrete surface strains along with monitoring long-term, time-dependent deformations. The primary objective of phase III was to monitor long-term prestress losses of bridge girders cast with both conventional concrete and self-consolidating concrete as placed in the field.

The test program was undertaken due to concerns for the low pullout values while performing large-block pullout tests (LBPTs) with prestressing strand in SCC. It must be noted that results obtained in this study are for the proposed SCC mixture, and other SCC mixtures may perform differently than the one tested in this program. While developing a new SCC mixture, it is not necessary to perform an extensive test program like the one carried out with this proposed SCC mixture, but it is imperative to confirm the long-term transfer length of the new SCC mixture. It has been shown that, in some cases, transfer lengths at release gave satisfactory results but then significantly increased with time. For the early age of the member, this will not be a problem; however, long-term issues could arise in the form of either shear or development length problems if strands continue to slip with time.

14.2 Conclusion Based on Flexural Specimens

The following can be concluded from the experimental studies conducted on the flexural specimens.

1. Large-block pullout test (LBPT) results for the strand used in this project and conducted with the mixture stipulated by Logan were above recommended minimum values for first-observed slip and maximum pullout force. Subsequent flexural beams fabricated with this strand and a proposed SCC all exhibited satisfactory flexural performance.
2. Recommended values for first-observed slip and maximum pullout force for 0.5-inch-diameter strand of 16 kip and 36 kip should not be used with LBPTs conducted with SCC. These values should be applied only when using a concrete mixture similar to the one stipulated by Logan.
3. Flexural tests indicated that current AASHTO (and also the ACI 318) equations for strand development length were conservative for the SCC and specimen geometry used in this study. Moreover, all specimens with an embedment length equal to 80% of the ACI development length, including those with more than 12 inches of concrete below the strand, failed in flexure by strand rupture.
4. Transfer lengths estimated from 18-day strand end-slip measurements were in general agreement with the values assumed by the AASHTO and ACI 318 specifications. Average implied transfer lengths for top-strand beams at 18

days and testing day were approximately 30% greater than those for the corresponding bottom-strand beams for all specimens with one strand.

5. There was an increase in implied transfer lengths during the first 18 days after detensioning. For specimens with strand cast two inches from the bottom, the average increase was 10 to 20%, while for specimens with the concrete cast more than 12 inches below the strand the increase was close to 100%. This suggests there is a top-strand effect for specimens cast with more than 12 inches of SCC below the stand.
6. Although a top-strand effect is present for members with this proposed SCC mixture, there was no evidence that it affected the development length for the members, just the transfer length.
7. No considerable increase in transfer length was measured after 18 days for the proposed SCC mixture.

14.3 Conclusions Based on IT Specimens

The following can be concluded from the experimental and analytical studies conducted on the IT specimens, along with the creep and shrinkage prisms.

1. Total observed losses for the experimental specimens were slightly less than those predicted by the current AASHTO, ACI/PCI, and KDOT design expressions.
2. Measured transfer lengths for the proposed SCC mixture and specimen geometry (IT) were in general agreement with the current AASHTO and ACI/PCI design assumptions, with the maximum measured transfer lengths

being 33% larger than the calculated value using equation 1.1, and close to values stipulated by AASHTO (60 d_b) and ACI (50 d_b) for shear design.

3. Using the proposed SCC mixture, it was found that effective prestress losses were in general accordance with current AASHTO, ACI/PCI, and KDOT code equations and no special design considerations need to be taken.
4. Creep coefficient and ultimate shrinkage strains were within general accordance with the values suggested by ACI Committee 209.
5. The ACI Committee 209 expression overestimated shrinkage for this proposed SCC mixture.

14.4 Conclusions Based on Cowley County Bridge

The following can be concluded from the experimental and analytical studies conducted on the girders used in the Cowley County Bridge.

1. Total observed losses for the bridge girders were slightly less than those predicted by current PCI design expressions.
2. Girders containing SCC had slightly larger prestress losses, and this can be attributed to a smaller modulus of elasticity of concrete for the SCC mixture.
3. Time-dependent deformations for the proposed SCC mixture are within acceptable range of design guideline equations recommended by the ACI, AASHTO, and KDOT, and no special design considerations need to be used when using this SCC mixture.
4. The current conventional concrete mixture is exhibiting satisfactory performance in prestressed bridge girders.

5. At time of publication, none of the girders instrumented with VWSGs had time-dependent deformations exceeding those predicted by code equations.

14.5 Recommendations Based on Experimental Results

As with any experimental program involving a limited number of tests, it is difficult to draw universal conclusions and recommendations. However, the following recommendations are made to the state of Kansas regarding the experimental procedure used when evaluating the proposed SCC mixture in state bridge girders.

1. Current KDOT design guidelines should be used when SCC is to be used in state girders and no changes should be made.
2. General code equations for predicting modulus of elasticity (E_c) for the SCC mixture should not be used. The current equation overestimates the modulus of elasticity for the proposed SCC mixture. For this reason, experimental results for modulus should be used until a more accurate model is developed for the propsed SCC mixture.
3. Further tests should be completed to examine the top-strand effect to determine if the increased transfer lengths are due to bleed water or the amount of concrete above of strand. It is believed that the pressure being applied by the concrete above the strand is contributing to smaller transfer lengths than those members with less concrete above the strand. The following test would confirm if the bleed water from below the strand or the amount of concrete above the strand affects the transfer length.

- Perform LBPTs on specimens in which the strand is cast and cured in the horizontal position.
- Have blocks with the strand at various amounts of concrete above and below the stand.
- For one of the blocks place a dead weight over the curing concrete to test if the consolidation pressure above is affecting pullout values.
- The following three blocks would be cast and tested to evaluation the bleed water effect and the amount of concrete above the strand. The side view of each block will be shown with the depth of each block being 24 inches. Block #1 (Figure 14.1) would be the control. Block #2 (Figure 14.2) would have two rows of strands to evaluate both the bleed water and amount of concrete above the strand. Block #3 (Figure 14.3 would have the same dimensions as Block #1, however it would have a dead load of 1400 pounds, the exact weight of concrete above the bottom row of strands of Block #2.

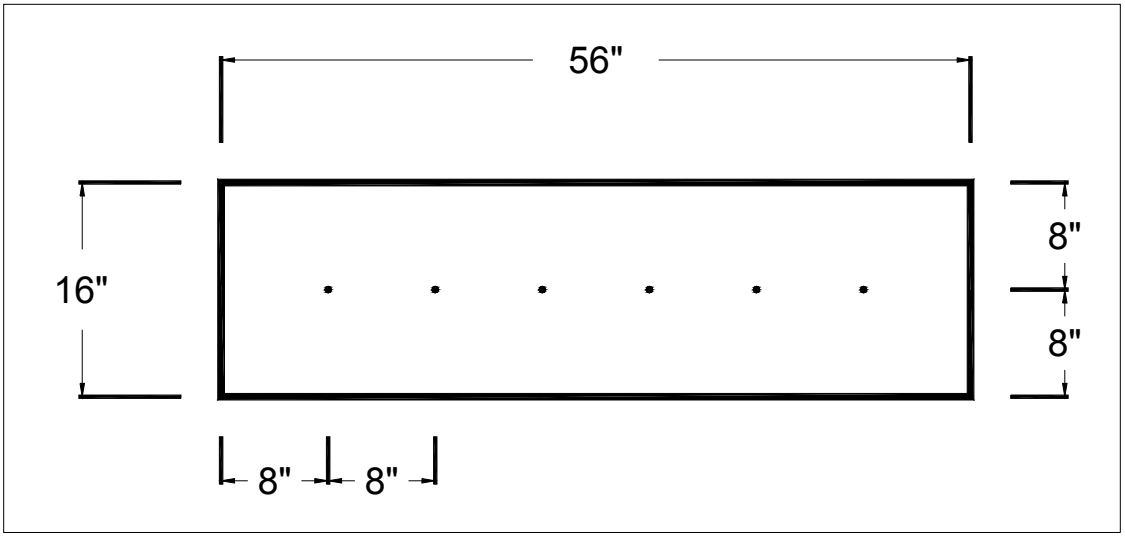

Figure 14.1 Block #1

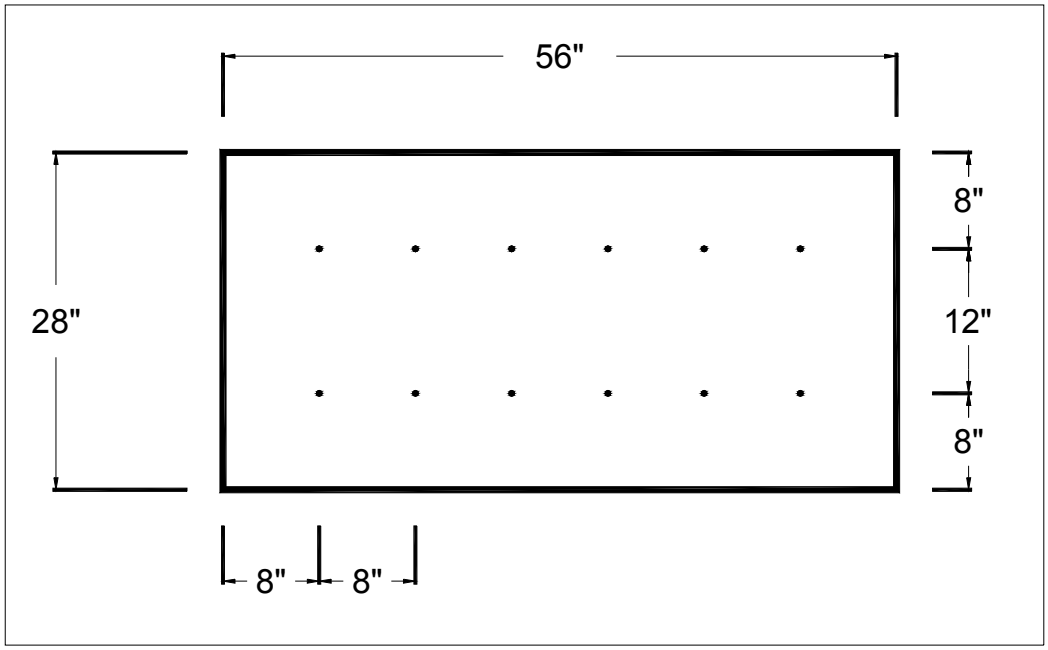

Figure 14.2 Block #2

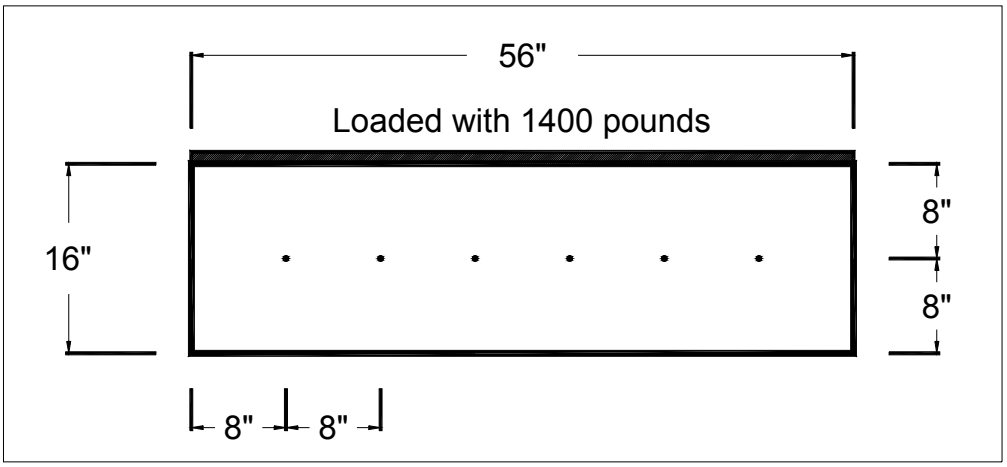

Figure 14.3 Block #3 (Loaded with 1400 pounds)

The following conclusions could be made depending of the results of the tests performed.

1. If the bleed water below the strand was the causing the poor bond of the top strands, then the pullout values of Blocks #1 and #3 would act the same as the bottom row of Block #2 having much higher pullout values the top row of Block #2.
2. If the amount of concrete above the strand is the major contributing factor to bond, then Block #1 and the top row of Block #2 would behave the same while Block #3 and the bottom row of Block #2 would act similar.

14.6 Recommendations Based on Plant Observations

The following recommendations are for KDOT to use after allowing SCC in state girders.

1. Consistency in the SCC mixture needs to be monitored, and a consistent spread for the concrete needs to be maintained throughout the placement of concrete. A

24 to 28-inch spread should be targeted when using the proposed SCC mixture. It has been seen that when the SCC spread gets below 24 inches the development of "bug" holes begin. This measurement needs to be taken at the site of the prestressing bed, not the batch plant. A mix can look good (spread and VSI) at the batch plant but segregation during handling can affect the concrete mix.

2. Long delays between placement of the SCC into the same girder needs to be eliminated. Cast lines can develop if too much time elapses from the time placement has ended with one truck and begins with the next. One way to eliminate these cast lines is to dispense the concrete at a slower rate, thus eliminating long breaks between trucks.
3. When hot temperatures exist (more than 90 degrees F), special precautions need to be made to prevent major (+6 inch) spread loss from batch plant to prestressing beds.
4. The state inspector should be trained in determining whether or not the SCC mixture is acceptable for use in girders.

14.7 Recommendations to Evaluate Other SCC Mixtures

The research program that was completed to evaluate the proposed SCC mixture was a long process. The following recommendations are made to evaluate other mixtures that are to be used in bridge girders.

1. The Large Block Pullout Tests fabricated with SCC are not a good indicator on whether the SCC mixture will perform well when the strand is in the horizontal position. LBPTs should only be used with the concrete stipulated by Logan.

2. Performing transfer length measurements on flexural specimens should be used when evaluating a potential SCC mixture. It is important to take readings well after detensioning to determine if the strand is continuing to "draw" in to the beam and the transfer length is getting longer over time. The use of Whittemore points to measure surface strains to determine transfer length was a lengthy process and could be eliminated since transfer lengths estimated from strand end-slip yield similar results.
3. Casting specimens with strand near the bottom and top of the specimens are important. However having three specimens for each embedment length was not needed. If one specimen (not three) was loaded similar to the 100% M_n loading condition and the beam had not failed after the 24 hour hold then it could be concluded that the mix would perform well in flexure. Additionally, only 80% embedment length specimens could be tested and if no failure before nominal capacity were seen then there would be no need to run the 100% embedment length specimens.
4. The placement of three VWSG's into a potential bridge girder cast with SCC would be a good indictor of determining long-term prestress losses. If any major differences are seen between the girder cast with SCC and those of code expressions then designs accounting for long-term losses should be based on experimental measurements for the actual SCC mixture, rather then code expressions. The casting of separate girders to isolate shrinkage alone is not needed to determine total losses

Notations

A	-	Cross-sectional area of member
AASHTO	-	American Association of State Highway Transportation Officials
ACI	-	American Concrete Institute
A_{ps}	-	Area of prestressing strand
CC	-	Conventional concrete
d_b	-	Diameter of prestressing strand
d_p	-	Depth of prestressing strand
E	-	Eccentricity
E_c	-	28-day modulus of elasticity of concrete
E_{ci}	-	Release modulus of elasticity of concrete
E_{ps}	-	Modulus of elasticity of prestressing strand
f'_c	-	28-day compressive concrete strength
f'_{ci}	-	Release compressive concrete strength
f_{pj}	-	Stress in strand after tensioning
f_{ps}	-	Stress in prestressing strand at failure
f_{se}	-	Effective prestress, after all time-dependent deformations
f_{si}	-	Prestress after transfer before time-dependent losses
FT	-	Fully tensioned
KDOT	-	Kansas Department of Transportation
LBPT	-	Large-block pullout test
RH	-	Relative humidity
I	-	Moment of inertia of cross section
IT	-	Inverted-T
L	-	Length of member
L_{dev}	-	Development length
L_e	-	Embedment length
L_{tr}	-	Transfer length
M_n	-	Nominal moment
M_{sw}	-	Moment due to self weight of member
P	-	Force in prestressing strand after release
PCI	-	Prestressed/Precast Concrete Institute
SCC	-	Self-consolidating concrete
SSB	-	Single-strand beam
TB	-	T-beam
TSB	-	Top-strand beam
UT	-	Untensioned
V/S	-	Volume-to-surface ratio
v_t	-	Creep coefficient at any given time
v_u	-	Ultimate creep coefficient
VWSG	-	Vibrating wire strain gage
Y	-	Distance to neutral axis
Δ	-	Measured end slip
ε	-	Strain

$(\varepsilon_{sh})_t$ - Shrinkage strain at any time
$(\varepsilon_{sh})_u$ - Ultimate shrinkage strain
σ - stress

References

1. Interim Guidelines for the Use of Self-Consolidating Concrete in Precast/ Prestressed Concrete Institute Member Plants, First Edition, Chicago, IL, 2003.

2. Russell, B.W., and Burns, N. H., "Design Guidelines for Transfer, Development and Debonding of Large Diameter Seven Wire Strands in Pretensioned Concrete Girders," Texas Department of Transportation, Research Project 3-5-89/2-1210, 286 pp., January 1993.

3. Peterman, R. J., Ramirez, J. A., and Olek, J., "Influence of Flexure-Shear Cracking on Strand Development Length in Prestressed Concrete Members," *PCI Journal*, V. 45, No. 5, September-October 2000, pp. 76-94.

4. ACI Committee 318, "Building Code Requirements for Structural Concrete (ACI 318-02) and Commentary (ACI 318R-02)," American Concrete Institute, Farmington Hills, MI, 2002.

5. AASHTO, *LRFD Bridge Design Specifications*, 3rd Ed., American Association of State Highway and Transportation Officials, Washington, DC, 2004.

6. Logan, Donald R., "Acceptance Criteria for Bond Quality of Strand for Pretensioned Prestressed Concrete Applications," *PCI Journal*, V.42, No. 2, March-April 1997, pp.52-90.

7. Nilson, A., *Design of Prestressed Concrete*, Second Edition, John Wiley & Sons, New York, New York, 1987.

8. Kansas Department of Transportation Design Manual, Bridge Section, V. 3, Version September 2003.

9. *PCI Design Handbook*, Sixth Edition, Precast/Prestressed Concrete Institute, Chicago, IL, 2004.

10. ACI Committee 209, "Prediction of Creep, Shrinkage, and Temperature Effects in Concrete Structures," American Concrete Institute, Farmington Hills, Mich., 1997.

11. Ouchi, M., "Self-Compacting Concrete Development, Applications and Investigations," *Proceedings of the Fourth International Conference on Materials Engineering for Resources*, V. 1, 2001, pp. 53-58.

12. Bury, A., and Christensen, B., "The Role of Innovative Chemical Admixtures in Producing Self-Consolidating Concrete," First North American Conference on the Design and Use of Self-Consolidating Concrete, 2002, pp. 137-140.

13. Ouchi, M.; Nakamura, S.; Osterberg, T.; Hallberg, S.; Lwin, M., "Applications of Self-Compacting Concrete in Japan, Europe, and the United States," 2003 ISHPC.

14. Janney, J., "Nature of Bond in Pre-tensioned Prestressed Concrete," *Journal of the American Concrete Institute*, May 1954, pp717-736.

15. Hanson, N., and Kaar, P., "Flexural Bond Tests of Pretensioned Prestressed Beams," *Journal of the American Concrete Institute*, V. 55, n. 51, January 1959, pp. 783-802.

16. Kaar, P., LaFraugh, R., and Mass, M., "Influence of Concrete Strength on Strand Transfer Length," *Ninth Annual Convention of the Prestressed Concrete Institute*, October 1963, pp. 47-67.

17. Janney, J., "Report of Stress Transfer Length Studies on 270 k Prestressing Strand," *PCI Journal*, February 1963, pp. 41-45.

18. Kaar, P., and Hanson, N., "Bond Fatigue Tests of Beams Simulating Pretensioned Concrete Crossties," *PCI Journal*, V. 20, n. 5, September- October 1975, pp 65-80.

19. Martin, L., and Scott, N., "Development of Prestressing Strand in Pretensioned Members," *ACI Journal*, V. 73, n. 8, August 1976, pp 453-453.

20. Zia, P., and Mostafa, T., Development Length of Prestressing Strands," *Journal of Prestressed Concrete Institute*, V. 22, n. 5, September-October 1977, pp. 54-65.

21. Cousins, T., Johnston, D., and Zia, P., "Transfer and Development Length of Epoxy Coated and Uncoated Prestressing Strand," *PCI Journal*, V. 35, n. 4, July-August 1990, pp. 92-103.

22. Cousin, T., Badeaux, M., and Moustafa, S., "Proposed Test for Determining Bond Characteristics of Prestressing Strand," *PCI Journal*, V. 37, n.1, January-Febuaury1992, pp. 66-73.

23. Shahawy, M., Issa, M., and Batchelor, B., "Strand Transfer Lengths in Full Scale AASHTO Prestressed Concrete Girders," *PCI Journal*, V. 37, n. 3, May-June 1992, pp. 84-96.

24. Mitchell, D., Cook, W., Khan, A., and Tham, T., "Influence of High Strength Concrete on Transfer and Development Length of Pretensioning Strand," PCI *Journal*, V. 38, n. 3, May-June 1993, pp. 52-66.

25. Buckner, D., "A Review of Strand Development Length for Pretensioned Concrete Members," *PCI Journal*, V. 40, No. 2, March-April 1995, pp.84-105.

26. Martin, L., and Korkosz, W., "Strength of Prestressed Concrete Members at Sections Where Strands are not Fully Developed," *PCI Journal*, V. 40, n. 5, September- October 1995, pp. 58-66.

27. Russell, B., and Burns, N., "Measured Transfer Lengths of 0.5 and 0.6 in. Strands in Pretensioned Concrete," *PCI Journal*, V. 41, n. 5, September-October 1996, pp. 44-64.

28. Rose, D., and Russell, B., "Investigation of Standardized Tests to Measure the Bond Performance of Prestressing Strand," *PCI Journal*, V. 42, n. 4, July-August 1997, pp. 44-66.

29. Lane, S., "A New Development Length Equation for Pretensioned Strands in Bridge Beams and Piles," Publication No. FHWA-RD-98-116, December 1996, pp. 123.

30. Steinberg, E., Beier, J., and Sargand, S., "Effects of Sudden Prestress Force Transfer in Pretensioned Concrete Beams," *PCI Journal*, V. 46, n. 1, January-February 2001, pp.64-75.

31. Oh, B., Kim, E., and Kim, K., "Correct Prediction of Transfer Lengths in Pretensioned Prestressed Concrete Structures," SmiRT 16, Washington DC, August 2001 pp. 1-8.

32. Barnes, R. W., Grove, J. W., and Burns, N. H., "Experimental Assessment of Factors Affecting Transfer Length," *ACI Structural Journal*, V. 100, No. 6, November-December 2004, pp. 740-748.

33. Khayat, K., Petrov, N., Attiogbe, E., and See, H., "Uniformity of Bond Strength of Prestressing Strands in Conventional Flowable and Self-Consolidating Concrete Mixtures," *3rd International Symposium on Self-Compacting Concrete*, August 17-20, 2003, Iceland, pp. 703-712.

34. Girgis, A., and Tuan, C., "Bond Strength and Transfer Length of Pretensioned Bridge Girders Cast with Self-Consolidating Concrete," *PCI Journal*, V. 50, n. 6, November-December 2005, pp. 72-87.

35. Burgueno, R., and Haq, M., "Transfer and Development Length of Prestressing Strands in Precast/Prestressed Girders using Self-Consolidating Concrete," SCC 2005 Proceedings, 6 pp.

36. The European Guidelines for Self-Compacting Concrete: Specification, Production and Use, May 2005.

37. Tabatabai, H.; Dickson, T., "The History of the Prestressing Strand Development Length Equation," *PCI Journal*, V. 38, No. 6. pp. 64-75.

38. Ahlborn, T., French, C., and Shield, C., "High-Strength Concrete Prestressed Bridge Girders: Long Term and Flexural Behavior," Final Report 2000-32, Minnesota Department of Transportation, Nov 2000, 357 pp.

39. Barr, E., Fekete, M., Eberhard, J., Stanton, B., Khaleghi, J., and Hsieh, J., "High Performance Concrete in Washington State SR 18/SR 516 Overcrossing: Interim Report on Girder Monitoring," Interim Report Jan 1996- Nov1998, Washington State Department of Transportation, April 2000 129 pp.

40. Ramakrishnan, V., and Sigi, A., "Evaluation of High Performance Concrete in Four Bridge Decks as well as Prestressed Girders for Two Bridges," Final Report Study SD98-06, South Dakota Department of Transportation, December 2001, 180 pp.

41. Onyemelukwe, O., Issa, M., and Mills, C., "Field Measured Pre-Stress Concrete Losses Versus Design Code Estimates," Experimental Mechanics, V. 43, n. 2, June 2003, pp.201-215.

42. Yang, Y., and Myers, J., "Prestress Loss Measurements in Missouri's First Fully Instrumented High-Performance Concrete Bridge," *Transportation Research Record: Journal of the Transportation Research Board*, No. 1928, 2005, pp.118-125.

43. ASTM C1611 Standard Test Method for Slump Flow of Self-Consolidating Concrete.

44. ASTM C1621 Standard Test Method for Passing Ability of Self-Consolidating Concrete by J-Ring.

45. Khayat, K. H., Assaad, J., and Daczko, J., "Comparison of Field-Oriented Test Methods to Assess Dynamic Stability of Self-Consolidating Concrete," ACI Materials Journal, V. 101, No. 2, March-April 2004, pp. 168-176.

46. Geokon Inc., "Installation Manual: Models VCE-4200/4202/4210 Vibrating Wire Strain Gages," Nebanon, New Hampshire, 2004.

47. Corley, W.G., and Sozen, M.A., "Time Dependent Deflections of Reinforced Concrete Beams," *Journal of the American Concrete Institute*, Proceedings V. 63, No. 3, March 1966, pp. 373-386.

48. Mokhtarzadeh, A., and French, C., "Time-Dependent Properties of High-Strength Concrete with Consideration for Precast Application," *ACI Materials Journal*, V. 97, No. 3. May-June 2000, pp. 263-271.

49. ASTM C512 Standard Test Method for Creep of Concrete in Compression.

APPENDIX

A.1 LBPT Tables

Table A.1 Mixture proportions stipulated by Logan

Materials	Quantity per yd^3
Cement (Type III)	660 lb
Concrete Sand	1100 lb
Crushed Gravel (Max 3/4")	1900 lb
Normal Range Water Reducer	26 oz
Air-Entraining Agent	0 oz
High Range Water Reducer	0 oz
Water	35 gal
w/c ratio	0.44

Note: The coarse aggregate had a maximum size of ¾" and an average Moh's hardness of 6.2 and the fineaggregate had a fineness modulus of 2.83

Table A.2 LBPT with SCC and control strand

SCC with Control Strand		
Specimen	**Max Load (kip)**	**Load at 1st Slip (kip)**
1	21.8	11.8
2	21.4	12.5
3	19.7	12.4
4	27.5	10.7
5	23.2	12.7
6	21.4	10.7
Average	**22.5**	**11.8**
Coeff of Var	**12.0%**	**7.7%**

Table A.3 LBPT with Logan concrete and control strand

Logan Concrete with Control Strand		
Specimen	**Max Load (kip)**	**Load at 1st Slip (kip)**
1	42.0	28.2
2	41.7	27.8
3	40.4	27.3
4	36.5	24.9
5	36.9	24.2
6	39.9	25.0
Average	**39.5**	**26.2**
Coeff of Var	**6.0%**	**6.6%**

A.2 Prestress Loss Equations

ACI and PCI METHOD

Elastic Shortening of Concrete (ES)

For members with bonded tendons,

$$ES = K_{es} E_s \frac{f_{cir}}{E_{ci}}$$

in which

K_{es} = 1.0 for pretensioned members
K_{es} = 0.5 for post-tensioned members when tendons are tensioned in sequential order to the same tension. With other post-tensioning procedures, the value for K_{es} may vary from 0 to 0.5.

$$f_{cir} = K_{cir} f_{cpi} - f_g$$

in which

K_{cir} = 1.0 for post-tensioned members.

K_{cir} = 0.9 for pretensioned members.

Creep of Concrete (CR)

For members with bonded tendons,

$$CR = K_{cr}\frac{E_s}{E_c}\left(f_{cir} - f_{cds}\right)$$

in which

K_{cr} = 2.0 for pretensioned members
K_{cr} = 1.6 for post-tensioned members

Shrinkage of Concrete (SH)

$$SH = 8.2x10^{-6} K_{sh} E_s \left(1 - 0.06\frac{V}{S}\right)\left(100 - RH\right)$$

in which

K_{sh} = 1.0 for pretensioned members
or
K_{sh} is taken from Table 1[9] for post-tensioned members.

Relaxation of Tendons (RE)

$$RE = \left[K_{re} - J\left(SH + CR + ES\right)\right]C$$

in which the values of K_{re}, J, and C are taken from Tables 2 and 3.[9]

AASHTO METHOD

Taken from the Third Edition[5] for pretensioned members

$$\Delta f_{pT} = \Delta f_{pES} + \Delta f_{pSR} + \Delta f_{pCR} + \Delta f_{pR2}$$

where:
Δf_{pT} = total loss (ksi)
Δf_{pES} = loss due to elastic shortening (ksi)
Δf_{pSR} = loss due to shrinkage (ksi)
Δf_{pCR} = loss due to creep of concrete (ksi)
Δf_{pR2} = loss due to relaxation of steel after transfer (ksi)

Elastic Shortening (Δf_{pES})

$$\Delta f_{pES} = \frac{E_p}{E_{ci}} f_{cgp}$$

where:

f_{cgp} = sum of concrete stresses at the center of gravity of prestressing tendons due to the prestressing force at transfer and the self-weight of the member at the sections of maximum moment (ksi)

E_p = modulus of elasticity of prestressing steel (ksi)

E_{ci} = modulus of elasticity of concrete at transfer (ksi)

Shrinkage (Δf_{pSR})

$$\Delta f_{pSR} = \left(17.0 - 0.150H\right)$$

where:

H = the average annual ambient relative humidity (percent)

Creep (Δf_{pCR})

$$\Delta f_{pCR} = 12.0 f_{cgp} - 7.0\Delta f_{cdp} \geq 0$$

where:

f_{cgp} = concrete stress at center of gravity of prestressing steel at transfer (ksi)

Δf_{cdp} = change in concrete stress at center of gravity of prestressing steel due to permanent loads with the exception of the load acting at the time the prestressing force is applied. Values of Δf_{cdp} should be calculated at the same section or at sections for which f_{cgp} is calculated (ksi)

Relaxation (Δf_{pR2})

At transfer

In pretensioned members, the relaxation loss in prestressing steel, initially stressed in excess of $0.50 f_{pu,}$ may be taken as:

For stress-relieved strand:

$$\Delta f_{pR1} = \frac{\log\left(24.0t\right)}{10.0}\left[\frac{f_{pj}}{f_{py}} - 0.55\right] f_{pj}$$

For low-relaxation strand:

$$\Delta f_{pR1} = \frac{\log(24.0t)}{40.0}\left[\frac{f_{pj}}{f_{py}} - 0.55\right] f_{pj}$$

where:

t = time estimated in days from stressing to transfer (days)
f_{pj} = initial stress in the tendon at the end of the stressing (ksi)
f_{py} = specified yield strength of prestressing steel (ksi)

After Transfer

Losses due to relaxation of prestressing steel may be taken as:

For pretensioning with stress-relieved strands:

$$\Delta f_{pR2} = 20.0 - 0.4\Delta f_{pES} - 0.2\left(\Delta f_{pSR} + \Delta f_{pCR}\right)$$

where:
Δf_{pES} = loss due to elastic shortening (ksi)
Δf_{pSR} = loss due to shrinkage (ksi)
Δf_{pCR} = loss due to creep of concrete (ksi)

For prestressing steels with low relaxation properties conforming to AASHTO M 203 (ASTM A 416 or E 328):

Use 30 percent of Δf_{pR2} given by equation 12.

KDOT METHOD

As described in the 2003 release[8].

The loss of stress in the prestressing steel is as follows:

Δf_S = SH + ES + CR_C +CR_S
Δf_S = Loss of stress, psi
SH = Loss due to concrete shrinkage, psi
ES = Loss due to elastic shortening, psi
CR_C = Loss due to creep of concrete, psi
CR_S = Loss due to relaxation of steel, psi

<u>Shrinkage</u>

The shrinkage loss is computed as follows,

$$SH = 17,000 - 150RH$$

Where RH is the average relative humidity in percent. For Kansas, the humidity may be assumed at 65 percent.

Elastic Shortening

Elastic shortening is computed as follows:

$$ES = \left(E_s \big/ E_{ci} \right) f_{cir}$$

in which

E_s = 28×10^6 psi

E_{ci} = Modulus of elasticity of concrete at transfer of stress ($33W^{3/2} \sqrt{f_{ci}^{'}}$ psi.)

W = 145 pcf for normal weight concrete

f_{cir} = Concrete stress at the center of gravity of the prestressing steel due top prestressing force and dead load of the beam immediately after transfer. (At this stage, the initial stress in the tendon has been reduced by elastic shortening of the concrete and tendon relaxation during placing and curing of the concrete.)

Creep of Concrete:

For pretensioned and post-tensioned members

$$CR_C = 12 f_{cir} - 7 f_{cds}$$

Where f_{cds} is the concrete stress at the center of gravity of prestressing steel due to all dead loads except the dead loads present at the time prestressing force is applied.

Relaxation of Prestressing Steel – (Low Relaxation Strand)

$$CR_S = 5,000 - 0.10ES - 0.05\left(SH + CR_C\right)$$

The values of *ES*, *SH*, and CR_C are those computed previously,

Total losses: $\Delta f = SH + ES + CR_C + CR_S$

The minimum loss of prestress to be used when computing service load stresses shall be 35,000 psi.

$$\lambda_t = (nf_c) + (nf_c)v_t\left(1 - \frac{F_t}{2F_0}\right) + \frac{(\varepsilon_{sh})_t E_s}{1 + n\rho\xi_s} + (f_{sr})_t$$

where

λ_t = total losses

n = modular ratio, E_S/E_{ci} at the time of loading;

f_c = concrete stress such as at steel c.g.s. due to prestress and precast beam dead load in the prestress loss equations;

v_t = creep coefficient at any time;

F_t = total loss of prestress at any time minus the inital elastic loss;

F_o = prestress force at transfer, after elastic loss;

$(\varepsilon_{sh})_t$ = shrinkage strain at any time;

E_s = modulus of elasticty of steel;

ρ = reinforcement ratio;

ξ_s = cross section shape coefficient;

$(f_{sr})_t$ = stress loss due to steel relaxation in prestressed member at any time.

A.3 Shear Calculations for Single Strand Specimens

Test Span $L_{test} = 12.83$ ft

Shear Span $a_{test} = 5.92$ ft

$M_D + M_L = 32.9$ kip-ft

$$\frac{(0.0933)\text{ x }(12.83)^2}{8} + \frac{P_F}{2}(5.92) = 32.9$$

$P_F = 10.5$ kips

$$V_{\max} = 0.0933\text{ x }(6) + \frac{10.5}{2} = 5.8\text{ kip}$$

$$V_c = 2 * \sqrt{f_c'}\text{ x }b\text{ x }d_p = 2\text{ x }\sqrt{8,000}\text{ x }8\text{ x }10 = 14.3\text{ kip}$$

$V_c > V_{\max}$ (Good)

A.4 Nominal Moment Calculations for Single Strand Specimens

$$P_e = f_{se} \text{ x } A_{ps} = 185 \text{ x } 0.153 = 28.3 \text{ kip}$$

$$\varepsilon_1 = f_{se} / E_p = 185 / 28,500 = 0.00649$$

$$\varepsilon_2 = \frac{1}{E_c}\left[\frac{P_e}{A} + \frac{P_e \text{ x } e^2}{I}\right] = \frac{1}{5000}\left[\frac{28.3}{96} + \frac{28.3 \text{ x } 4^2}{1152}\right] = .000138$$

Assume $f_{ps} = 268.2 \text{ ksi}$

$$a = \frac{A_{ps} \text{ x } f_{ps}}{0.85 \text{ x } f_c^{'} * b} = \frac{0.153 \text{ x } 268.2}{0.85 \text{ x } 8 \text{ x } 8} = 0.754$$

$$c = a / \beta_1 = 0.754 / 0.65 = 1.16$$

$$\varepsilon_3 = \left(\frac{d_p - c}{c}\right) \text{x } \varepsilon_c = \left(\frac{10 - 1.16}{1.16}\right) \text{x } 0.003 = 0.0229$$

$$\varepsilon_{ps} = \varepsilon_1 + \varepsilon_2 + \varepsilon_3 = 0.00649 + 0.000138 + 0.0229 = 0.0295$$

From strand stress-strain curve in PCI Design Handbook

$$f_{ps} = 270 - \frac{0.04}{\varepsilon_{ps} - 0.007} = 268.2 \text{ ksi (Equals assumed value)}$$

$$M_n = A_{ps} \text{ x } f_{ps} \text{ x} \left(d_p - \frac{a}{2}\right) = 0.153 \text{ x } 268.2 \text{ x} \left(10 - \frac{.754}{2}\right) = 394.9 \text{ kip-in.}$$

$$= 32.9 \text{ kip-ft}$$

A.5 Nominal Moment Calculations for TB Specimens

$$P_e = f_{se} \text{ x } A_{ps} = 181\big((5)0.153\big) = 138.5 \text{ kip}$$

$$\varepsilon_1 = f_{se} / E_p = 181/28{,}500 = 0.00635$$

$$\varepsilon_2 = \frac{1}{E_c}\left[\frac{P_e}{A} + \frac{P_e \text{ x } e^2}{I}\right] = \frac{1}{5000}\left[\frac{138.5}{466} + \frac{138.5 \text{ x } 10.52^2}{17733}\right] = .000232$$

Assume $f_{ps} = 268.8$ ksi and compression in flange

$$a = \frac{A_{ps} \text{ x } f_{ps}}{0.85 \text{ x } f_c^{'} * b} = \frac{(5)0.153 \text{ x } 268.8}{0.85 \text{ x } 8 \text{ x } 36} = 0.84$$

$$c = a / \beta_1 = 0.84 / 0.65 = 1.29$$

$$\varepsilon_3 = \left(\frac{d_p - c}{c}\right) \text{x } \varepsilon_c = \left(\frac{19 - 1.29}{1.29}\right) \text{x } 0.003 = 0.0411$$

$$\varepsilon_{ps} = \varepsilon_1 + \varepsilon_2 + \varepsilon_3 = 0.00635 + .000232 + .0411 = 0.0477$$

From strand stress-strain curve in PCI Design Handbook

$$f_{ps} = 270 - \frac{0.04}{\varepsilon_{ps} - 0.007} \approx 268.8 \text{ ksi (Equals assumed value)}$$

$$M_n = A_{ps} \text{ x } f_{ps} \text{ x}\left(d_p - \frac{a}{2}\right) = (5)0.153 \text{ x } 268.8 \text{ x}\left(19 - \frac{.84}{2}\right) = 3821 \text{ kip-in.}$$

$$= 318 \text{ kip-ft}$$

A.6 Calculations of Losses for Flexural Specimens

(using PCI Method)

Single-strand specimens

Elastic Shortening of Concrete (ES)

$$ES = K_{es} E_s \frac{f_{cir}}{E_{ci}}$$

K_{es} = 1.0 for pretensioned members
E_{ci} = 3,600 ksi
Es = 28,500 ksi

$$f_{cir} = K_{cir} f_{cpi} - f_g$$

K_{cir} = 0.9 for pretensioned members.

$$f_{cpi} = 0.9\left(\frac{31}{96} + \frac{31(4)^2}{1152}\right) = .68\,ksi$$

$$f_g = \frac{2.0(12)4}{1152} = 0.08\,ksi$$

$$f_{cir} = 1.0(.68) - .08 = 0.6\,ksi$$

$$ES = 1.0(28500)\frac{0.6}{3600} = 4.8\,ksi$$

Creep of Concrete (CR)

For members with bonded tendons,

$$CR = K_{cr}\frac{E_s}{E_c}(f_{cir} - f_{cds})$$

K_{cr} = 2.0 for pretensioned members

$$f_{cds} = 0\,ksi$$

$$CR = 2\frac{28500}{5000}(0.6 - 0) = 6.8\,ksi$$

Shrinkage of Concrete (SH)

$$SH = 8.2x10^{-6} K_{sh} E_s \left(1 - 0.06\frac{V}{S}\right)(100 - RH)$$

K_{sh} = 1.0 for pretensioned members

V / S =2.33

RH = 65%

$$SH = 8.2x10^{-6}(1.0)28500(1 - .06(2.33))(100 - 65) = 7.0\,ksi$$

Relaxation of Tendons (RE)

$$RE = \left[K_{re} - J(SH + CR + ES)\right]C$$

K_{re} = 5.0
J = 0.04
C = 1.0

$$RE_L = \left[5.0 - .04\left(4.8 + 6.8 + 7.0\right)\right]1 = 4.3\,ksi$$

$$RE_i = f_{st}\left\{\left[\log 24t - \log 24t_1\right]/24\right\}\text{x}\left[f_{st}/f_{py} - .55\right]$$
$$= 202{,}500\,\text{x}\left[\log 18\right]/45\,\text{x}\left[202{,}500/243{,}000 - .55\right] = 1.60\,\text{ksi}$$

Total Losses

$$f_{si} = f_{pj} - ES - RE_i$$
$$= 202.5 - 4.8 - 1.6 \approx 196\,\text{ksi}$$
$$f_{se} = f_{pj} - ES - CR - SH - RE_L$$
$$= 202.5 - 4.8 + 6.8 + 7.0 + 4.3 \approx 180\,\text{ksi}$$
$$f_{se@90} = 185\,\text{ksi}^*$$

$^*f_{se}$ of 90 days was used for calculations because that was the average age of the specimens at the time of testing.

Calculated Transfer Length (using equation 1.1)

$$L_{tr} = f_{se}d_b/3$$
$$185\,\text{x}\,.5/3 = 31\text{ in.}$$

Calculated Development Length (using equation 1.2)

$$L_{dev} = f_{se}d_b/3 + (f_{ps} - f_{se})d_b$$
$$= 185\,\text{x}\,.5/3 + \left(268.2 - 185\right)\text{x}\,.5 = 72.5\,\text{in.} \approx 6\text{'-}1\text{"}$$

Multiple-strand specimens

Elastic Shortening of Concrete (ES)

$$ES = K_{es}E_s\frac{f_{cir}}{E_{ci}}$$

K_{es} = 1.0 for pretensioned members
E_{ci} = 3,600 ksi
Es = 28,500 ksi

$$f_{cir} = K_{cir} f_{cpi} - f_g$$

K_{cir} = 0.9 for pretensioned members.

$$f_{cpi} = 0.9\left(\frac{155}{466} + \frac{155(10.52)^2}{17733}\right) = 1.17\,ksi$$

$$f_g = \frac{11.4(12)10.52}{17733} = 0.08\,ksi$$

$$f_{cir} = 1.0(1.17) - .08 = 1.09\,ksi$$

$$ES = 1.0(28500)\frac{1.08}{3600} = 8.55\,ksi$$

Creep of Concrete (CR)

For members with bonded tendons,

$$CR = K_{cr}\frac{E_s}{E_c}\left(f_{cir} - f_{cds}\right)$$

K_{cr} = 2.0 for pretensioned members

$$f_{cds} = 0\,ksi$$

$$CR = 2\frac{28500}{5000}(1.09 - 0) = 12.4\,ksi$$

Shrinkage of Concrete (SH)

$$SH = 8.2x10^{-6} K_{sh} E_s \left(1 - 0.06\frac{V}{S}\right)(100 - RH)$$

K_{sh} = 1.0 for pretensioned members
V/S =3.91
RH = 65%

$$SH = 8.2x10^{-6}(1.0)28500\left(1 - .06(3.91)\right)(100 - 65) = 6.3\,ksi$$

Relaxation of Tendons (RE)

$$RE = \left[K_{re} - J\left(SH + CR + ES\right)\right] C$$

K_{re} = 5.0
J = 0.04
C = 1.0

$$RE_L = \left[5.0 - .04\left(8.6 + 12.4 + 6.3\right)\right] 1 = 3.9\, ksi$$

$$RE_i = f_{st}\left\{\left[\log 24t - \log 24t_1\right] / 24\right\} \text{x} \left[f_{st} / f_{py} - .55\right]$$

$$= 202,500 \text{ x} \left[\log 18\right] / 45 \text{ x} \left[202,500 / 243,000 - .55\right] = 1.60 \text{ ksi}$$

Total Losses

$$f_{si} = f_{pj} - ES - RE_i$$

$$= 202.5 - 8.6 - 1.6 \approx 192 \text{ ksi}$$

$$f_{se} = f_{pj} - ES - CR - SH - RE_L$$

$$= 202.5 - 8.6 - 12.4 - 6.3 - 3.9 \approx 171 \text{ ksi}$$

$$f_{se@90} = 181 \text{ ksi}^*$$

$^*f_{se}$ of 90 days was used for calculations because that was the average age of the specimens at the time of testing.

Calculated Transfer Length (using equation 1.1)

$$L_{tr} = f_{se} d_b / 3$$

$$181 \text{ x } .5 / 3 = 30 \text{ in.}$$

Calculated Development Length (using equation 1.2)

$$L_{dev} = f_{se} d_b / 3 + (f_{ps} - f_{se}) d_b$$

$$= 181 \text{ x } .5 / 3 + \left(268.8 - 181\right) \text{x } .5 = 73 \text{ inch} \approx 6\text{'-}1\text{"}$$

A.7 As-Built Dimensions for Flexural Specimens

Table A.4 As-built dimensions for SSB specimens

Specimen	Heigth (inch)	Width (inch)	Strand Depth (inch)
SSB A	12	8.25	9.88
SSB C	12	8.25	9.88
SSB D	12	8.25	10
SSB E	12	8.25	9.88
SSB F	12	8.25	10

Table A.5 As-built dimensions for TSB specimens

Specimen	Heigth (inch)	Width (inch)	Strand Depth (inch)
TSB A	12.5	8	10
TSB B	12.5	8	10
TSB C	12.5	8	10
TSB D	12.25	8.13	9.75
TSB E	12	8.25	9.5
TSB F	12	7.88	9.5

Table A.6 As-built dimensions for TB specimens

Specimen	Height (inch)	Flange Width (inch)	Flange Heigth (inch)	Web Width (inch)	Strand Depth (inch)
TB A	20.63	36	6.38	16.06	18.63
TB B	21.63	35.88	6.75	15.94	19.63
TB C	20.63	36	6.38	16.06	18.63
TB D	21.63	35.88	6.75	15.94	19.63

A.8 Calculations of Prestress Losses for IT Specimens

ACI and PCI METHOD

Elastic Shortening of Concrete (ES)

$$ES = K_{es} E_s \frac{f_{cir}}{E_{ci}}$$

K_{es} = 1.0 for pretensioned members
E_{ci} = 3,600 ksi
Es = 28,500 ksi

$$f_{cir} = K_{cir} f_{cpi} - f_g$$

K_{cir} = 0.9 for pretensioned members.

$$f_{cpi} = 0.9\left(\frac{484}{256} + \frac{484(3.86)^2}{12822}\right) = 2.21 ksi$$

$$f_g = \frac{4.41(12)3.86}{12822} = 0.02 ksi$$

$$f_{cir} = 1.0(2.21) - .02 = 2.19 ksi$$

$$ES = 1.0(28500)\frac{2.19}{3600} = 17.3 ksi$$

Creep of Concrete (CR)

For members with bonded tendons,

$$CR = K_{cr} \frac{E_s}{E_c}\left(f_{cir} - f_{cds}\right)$$

K_{cr} = 2.0 for pretensioned members

$$f_{cds} = 0 ksi$$

$$CR = 2\frac{28500}{5300}(2.19 - 0) = 23.6 ksi$$

Shrinkage of Concrete (SH)

$$SH = 8.2x10^{-6} K_{sh} E_s \left(1 - 0.06\frac{V}{S}\right)(100 - RH)$$

K_{sh} = 1.0 for pretensioned members
V / S =2.87
RH = 65%

$$SH = 8.2x10^{-6}(1.0)28500\left(1 - .06(2.87)\right)(100 - 65) = 6.8\,ksi$$

Relaxation of Tendons (RE)

$$RE = \left[K_{re} - J\left(SH + CR + ES\right)\right]C$$

K_{re} = 5.0
J = 0.04
C = 1.0

$$RE = \left[5.0 - .04\left(17.3 + 23.6 + 6.8\right)\right]1 = 3.1\,ksi$$

Total Losses

$$TL = 17.3 + 23.6 + 6.8 + 3.1 = 50.8\,ksi$$
$$f_{se} = 198 - 50.8 \approx 147\,ksi$$

AASHTO METHOD

$$\Delta f_{pT} = \Delta f_{pES} + \Delta f_{pSR} + \Delta f_{pCR} + \Delta f_{pR2}$$

Elastic Shortening (Δf_{pES})

$$\Delta f_{pES} = \frac{E_p}{E_{ci}} f_{cgp}$$

f_{cgp} = $\left(\frac{484}{256} + \frac{484(3.86)^2}{12822}\right) - \frac{4.41(12)3.86}{12822} = 2.44\,ksi$

$$\Delta f_{pES} = \frac{28500}{3600} 2.44 = 19.3\,ksi$$

Shrinkage (Δf_{pSR})

$$\Delta f_{pSR} = \left(17.0 - 0.150H\right)$$

$H = 65$

$$\Delta f_{pSR} = \left(17.0 - 0.150\left(65\right)\right) = 7.25\,ksi$$

Creep (Δf_{pCR})

$$\Delta f_{pCR} = 12.0 f_{cgp} - 7.0\Delta f_{cdp} \geq 0$$

f_{cgp} = 2.44 ksi
Δf_{cdp} = 0 ksi

$$\Delta f_{pCR} = 12.0\left(2.44\right) - 7.0\left(0\right) = 29.3\,ksi$$

Relaxation (Δf_{pR2})

After Transfer

$$\Delta f_{pR2} = \left(20.0 - 0.4\Delta f_{pES} - 0.2\left(\Delta f_{pSR} + \Delta f_{pCR}\right)\right).30$$

$$\Delta f_{pR2} = \left(20.0 - 0.4\left(19.3\right) - 0.2\left(7.25 + 29.3\right)\right).30 = 1.5\,ksi$$

Total Losses

$$TL = 19.3 + 29.3 + 7.3 + 1.5 = 57.4$$
$$f_{se} = 198 - 57.4 \approx 141\,ksi$$

KDOT METHOD

Shrinkage

$$SH = 17,000 - 150RH$$

H =65

$$SH = 17,000 - 150\left(65\right) = 7250\ psi = 7.3\,ksi$$

Elastic Shortening

$$ES = \left(E_s \big/ E_{ci}\right) f_{cir}$$

$E_s =$ 28 x 10^6 psi
$f_{cir} =$ 2440 psi

$$ES = \left(28000 \big/ 3600\right) 2440 = 18900\ psi = 18.9\ ksi$$

Creep of Concrete:

$$CR_C = 12 f_{cir} - 7 f_{cds}$$

$f_{cds} =$ 0 ksi

$$CR_c = 12\left(2.44\right) - 7\left(0\right) = 29.3\ ksi$$

Relaxation of Prestressing Steel

$$CR_S = 5{,}000 - 0.10ES - 0.05\left(SH + CR_C\right)$$

$$CR_s = 5 - .1\left(18.9\right) - .05\left(7.3 + 29.3\right) = 1.3\ ksi$$

Total Losses

$$TL = 18.9 + 29.3 + 7.3 + 1.3 = 56.8$$
$$f_{se} = 198 - 56.8 \approx 141\ ksi$$

A.9 Calculation of ACI 209 Prestress Losses for IT specimen

Elastic shortening

$$ES = nf_c$$

$$n = 28500 \big/ 3500 = 8.14$$

$$f_c = \frac{484}{256} + \frac{484\left(3.86\right)^2}{12822} - \frac{4.41\left(12\right)3.86}{12822} = 2.44\ ksi$$

$$ES = 8.14\left(2.44\right) = 19.9\ ksi$$

Creep

$$CR = (nf_c)v_u\left[1 - \Delta F_t / 2F_o\right]$$

$$n = 28500/3750 = 7.6$$

$$f_c = 2.44\,ksi$$

$$v_u = 1.75$$

$$\Delta F_t / F_o = .18$$

$$CR = \left(7.6(2.44)\right)1.75\left[1 - .18/2\right] = 29.5\,ksi$$

Shrinkage

$$SH = \frac{(\varepsilon_{sh})_u E_s}{1 + n\rho k_s}$$

$$(\varepsilon_{sh})_u = 550\,\mu\varepsilon$$

$$E_s = 28500\,ksi$$

$$n = 28500/3750 = 7.6$$

$$\rho = \frac{14(.153)}{6.35(21)} = 0.016$$

$$k_s = 1 + e^2/r^2 = 1 + 3.86^2 \Big/ 12822/256 = 1.30$$

$$SH = \frac{550/10^6\ 28500}{1 + 7.6(.016)1.3} = 13.5\,ksi$$

Relaxation

$$RE = (f_{sr})_t$$

$$\left(f_{sr}\right)_u = .025(198) = 5.0$$

$$RE = 5.0\,ksi$$

Total Losses

$$TL = 19.9 + 29.5 + 13.5 + 5 = 67.9\,ksi$$
$$f_{se} = 198 - 67.9 \approx 130\,ksi$$

A.10 Calculation of Prestress Losses for K3 Girders

ACI and PCI METHOD (Conventional Concrete)

Elastic Shortening of Concrete (ES)

$$ES = K_{es} E_s \frac{f_{cir}}{E_{ci}}$$

K_{es} = 1.0 for pretensioned members
E_{ci} = 4,500 ksi
Es = 28,500 ksi

$$f_{cir} = K_{cir} f_{cpi} - f_g$$

K_{cir} = 0.9 for pretensioned members.

$$f_{cpi} = 0.9\left(\frac{496}{525} + \frac{496(13.27)^2}{127490}\right) = 1.47ksi$$

$$f_g = \frac{171(12)13.27}{127490} = 0.21ksi$$

$$f_{cir} = 1.0(1.47) - .21 = 1.26\,ksi$$

$$ES = 1.0(28500)\frac{1.26}{4500} = 8.0\,ksi$$

Creep of Concrete (CR)

For members with bonded tendons,

$$CR = K_{cr}\frac{E_s}{E_c}\left(f_{cir} - f_{cds}\right)$$

K_{cr} = 2.0 for pretensioned members

$$f_{cds} = \frac{850(50)^2\,12(13.27)}{8(127490)} = .33\,ksi$$

$$CR = 2\frac{28500}{4600}(1.26 - .33) = 11.5\,ksi$$

Shrinkage of Concrete (SH)

$$SH = 8.2x10^{-6}K_{sh}E_s\left(1 - 0.06\frac{V}{S}\right)(100 - RH)$$

K_{sh} = 1.0 for pretensioned members
V/S = 3.56
RH = 65%

$$SH = 8.2x10^{-6}(1.0)28500\left(1 - .06(3.56)\right)(100 - 65) = 6.4\,ksi$$

Relaxation of Tendons (RE)

$$RE = \left[K_{re} - J\left(SH + CR + ES\right)\right]C$$

K_{re} = 5.0
J = 0.04
C = 1.0

$$RE = \left[5.0 - .04\left(8.0 + 11.5 + 6.4\right)\right]1 = 4.0\,ksi$$

Total Losses

$$TL = 8.0 + 11.5 + 6.4 + 4.0 = 29.9\,ksi$$
$$f_{se} = 202.5 - 29.9 \approx 173\,ksi$$

AASHTO METHOD (Conventional Concrete)

$$\Delta f_{pT} = \Delta f_{pES} + \Delta f_{pSR} + \Delta f_{pCR} + \Delta f_{pR2}$$

Elastic Shortening (Δf_{pES})

$$\Delta f_{pES} = \frac{E_p}{E_{ci}} f_{cgp}$$

$$f_{cgp} = \left(\frac{496}{525} + \frac{496(13.27)^2}{127490} \right) - \frac{171(12)13.27}{127490} = 1.42\,ksi$$

$$\Delta f_{pES} = \frac{28500}{4500} 1.42 = 9.0\,ksi$$

Shrinkage (Δf_{pSR})

$$\Delta f_{pSR} = (17.0 - 0.150H)$$

$H = 65$

$$\Delta f_{pSR} = \left(17.0 - 0.150(65)\right) = 7.25\,ksi$$

Creep (Δf_{pCR})

$$\Delta f_{pCR} = 12.0 f_{cgp} - 7.0\Delta f_{cdp} \geq 0$$

f_{cgp} = 1.42 ksi
Δf_{cdp} = .33 ksi

$$\Delta f_{pCR} = 12.0(1.42) - 7.0(.33) = 14.7\,ksi$$

Relaxation (Δf_{pR2})

After Transfer

$$\Delta f_{pR2} = \left(20.0 - 0.4\Delta f_{pES} - 0.2\left(\Delta f_{pSR} + \Delta f_{pCR}\right)\right).30$$

$$\Delta f_{pR2} = \left(20.0 - 0.4(9.0) - 0.2\left(7.25 + 14.7\right)\right).30 = 3.6\,ksi$$

Total Losses

$$TL = 9.0 + 14.7 + 7.3 + 3.6 = 34.6$$
$$f_{se} = 202.5 - 34.6 \approx 168\,ksi$$

KDOT METHOD (Conventional Concrete)

Shrinkage

$$SH = 17,000 - 150RH$$

H =65

$$SH = 17,000 - 150(65) = 7250\ psi = 7.3\ ksi$$

Elastic Shortening

$$ES = \left({}^{E_s}\!\!\diagup\!\!{}_{E_{ci}} \right) f_{cir}$$

E_s = 28 x 10^6 psi
f_{cir} = 1420 psi

$$ES = \left({}^{28000}\!\!\diagup\!\!{}_{4500} \right) 1420 = 8840\ psi = 8.8\ ksi$$

Creep of Concrete:

$$CR_C = 12 f_{cir} - 7 f_{cds}$$

f_{cds} = .33 ksi

$$CR_c = 12(1.42) - 7(.33) = 14.7\ ksi$$

Relaxation of Prestressing Steel

$$CR_S = 5,000 - 0.10ES - 0.05(SH + CR_C)$$

$$CR_s = 5 - .1(8.8) - .05(7.3 + 14.7) = 3.0\ ksi$$

Total Losses

$$TL = 8.8 + 14.7 + 7.3 + 3.0 = 33.8$$
$$f_{se} = 202.5 - 33.8 \approx 169\ ksi$$

ACI and PCI METHOD (SCC)

Elastic Shortening of Concrete (ES)

$$ES = K_{es} E_s \frac{f_{cir}}{E_{ci}}$$

K_{es} = 1.0 for pretensioned members
E_{ci} = 3,500 ksi
Es = 28,500 ksi

$$f_{cir} = K_{cir} f_{cpi} - f_g$$

K_{cir} = 0.9 for pretensioned members.

$$f_{cpi} = 0.9\left(\frac{496}{525} + \frac{496(13.27)^2}{127490}\right) = 1.47 ksi$$

$$f_g = \frac{171(12)13.27}{127490} = 0.21 ksi$$

$$f_{cir} = 1.0(1.47) - .21 = 1.26 ksi$$

$$ES = 1.0(28500)\frac{1.26}{3500} = 10.3 ksi$$

Creep of Concrete (CR)

For members with bonded tendons,

$$CR = K_{cr} \frac{E_s}{E_c}(f_{cir} - f_{cds})$$

K_{cr} = 2.0 for pretensioned members

$$f_{cds} = \frac{850(50)^2 12(13.27)}{8(127490)} = .33 ksi$$

$$CR = 2\frac{28500}{3750}(1.26 - .33) = 14.1 ksi$$

Shrinkage of Concrete (SH)

$$SH = 8.2x10^{-6} K_{sh} E_s \left(1 - 0.06\frac{V}{S}\right)(100 - RH)$$

K_{sh} = 1.0 for pretensioned members
V / S =3.56
RH = 65%

$$SH = 8.2x10^{-6}(1.0)28500\left(1 - .06(3.56)\right)(100 - 65) = 6.4\,ksi$$

Relaxation of Tendons (RE)

$$RE = \left[K_{re} - J\left(SH + CR + ES\right)\right]C$$

K_{re} = 5.0
J = 0.04
C = 1.0

$$RE = \left[5.0 - .04\left(10.3 + 14.1 + 6.4\right)\right]1 = 3.8\,ksi$$

Total Losses

$$TL = 10.3 + 14.1 + 6.4 + 3.8 = 34.6\,ksi$$
$$f_{se} = 202.5 - 34.6 \approx 168\,ksi$$

AASHTO METHOD (SCC)

$$\Delta f_{pT} = \Delta f_{pES} + \Delta f_{pSR} + \Delta f_{pCR} + \Delta f_{pR2}$$

Elastic Shortening (Δf_{pES})

$$\Delta f_{pES} = \frac{E_p}{E_{ci}} f_{cgp}$$

$$f_{cgp} = \left(\frac{496}{525} + \frac{496(13.27)^2}{127490}\right) - \frac{171(12)13.27}{127490} = 1.42\,ksi$$

$$\Delta f_{pES} = \frac{28500}{3500}1.42 = 11.6\,ksi$$

Shrinkage (Δf_{pSR})

$$\Delta f_{pSR} = \left(17.0 - 0.150H\right)$$

$H = 65$

$$\Delta f_{pSR} = \left(17.0 - 0.150\left(65\right)\right) = 7.25\,ksi$$

Creep (Δf_{pCR})

$$\Delta f_{pCR} = 12.0 f_{cgp} - 7.0\Delta f_{cdp} \geq 0$$

f_{cgp} = 1.42 ksi
Δf_{cdp} = .33 ksi

$$\Delta f_{pCR} = 12.0\left(1.42\right) - 7.0\left(.33\right) = 14.7\,ksi$$

Relaxation (Δf_{pR2})

After Transfer

$$\Delta f_{pR2} = \left(20.0 - 0.4\Delta f_{pES} - 0.2\left(\Delta f_{pSR} + \Delta f_{pCR}\right)\right).30$$

$$\Delta f_{pR2} = \left(20.0 - 0.4\left(11.6\right) - 0.2\left(7.25 + 14.7\right)\right).30 = 3.3\,ksi$$

Total Losses

$$TL = 11.6 + 14.7 + 7.3 + 3.3 = 36.9$$
$$f_{se} = 202.5 - 36.9 \approx 166\,ksi$$

KDOT METHOD (SCC)

Shrinkage

$$SH = 17,000 - 150RH$$

H =65

$$SH = 17,000 - 150\left(65\right) = 7250\ psi = 7.3\,ksi$$

Elastic Shortening

$$ES = \left(E_s \big/ E_{ci}\right) f_{cir}$$

$E_s =$ 28 x 10^6 psi
$f_{cir} =$ 1420 psi

$$ES = \left(28000 \big/ 3500\right) 1420 = 11360\ psi = 11.4\ ksi$$

Creep of Concrete:

$$CR_C = 12 f_{cir} - 7 f_{cds}$$

$f_{cds} =$ .33 ksi

$$CR_c = 12(1.42) - 7(.33) = 14.7\ ksi$$

Relaxation of Prestressing Steel

$$CR_S = 5{,}000 - 0.10ES - 0.05(SH + CR_C)$$

$$CR_s = 5 - .1(11.4) - .05(7.3 + 14.7) = 2.8\ ksi$$

Total Losses

$$TL = 11.4 + 14.7 + 7.3 + 2.8 = 36.2$$
$$f_{se} = 202.5 - 36.2 \approx 166\ ksi$$

ACI 209 METHOD (SCC)

Elastic shortening

$$ES = nf_c$$

$$n = 28500 \big/ 3500 = 8.14$$

$$f_c = \frac{496}{525} + \frac{496(13.27)^2}{127490} - \frac{171(12)13.27}{127490} = ksi$$

$$ES = 8.14(1.42) = 11.6\ ksi$$

Creep

$$CR = (nf_c)v_u\left[1 - \Delta F_t / 2F_o\right]$$

$$n = 28500/3750 = 7.6$$

$$f_c = 1.42 - \frac{266(12)13.27}{127490} = 1.09\,ksi$$

$$v_u = 1.75$$

$$\Delta F_t / F_o = .14$$

$$CR = \left(7.6(1.09)\right)1.75\left[1 - .14/2\right] = 13.5\,ksi$$

Shrinkage

$$SH = \frac{(\varepsilon_{sh})_u E_s}{1 + n\rho k_s}$$

$$(\varepsilon_{sh})_u = 550\,\mu\varepsilon$$

$$E_s = 28500\,ksi$$

$$n = 28500/3750 = 7.6$$

$$\rho = \frac{16(.153)}{22(42)} = 0.0026$$

$$k_s = 1 + e^2/r^2 = 1 + 13.27^2 \Big/ 127490/525 = 1.73$$

$$SH = \frac{\frac{550}{10^6}28500}{1 + 7.6(.0026)1.73} = 15.2\,ksi$$

Relaxation

$$RE = (f_{sr})_t$$

$$\left(f_{sr}\right)_u = .025(198) = 5.0$$

$$RE = 5.0\,ksi$$

Total Losses

$$TL = 11.6 + 13.5 + 15.2 + 5 = 45.3\,ksi$$
$$f_{se} = 202.5 - 45.3 \approx 157\,ksi$$